

**Clamped-Mode Fixed Frequency Series Resonant Converter:Off-line Application,
Analysis and Implementation.**

by

Juan A. Sabate

Thesis submitted to the Faculty of the
Virginia Polytechnic Institute and State University
in partial fulfillment of the requirements for the degree of
Master of Science
in
Electrical Engineering

APPROVED:



Fred C. Lee, Chairman



B. H. Cho



V. Vorperian

October, 1988.

Blacksburg, Virginia

2

LD
5655
V855
1988
5227
C.2

**Clamped-Mode Fixed Frequency Series Resonant Converter:Off-line Application,
Analysis and Implementation.**

by

Juan A. Sabate

Fred C. Lee, Chairman

Electrical Engineering

(ABSTRACT)

The performance of the clamped-mode series resonant converter operating at a fixed frequency is studied for off line applications. A new set of characteristics for the converter operating above and below resonant frequency has been developed by including the effect of losses in the analysis.

Based on the analytical results, design guidelines are established and two prototypes were built to operate below and above resonant frequency respectively. The advantages and limitations of the two breadboards are assessed and their major sources of loss identified.

Acknowledgements

I am deeply indebted to Dr. Fred C. Lee for offering me the opportunity to study with the Virginia Tech Power Electronics Center. His continued encouragement and technical expertise provided throughout my research and thesis is especially appreciated.

Special thanks are extended to the other members of my advisory committee: Dr. Vatche Vorperian and Dr. Bo H. Cho. I have benefitted greatly from their advice and guidance.

I wish to thank all of my professors in my Master's program; their instruction has allowed me to broaden and enhance my knowledge.

Special thanks are due to Mr. F. S. Tsai and to Mr. Peter Materu who shared their knowledge and experience of clamped-mode resonant converters.

I would also like to thank my fellow students and colleagues in the power electronics research group at Virginia Polytechnic Institute and State University. Especially the following, whose friendship and suggestions have been invaluable

in the completion of thesis work, thank you to: Mr. A. Lotfi, Mr. L. Chang, Mr. P. Gradzki, Mr. W. Tabisz, Dr. Milan M. Jovanovic, Mr. R. Ridley, Mr. C. J. Hsiao, Mr. A. Ghahary, Mr. Grant Carpenter and all of the graduate students and technicians at VPEC.

I also deeply appreciate the help of Mrs. Tammy J. Hinner, Mrs. Justice McCormick and Mis. Gayle Noyes.

My sincere thanks to Mis. Monica C. Lluch, for her understanding, encouragement and constant support.

Finally, I particularly would like to offer my sincerest gratitude to my parents and brother, for their encouragement and support have provided the strength and determination needed to pursue and fulfill my studies.

Table of Contents

- Introduction** 1

- Description of the operation** 4
 - 2.1 Introduction 4
 - 2.2 Constant frequency operation 5
 - 2.3 Circuit parameters 10
 - 2.4 Operating regions 11
 - 2.4.1 Operation below resonant frequency 11
 - 2.4.2 Operation above resonant frequency 16

- Analysis and design characteristics** 23
 - 3.1 Ideal case analysis 23
 - 3.1.1 DC characteristics below resonant frequency 25
 - 3.1.2 DC characteristics above resonant frequency 26
 - 3.2 Analysis including losses 30
 - 3.2.1 Model Including Losses 31
 - 3.2.2 DC characteristics for operation above resonant frequency 33

3.2.3 DC characteristics for operation below resonant frequency	34
Design considerations	39
4.1 Design guidelines	40
4.1.1 Case below resonant frequency	43
4.1.2 Case above resonant frequency	49
4.1.3 Control logic and gate driver.	53
4.2 Performance evaluation	58
4.2.1 Prototype operating below resonant frequency	58
4.2.2 Case above resonant frequency	65
Verification of the characteristics	75
5.1 DC characteristics	76
5.2 Simulation results	77
Conclusions and summary	86
State plane analysis of the clamped mode series resonant converter including parasitic losses .	89
A.1 Introduction	89
A.2 State plane analysis	90
A.2.1 Equilibrium trajectories above resonant frequency	94
A.2.2 DC characteristics above resonant frequency	105
A.2.3 Equilibrium trajectories below resonant frequency	106
A.2.4 DC characteristics below resonant frequency	113
Fortran programs	114
B.1 Programs to calculate DC characteristics for the ideal case	114
Table of Contents	vi

B.1.1	Case above resonant frequency	114
B.1.2	Case below resonant frequency	125
B.2	Programs to calculate DC characteristics for the case including loss	135
B.2.1	Case above resonant frequency	135
B.2.2	Case below resonant frequency	155
	Spice listings	182
C.1	Simulation of the model including loss	182
C.2	Simulation of switching conditions	184
	References:	187
	Vita	190

Chapter 1

Introduction

The new trend in power electronics reveals an increased demand for power supplies with higher power density. The size of the filtering elements and transformers can be reduced by increasing the operation frequency. However, the losses in these elements increase in proportion to the operation frequency. Reduction of the overall equipment size is achieved only if the losses in these elements can be kept reasonably low.

Although better core materials and capacitors are available for high-frequency operation, a major problem is associated with the switching losses of semiconductor devices. Even with the fastest devices (MOSFETs) available for power processing, the turn on and turn off processes are always accompanied with current and voltage overlap. When operating at high frequencies, the switching loss can offset the benefit of high-frequency operation.

PWM converters have been widely used because of their simplicity and relatively good performance. However, PWM converters operate with square-wave current and voltages which impose high dv/dt and di/dt on the devices, resulting in high switching stress and switching loss. Other sources of stress and loss in PWM converters are the parasitic elements associated with the switching devices. Recently, resonant switch concepts were proposed to alleviate these problems. The appropriate design of resonant converters allows operation with either zero current switching (ZCS) or zero voltage switching (ZVS) and utilization of the parasitic elements. By introducing the resonant switch concept, a large family of quasi-resonant converters has been developed directly from their PWM counterparts [23], resulting in a drastic reduction of switching loss and stress. This family of converters can therefore operate at a much higher switching frequency and maintain high conversion efficiency.

Control of resonant converters or quasi-resonant converters has been accomplished by modulating the operation frequency of the circuit to regulate the output. This variable frequency operation imposes a penalty on the design of input and output filters and it is not suitable for certain applications where a fixed frequency operation is necessary.

A phase control technique for resonant converters was proposed recently [14]. This technique permits output regulation without changing the operating frequency. Converters using this control principle are called constant frequency clamped-mode resonant converters. Several studies have been reported [10-12,24] explaining its operation and providing design characteristics.

The purpose of this work is to study in detail the clamped mode series resonant converter topology. A breadboard is built to provide an experimental verification of this concept.

Chapter 2 presents an overview of the circuit operation, with an emphasis on the switching conditions of the devices. The operating range where the circuit operates with zero voltage turn on or zero current turn off is defined analytically. Chapter 3 presents the analysis of the circuit and calculation of the DC characteristics. Previous studies [10-12,24] based on the assumption of ideal components are improved by incorporating losses in the tank. Chapters 4 and 5 describe the design guidelines and present the experimental results, respectively. The operating ranges for zero current turn off and zero voltage turn on are identified for operation above and below resonant frequency. The results of the experimental work are used to verify the accuracy of the model developed by including losses in the determination of DC characteristics.

Chapter 2

Description of the operation

2.1 Introduction

The conventional series resonant converter has been extensively studied [1-7,8]. This converter can be operated with a switching frequency either above or below the resonant frequency of the LC tank, and with the output load linked to the current in the tank through a rectifier. Since the current in the tank is sinusoidal, the only output filter required is a capacitor. The circuit operates with all active switches commutated at zero current below resonant frequency and with the active switches turned on at zero voltage above resonant frequency.

The conventional resonant converter is controlled by modulating the switching frequency. Problems with this method occur when the converter is operated

with variable loads. If there is a wide range of input and load, in order to regulate the output, the switching frequency must be varied over a wide range.

It is desirable to be able to retain the main features of the resonant converters and to operate at a fixed frequency. The recently proposed clamped-mode resonant converters [10-13,24] can be regulated without changing the frequency of operation.

2.2 Constant frequency operation

The clamped mode series resonant converter is implemented with a full bridge structure either with or without isolation (Figs. 2.1 and 2.2). The operation is based on a phase shifting between the gating signals applied to the devices in the two legs of the bridge. The two devices of each leg are operated complementarily (delayed 180 deg.) with a 50 percent duty ratio, as well as simultaneously with a phase lag between each device and its diagonally opposing device in the bridge.

This sequence of operation causes the voltage applied to the resonant element to be quasi-square wave as shown in Fig. 2.3. Between the positive and negative pulses there exists a time interval when the tank voltage is clamped to zero. The time that the tank is connected to the supply is controlled by varying the phase lag between the two diagonal devices.

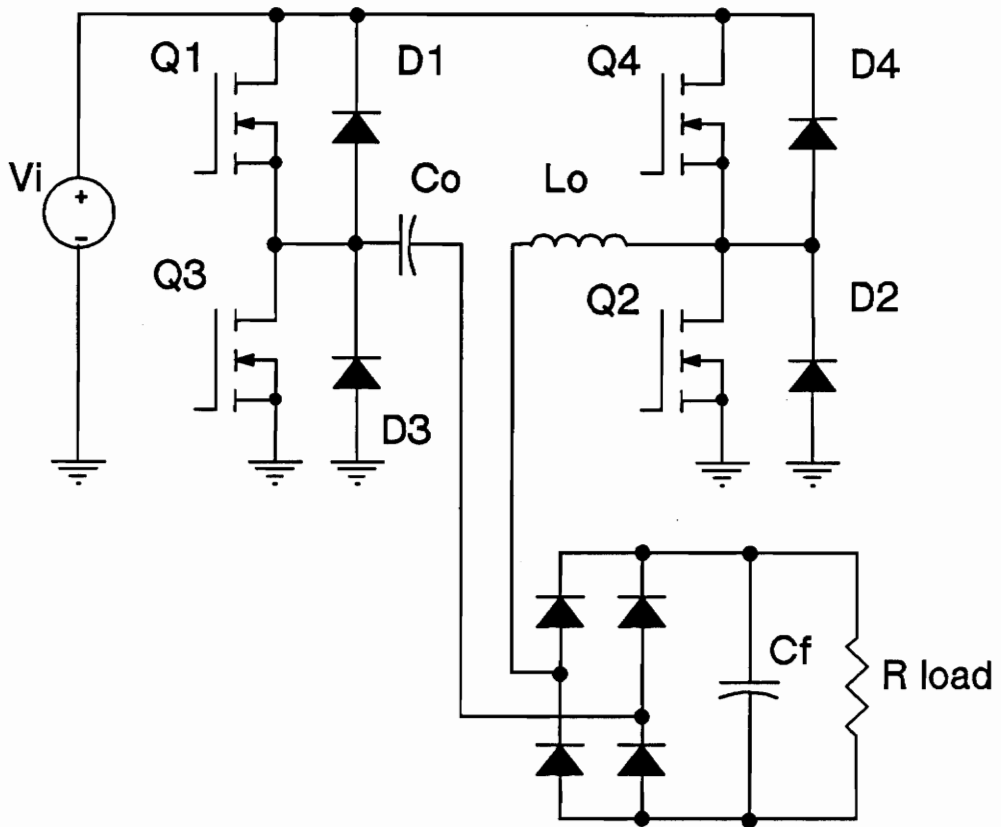


Figure 2.1: Circuit without isolation.

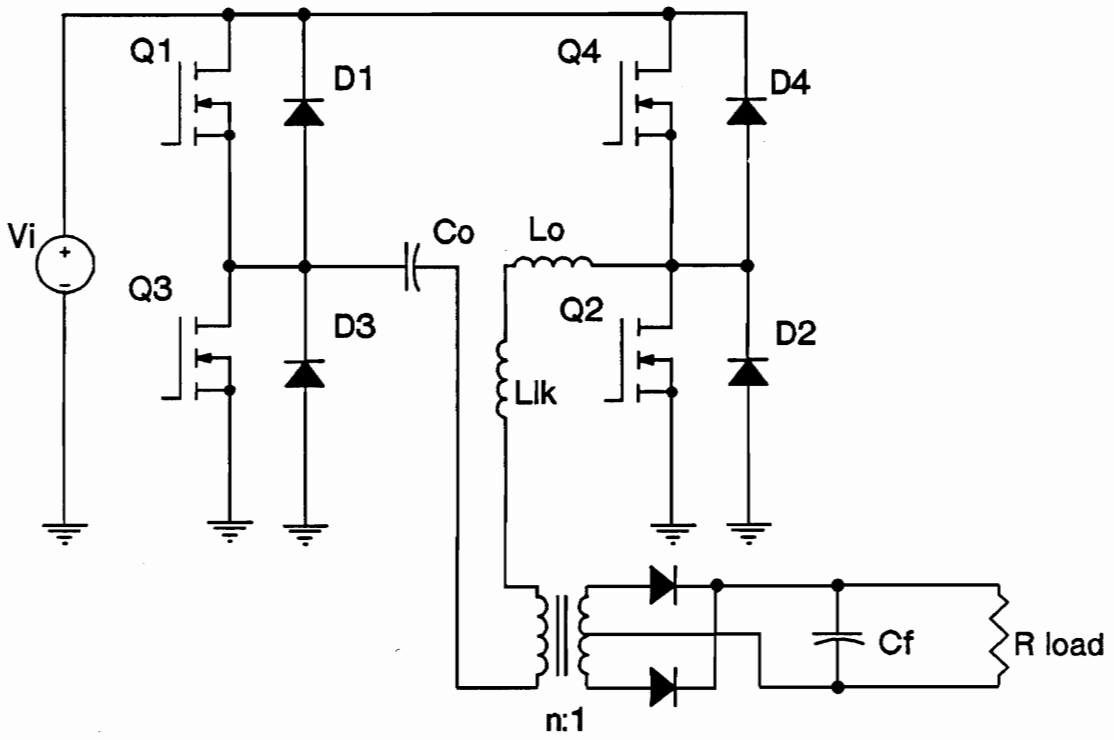


Figure 2.2: Circuit with isolation.

The control parameter is defined as the time that the tank is connected directly to the input supply, and its value in degrees with reference to the switching frequency is defined as β . Mathematically it can be expressed as

$$\beta = \frac{t_{\beta}}{T_s/2} \times 180 \text{ degrees}$$

where t_{β} is the amount of time the tank is directly connected to the input source and T_s is the switching period. (Fig. 2.3).

It is important to emphasize the similarity between β and the duty ratio for PWM converters. In clamped-mode series resonant converters, the output can be regulated by controlling β

There exists many different operating modes depending upon the design of the resonant tank elements and the load conditions. The next section of this chapter presents an overview of all possible modes, including the cases when switching frequency is above and below resonant frequency (Secs. 2.4.1 and 2.4.2). Zero voltage turn-on or zero current turn-off operation not only depends on the operation above or below resonant frequency ratio, but also on the load. Consequently, since regulation is achieved by varying β according to the load, the zero voltage turn-on and zero current turn-off conditions are expressed as function of the operating frequency and β .

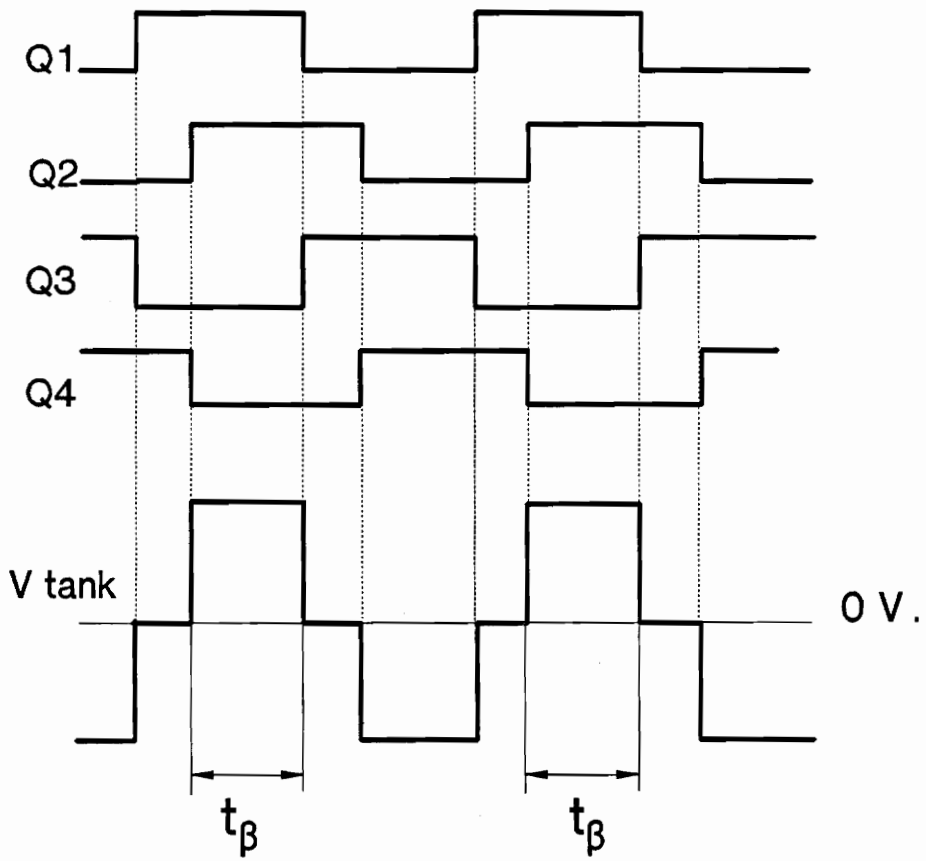


Figure 2.3: Timing waveforms and tank voltage.

2.3 *Circuit parameters*

The series resonant converter is characterized by the resonant frequency and the characteristic impedance of the resonant tank,

$$f_o = \frac{1}{2\pi\sqrt{LC}} \text{ Hz} \quad (2.1)$$

and

$$Z_o = \sqrt{\frac{L}{C}} \ \Omega \quad (2.2)$$

All circuit currents and voltages are normalized for simplicity and generality of results, as is common practice in the analysis of the resonant converters [1-5,6,8,10,11]. The normalized quantities are defined as

$$I_n = \frac{I}{I_o} \quad (2.3)$$

$$V_n = \frac{V}{V_i} \quad (2.4)$$

$$f_n = \frac{f}{f_o} \quad (2.5)$$

where V_i is the input voltage, and the n subscript indicates normalized value.

2.4 Operating regions

Circuit operation below resonant frequency has been fully characterized in previous studies [10,11], showing that many different modes of operation are possible. It is necessary to evaluate them to determine suitability for particular applications.

Switching conditions for the devices are major factors when high-frequency operation is desired. In the following sections, various operating modes and corresponding regions are defined. The cases when the switching frequency is above or below the resonant frequency present different features and are discussed separately. The regions of operation define operating conditions with identical switching conditions. In every region, different modes of operation or different sequences of conduction for the devices are possible. Continuous conduction mode (CCM) or discontinuous conduction mode (DCM) refer to the inductor current which is either continuous or discontinuous.

2.4.1 Operation below resonant frequency

Six different modes of operation are possible below resonant frequency. Depending on the switching conditions, only two different commutation situations are possible. One is when the four active devices are turned-off naturally. The other is when two active devices are turned off naturally and two are force

turned-off with current. In the second case, however, the force commutated devices turn on with no voltage applied. For the first case, the region of operation is called region A and for the second, region B. These regions are drawn with respect to load (β) and normalized output voltage for every ω_n , as shown in Fig 2.4.

Only one mode of operation is possible in region A (Fig. 2.5). In this mode before the gate voltage is removed from a particular MOSFET the corresponding parallel diode is already conducting, due to the reversed tank current. However, the four diodes of the bridge are reverse biased by the input voltage when the corresponding MOSFET in series is turned on. This fact plays an important roll in the turn on losses as shown in the experimental results.

In region B, five operating modes are possible [11]. However, two occur when operating at frequencies less than $0.8 f_s$, and another occurs when the normalized output voltage is close to unity [10,11]. Since these conditions are not practical in an actual design, only two possibilities are described here.

The two cases of interest in region B are shown in Fig 2.6. Prior to the reversal of current through Q1 and Q2 , Q1 is force turned-off. Energy stored in the resonant tank is resonating through Q2 and D3. In this case, Q1 and Q3 are force commutated and Q2 and Q3 are naturally commutated, however, Q1 and Q3 are gated when the corresponding parallel diode is still conducting. Consequently, they turn on with zero voltage, and a simple capacitor snubber across Q1 and Q3 can be used to reduce their turn-off losses.

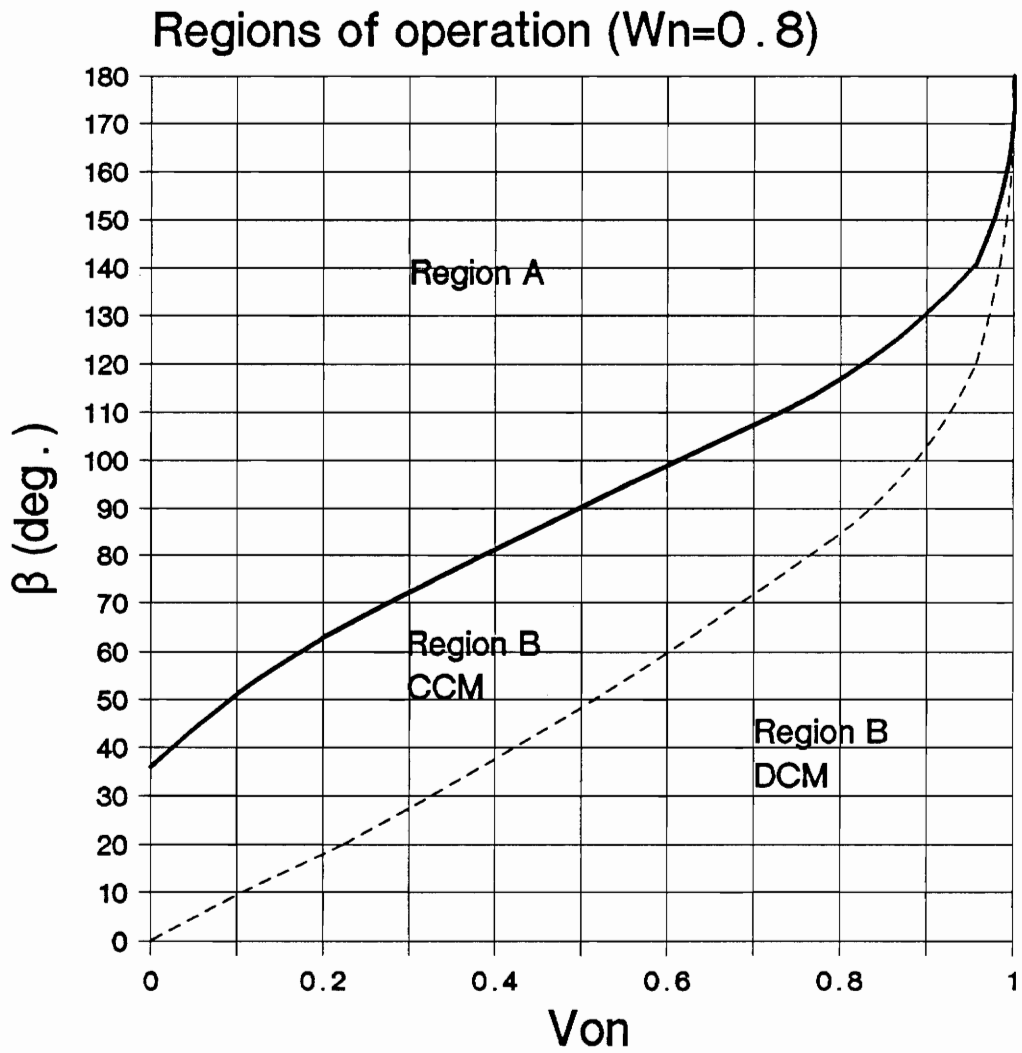


Figure 2.4: Operating regions below resonant frequency.

REGION A

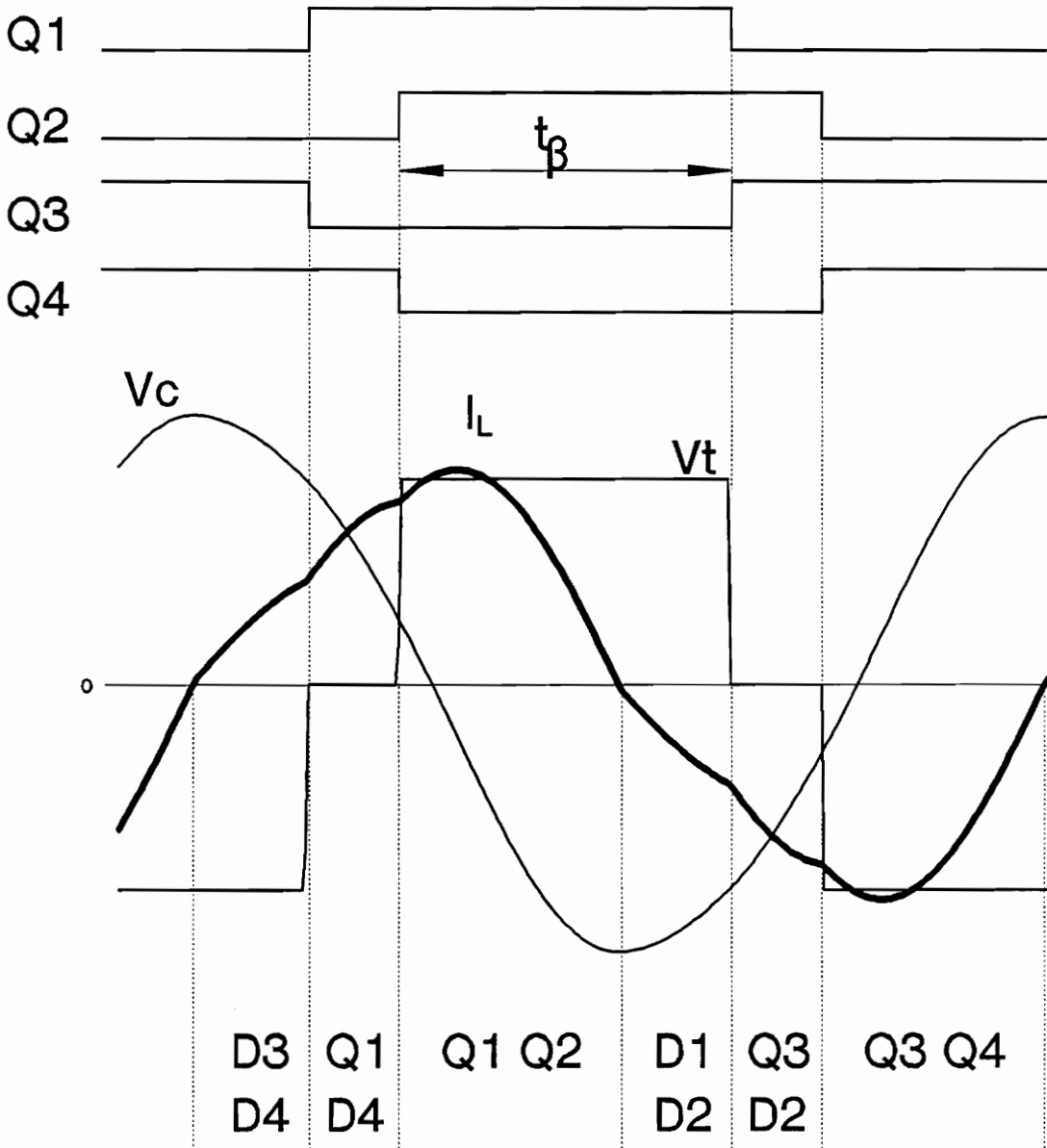
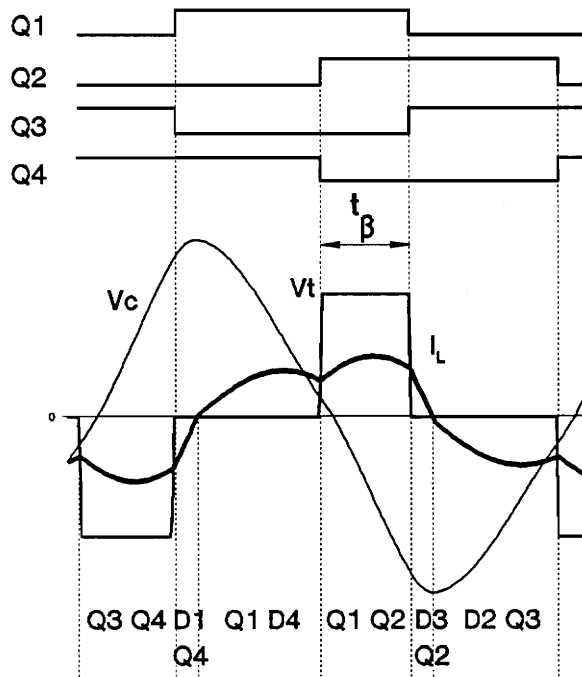
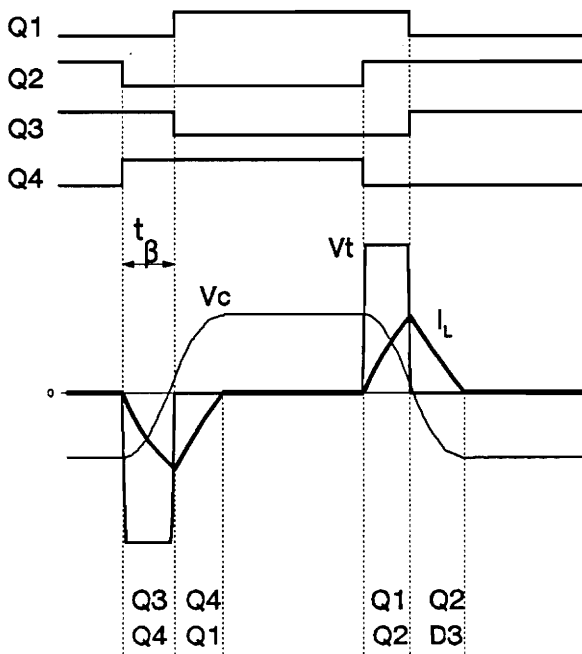


Figure 2.5: Inductor current, tank and capacitor voltages. Region A.

REGION B



CCM



DCM

Figure 2.6: Inductor current, tank and capacitor voltages . Region B.

The second possible mode of region B is the discontinuous conduction mode (DCM). DCM occurs when the voltage across the resonant capacitor is not high enough to forward bias the rectifier against the output voltage. This mode of operation invariably occurs under very light loads.

Figure 2.7 shows the topological modes for regions A and B.

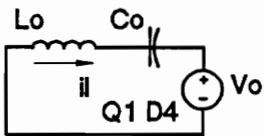
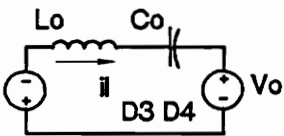
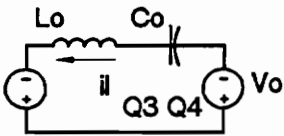
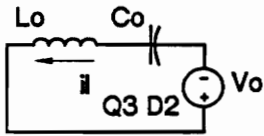
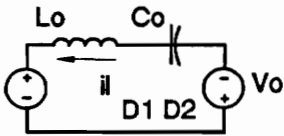
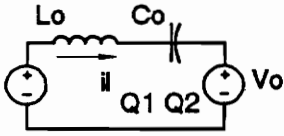
2.4.2 Operation above resonant frequency

Similar to the case below resonant frequency, two operating regions are defined when operating above resonant frequency [27]. Region A' is where the four active devices are turned on with zero voltage. Region B' is where two turn on with zero voltage and two turn off with zero current (as for region B below resonant frequency). Figure 2.8 shows the regions with respect to load, β and normalized output voltage.

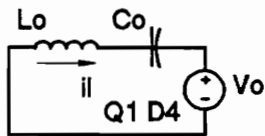
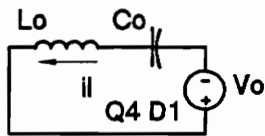
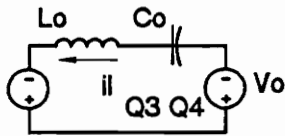
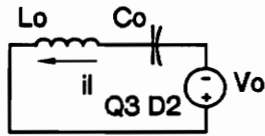
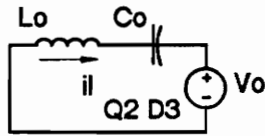
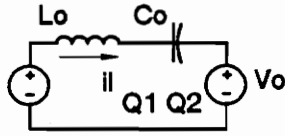
Only one mode of operation is possible when operating in region A' [27]. When voltage is applied to the gate of each MOSFET, the corresponding parallel diode is conducting. The four MOSFETs turn on with zero voltage and the diodes turn off naturally because the current reverses (Fig 2.9).

In region B', two modes of operation are possible, CCM and DCM. For both modes, two of the active devices turn on with zero voltage and the other two turn off with zero current but turn on with voltage. It can be seen in Fig 2.10 that the current reverses before the two active devices, Q2 and Q4, are turned on. Nevertheless Q2 and Q4 are turned off naturally.

Region A



CCM



Region B

DCM

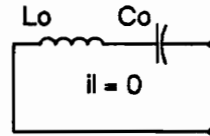
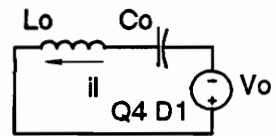
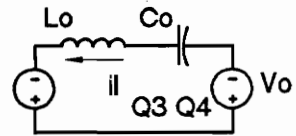
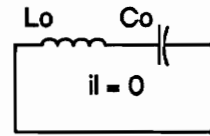
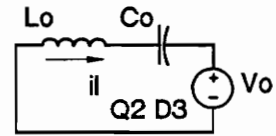
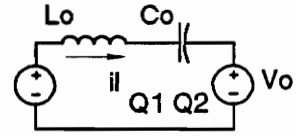


Figure 2.7: Topological modes for regions A and B (CCM and DCM)

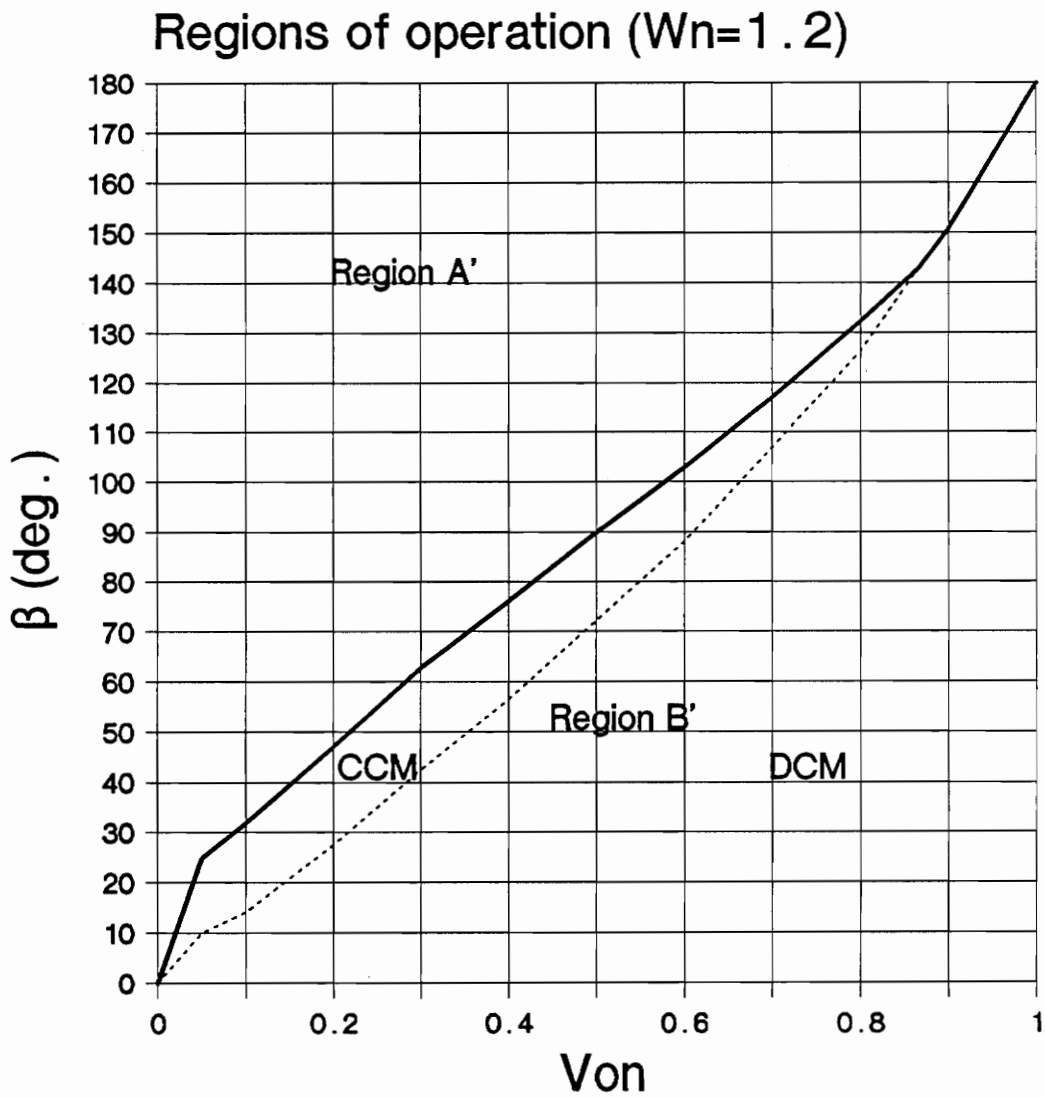


Figure 2.8: Regions of operation above resonant frequency

REGION A'

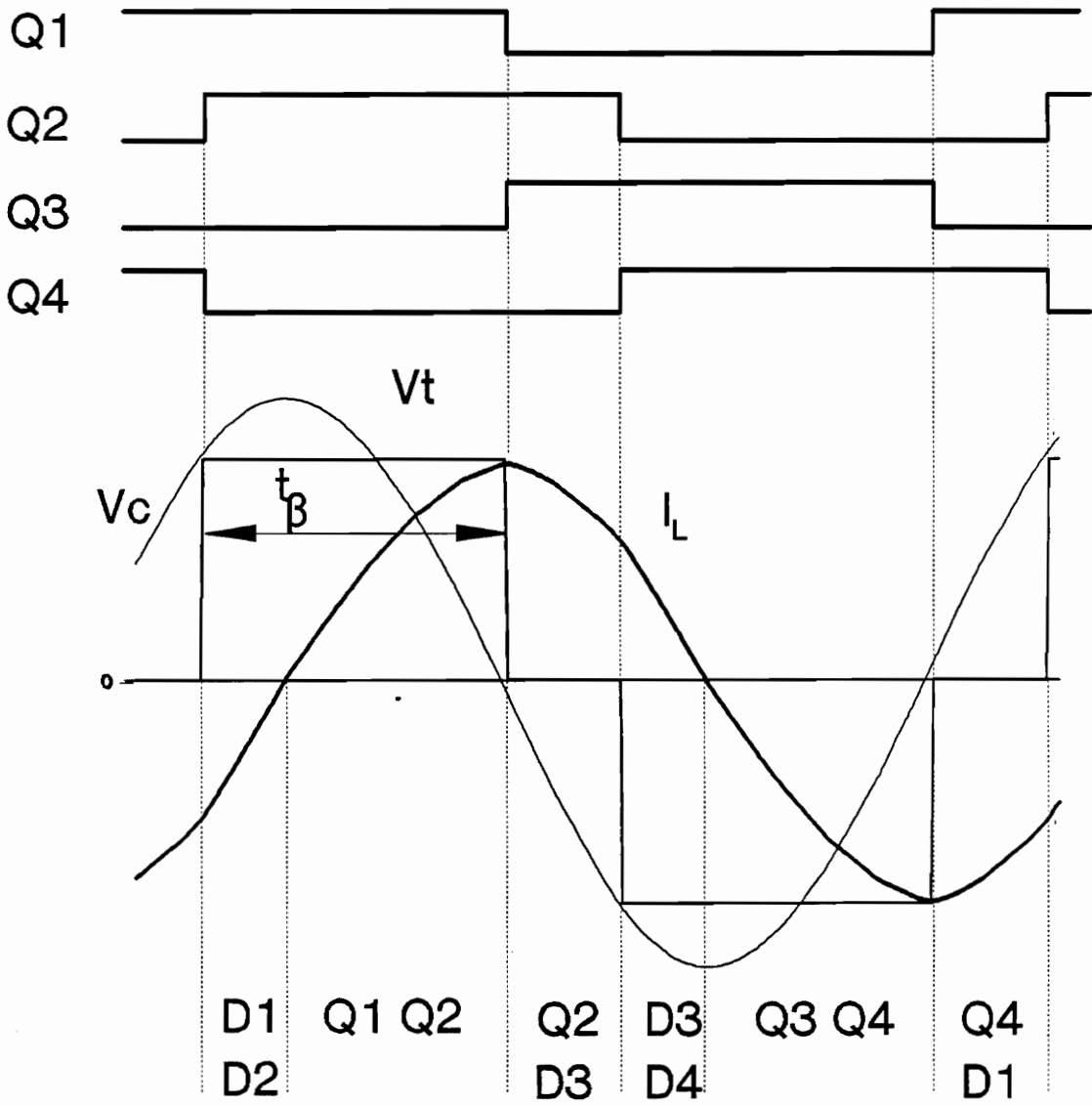
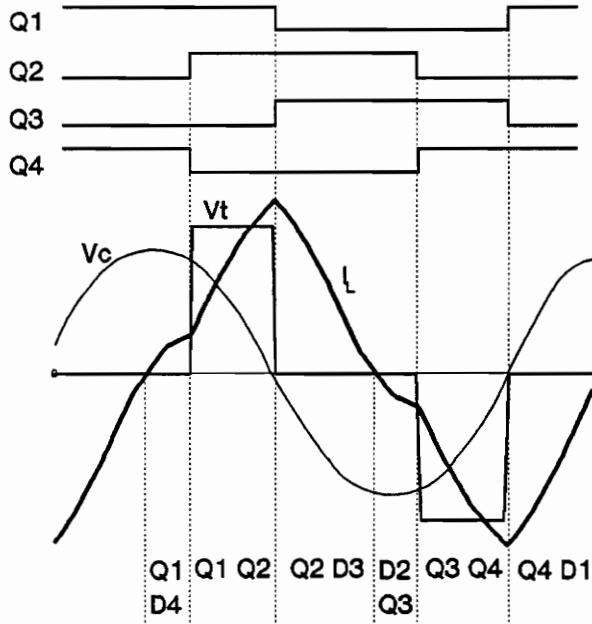
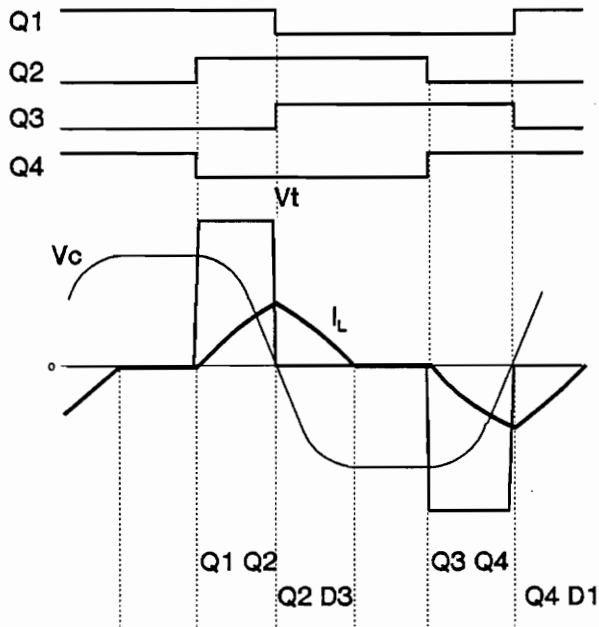


Figure 2.9: Inductor current, tank and capacitor voltages. Region A'.

REGION B'



CCM



DCM

Figure 2.10: Inductor current, tank and capacitor voltages. Region B'.

Figure 2.11 shows the topological sequences the converter goes through in one operating cycle. In region B', DCM occurs when the capacitor is not charged with sufficient voltage to forward bias the rectifier against the output voltage. As in the operation below resonant frequency, this occurs with light load.

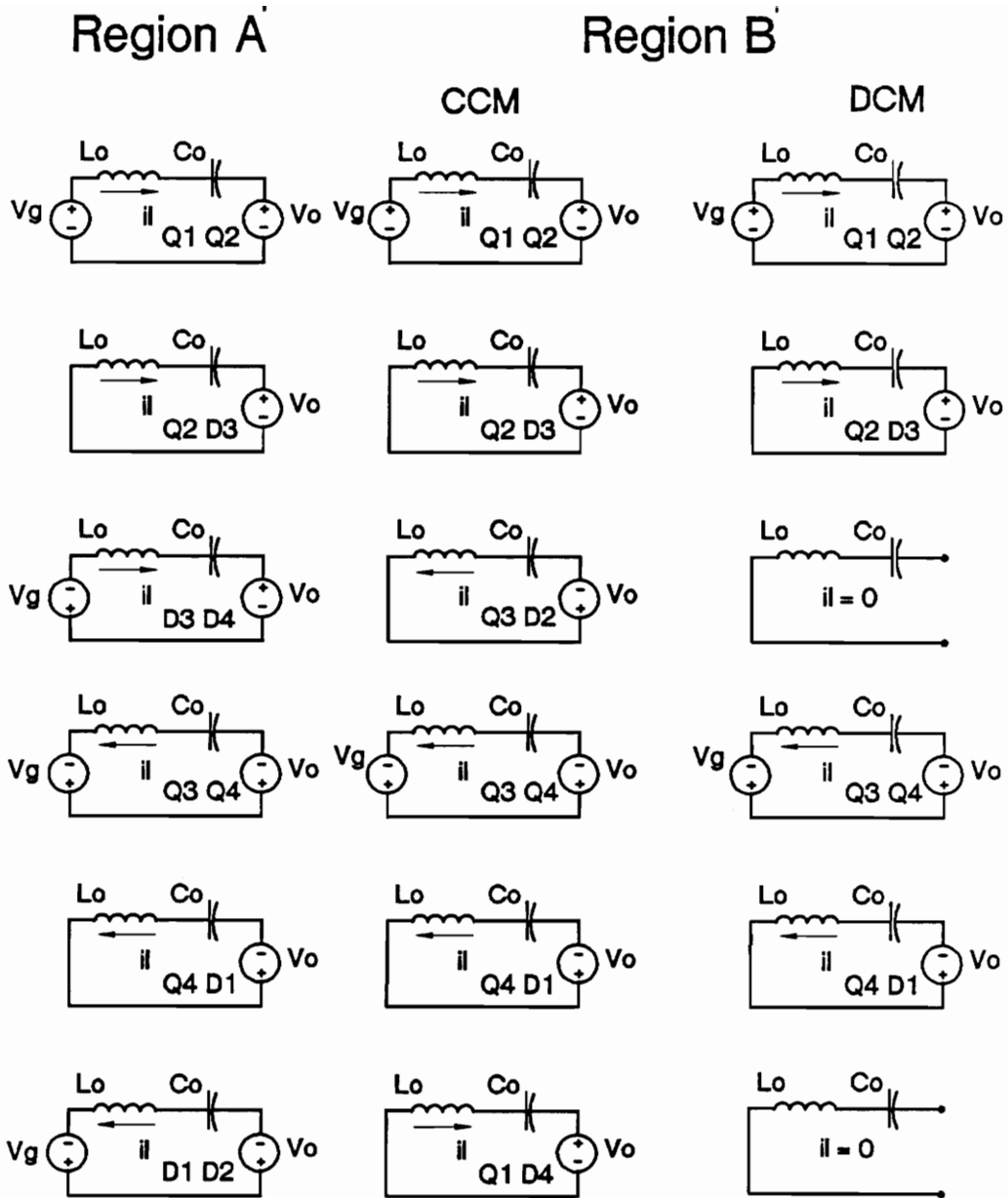


Figure 2.11: Topological modes for regions A' and B'.

Chapter 3

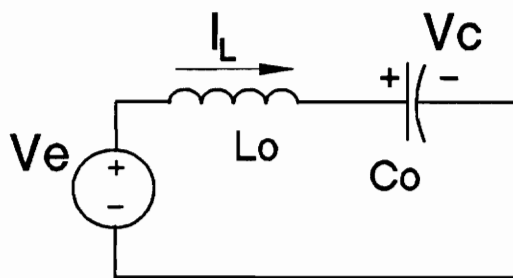
Analysis and design characteristics

3.1 Ideal case analysis

Previous analysis of clamped-mode resonant converters characterize the DC operation [10,11,24]. The method of analysis used for the series resonant circuit is based on the determination of equilibrium trajectories on the state plane [6,9].

The model used for DC characterization assumes the tank is ideal and the output is a constant voltage source (Figure 3.1). The voltage source of the model varies according to the conduction sequence of the switching devices and includes the output voltage source with the polarity corresponding to the current in the tank.

The procedure to determine the DC characteristics using the equilibrium state-plane trajectories is the following:



Dev . on	V_e
Q1 Q2	$V_s - V_o$
D1 D2	$V_s + V_o$
Q2 D3	$-V_o$
Q3 D2	$+V_o$
Q3 Q4	$-V_s + V_o$
D3 D4	$-V_s - V_o$
Q4 D1	$+V_o$
Q1 D4	$-V_o$

Figure 3.1: Converter model for an ideal tank.

- Identify all topological sequences corresponding to the different operating modes.
- Draw an equilibrium trajectory for each topological sequence.
- Since each operating mode is only possible for a given β angle range, geometrical constraints define the boundary trajectories between modes. These boundary trajectories allow the calculation of the boundary β angles.
- Given the boundary β angles, the values of the control parameter (β) and the equilibrium trajectory for each mode, a program using the geometrical characteristics of a trajectory allows calculation of the parameters for every operating point [11].

(Refer to APPENDIX A for more details)

3.1.1 DC characteristics below resonant frequency

Considering the operating modes described in the former chapter, a FORTRAN program has been written (Appendix B), according to the algorithm given in [10] and [11], to plot the DC characteristics and define the regions of operation.

In Figure 3.2, the graph shows a curve of I_{LAVN} (normalized output current) vs. β for every V_{on} at $f_n = 0.8$, where the dotted line separates region A and region

B. The abrupt change in slope in region B corresponds to the transition between the discontinuous operating mode (lowest currents) and the continuous operating mode.

The fact that the graph corresponds to $f_n = 0.8$ does not affect the generality of the qualitative comments that follow. Although the shape of the characteristics and regions distributions is the same for all frequencies, the numerical values are different in each case. The program permits calculation for different f_n values incorporating the three different operating modes of interest.

In Figure 3.2, it is interesting to note that region A is available only for a limited load range, while region B permits operation from 0 current to the boundary. When operating in region B, the control gain changes significantly when moving from discontinuous to continuous operating modes. This change must be considered when designing the feedback regulation loop.

3.1.2 DC characteristics above resonant frequency

A FORTRAN program (Appendix B) has been written to calculate boundaries and characteristics above resonant frequency. Figure 3.3 shows I_{LAVN} and β for different output voltages at a switching frequency $f_n = 1.2$.

When operating above resonant frequency, region A' is only available for a limited load range when load current is higher. Region B', however, operates from no load to the region A' boundary (dotted line).

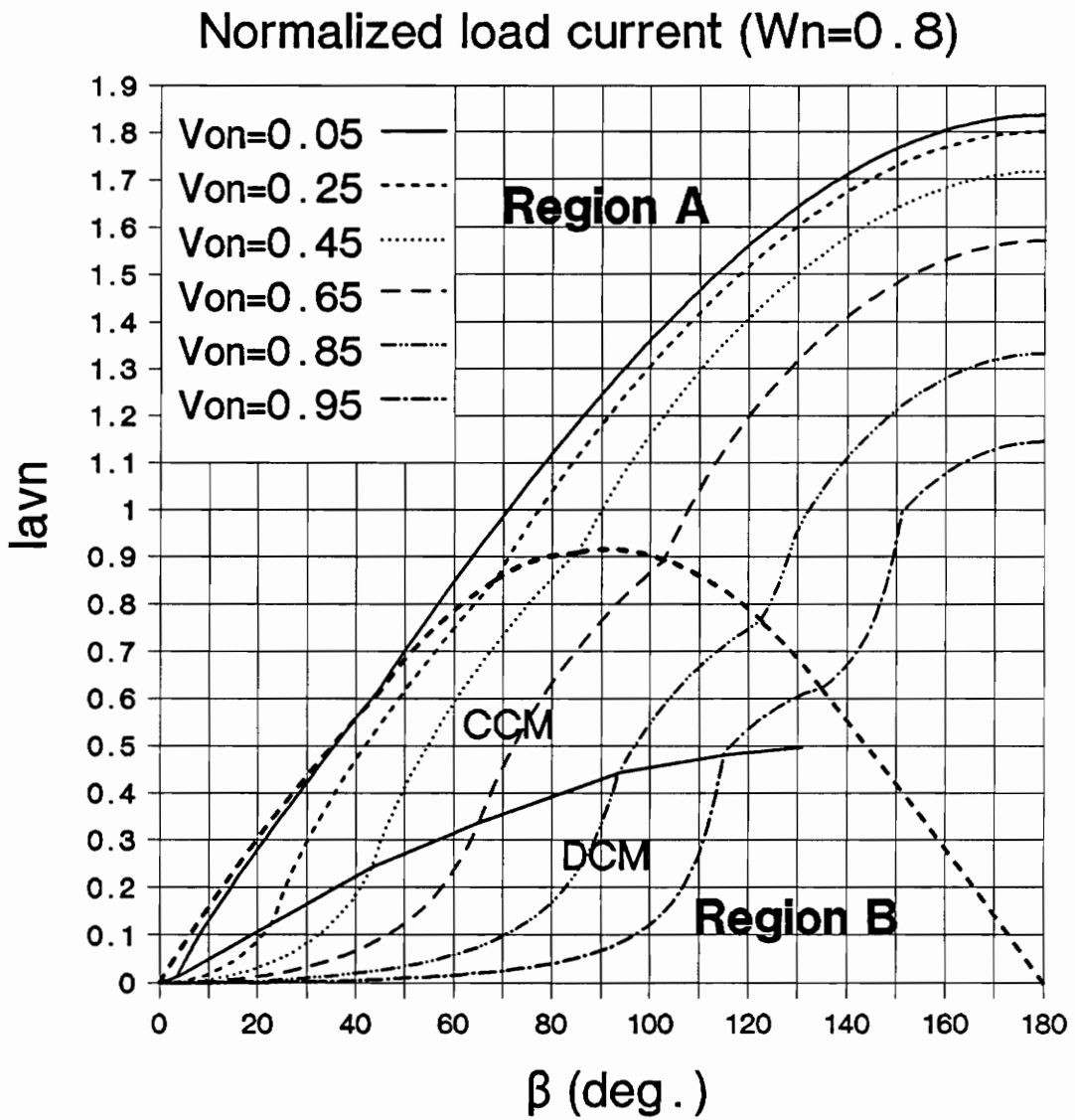


Figure 3.2: DC characteristics below resonant frequency. (Region A: all switches ZCS ; Region B: 2 switches ZCS and 2 ZVS)

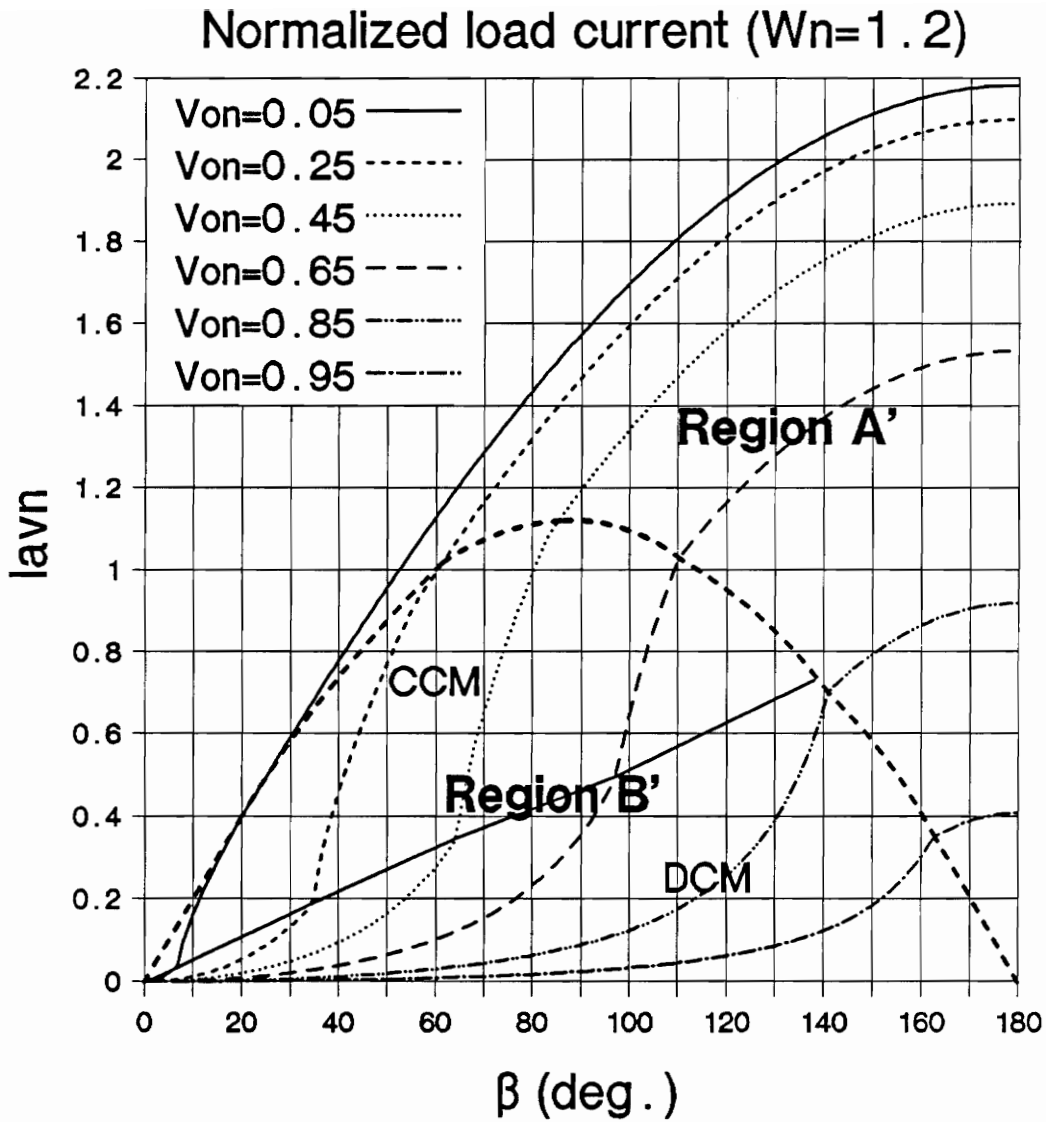


Figure 3.3: DC characteristics above resonant frequency. (Region A': all switches ZVS ; Region B': 2 switches ZCS and 2 with ZVS)

Above resonant frequency there are two slope changes in each curve, corresponding to each V_{on} . The first is the transition from discontinuous conduction, at low current, and the other is the boundary between region A' and region B'.

Comparing the characteristics below and above resonant frequency, the following facts are noteworthy:

- Operation with heavy load gives zero voltage switching above resonant frequency and zero current switching below resonant frequency.
- When operating either above or below resonant frequency, regions A and A' are only available for a limited load range.
- The switching conditions for the devices are qualitatively the same in regions B and B'. Two active switches are turned off naturally and the other two are turned on with zero voltage.
- An overload of a circuit designed to operate in region B (or B') may signify entrance into region A (A') and circuit damage may result. The reciprocal is true for regions A (A') designs when going below a minimum load. The time recovery of the internal diode of the MOSFETS may not be tolerable when the device operates with ZCS.
- Regions B or B' are considered one region because the switching conditions are the same in either continuous or discontinuous conduction mode. Also, the external elements needed for the proper operation of the converter can be

used for the whole region. This is not true when moving from region B to region A, because the lossless snubbers added to two of the devices do not allow for proper operation in region A.

3.2 Analysis including losses

The characteristics presented in the previous section have been derived with the assumption that all the circuit components are ideal. Although this results in a reasonable approximation of the high Q tank circuit, the load range and the boundary conditions of different regions of operation are significantly affected by the losses in the tank circuit.

Studies of the effect of losses in the clamped-mode series resonant converter have not been reported. For the conventional series resonant converter, the losses effect have been modelled and analyzed for the operation below resonant frequency [8] and [9].

The analysis of the conventional series resonant converter is used to predict the effect of losses in the clamped-mode series resonant circuit. To do this, the conventional series resonant converter is considered a particular case of the clamped mode operation, when the control angle is maximum ($\beta = 180^\circ$). The operation of the conventional series resonant converter is then the upper boundary for DC voltage conversion and power delivered to the load.

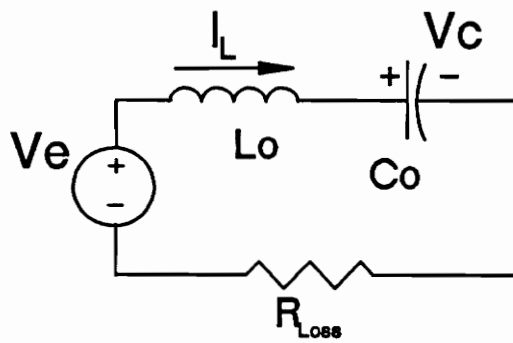
Studies of the conventional series resonant converter show that the effect of losses in the converter performance is due to a reduction of the maximum average current that can be delivered to the load for a given set of operating conditions and tank values. This reduction in current is also expected to affect the boundary conditions of the operating regions of the clamped mode series resonant converter. This effect is more pronounced when resonant frequency is closer to switching frequency and when the normalized output voltage is higher.

Discrepancies between the ideal case estimation and the actual results suggested a more accurate study. The analysis presented here permits the determination of DC characteristics for a circuit when the losses are not negligible. A comparison is made between DC characteristics calculated for the ideal model and the ones obtained with the model considering the losses. The cases above and below resonant frequency are presented.

3.2.1 Model Including Losses

A new model is defined to analyze the clamped mode series resonant converter. Following the guidelines of studies of loss effect in conventional series resonant converters [8,9], a damping resistor is placed in series with the resonant tank in the circuit model (Fig. 3.4). The losses are then modelled as:

- Losses in the primary (bridge, resonant tank and transformer) are approximated with a lumped resistor in series with the LC resonant element.



Dev. on	V_e
Q1 Q2	$V_s - V_o$
D1 D2	$V_s + V_o$
Q2 D3	$-V_o$
Q3 D2	$+V_o$
Q3 Q4	$-V_s + V_o$
D3 D4	$-V_s - V_o$
Q4 D1	$+V_o$
Q1 D4	$-V_o$

Figure 3.4: Converter model for finite Q.

- Losses on the rectifier are modelled by adding the forward voltage drop of the diodes to the load voltage.

The circuit model (Fig 3.4) is very similar to the one used for the ideal case, and includes the reflected voltage from the load.

The method used to analyze the circuit is the state plane analysis and is fully described in Appendix A.

The following sections describe the results obtained for the cases below and above resonant frequency.

3.2.2 DC characteristics for operation above resonant frequency

The normalized average load current I_{AVN} vs. control angle β is plotted with $\omega_n = 1.2$ and a damping coefficient of $\xi = 0.02$ for several normalized output voltages in Figure 3.5 and for different damping factors in Figure 3.6.

The results confirm the expected effects. The difference with the ideal case is larger for higher normalized output voltages and the boundary line between regions A and B occurs at lower I_{AVN} (dotted line in Fig 3.5). As the damping increased, the deviation from the ideal case also increased, as shown in Fig. 3.6.

3.2.3 DC characteristics for operation below resonant frequency

The results are plotted compared with the ideal case for different normalized output voltages (Fig 3.7) and for different damping factors (Fig. 3.8) with a normalized operating frequency of $\omega_n = 0.8$. The comments for the case apply to this case too :

- Increasing effect when the normalized output voltage increases.
- Boundary between Regions A and B regions at lower I_{AVN} values.

At a normalized frequency, $\omega_n = 0.8$, the deviation from the ideal case is smaller than that at $\omega_n = 1.2$. This occurs because the voltage gain as function of the frequency for the series resonant converter is not symmetrical with respect to resonant frequency.

Normalized load current ($W_n=1.2$)

Ideal — $\xi = 0.02$ - - - -

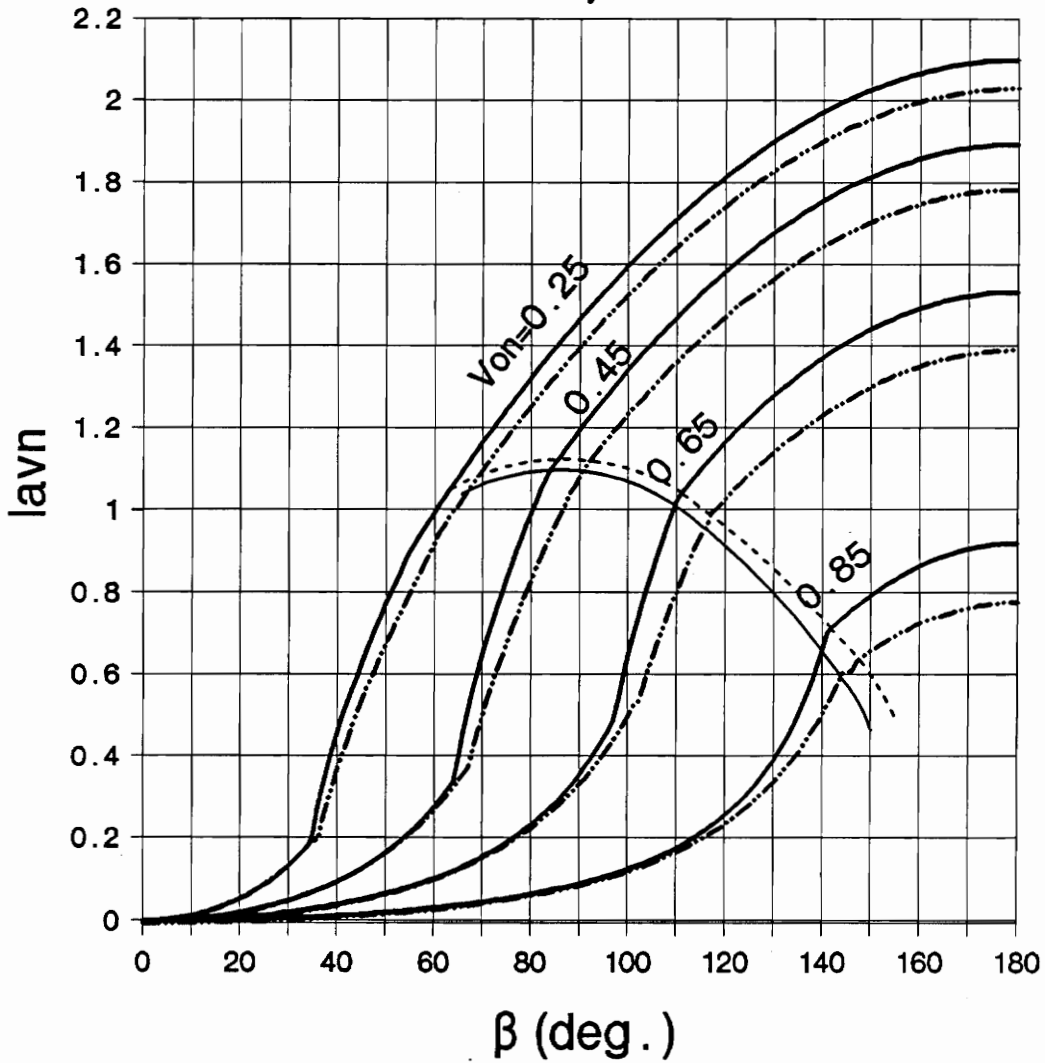


Figure 3.5: Characteristics for the cases with and without loss.

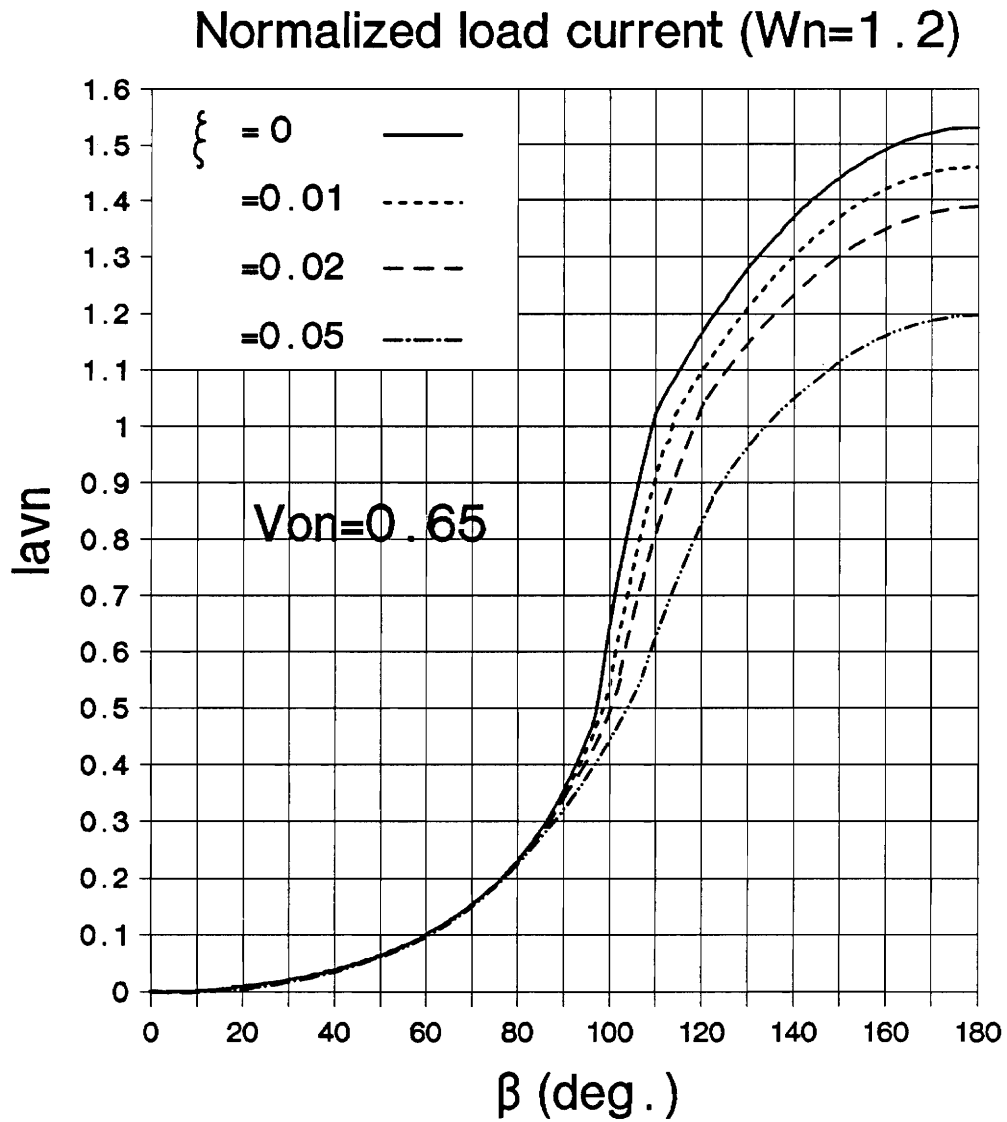


Figure 3.6: Characteristics for different Q values.

Normalized load current ($W_n=0.8$)

$\xi = 0.02$ — Ideal

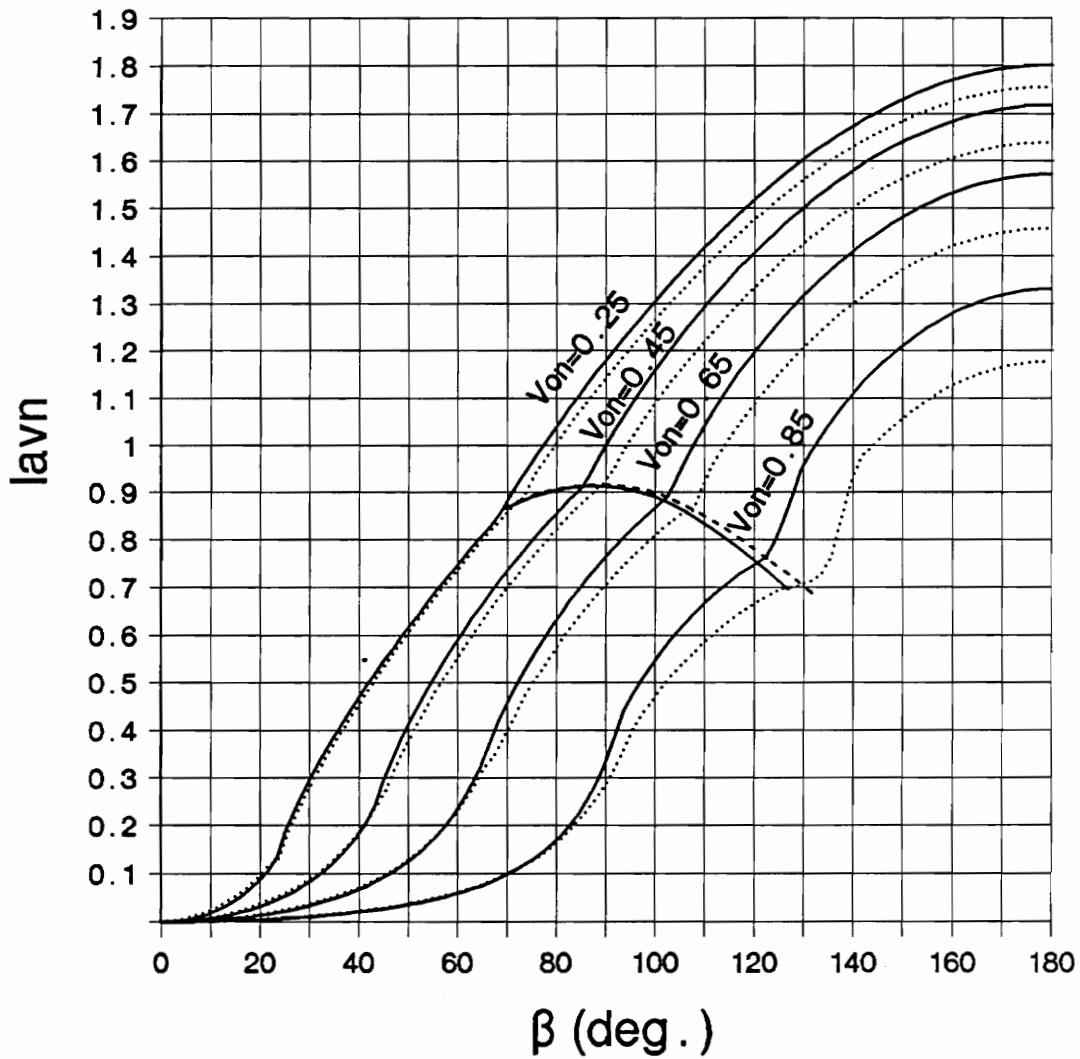


Figure 3.7: Characteristics for the cases with and without loss.

Normalized load current ($W_n=0.8$)

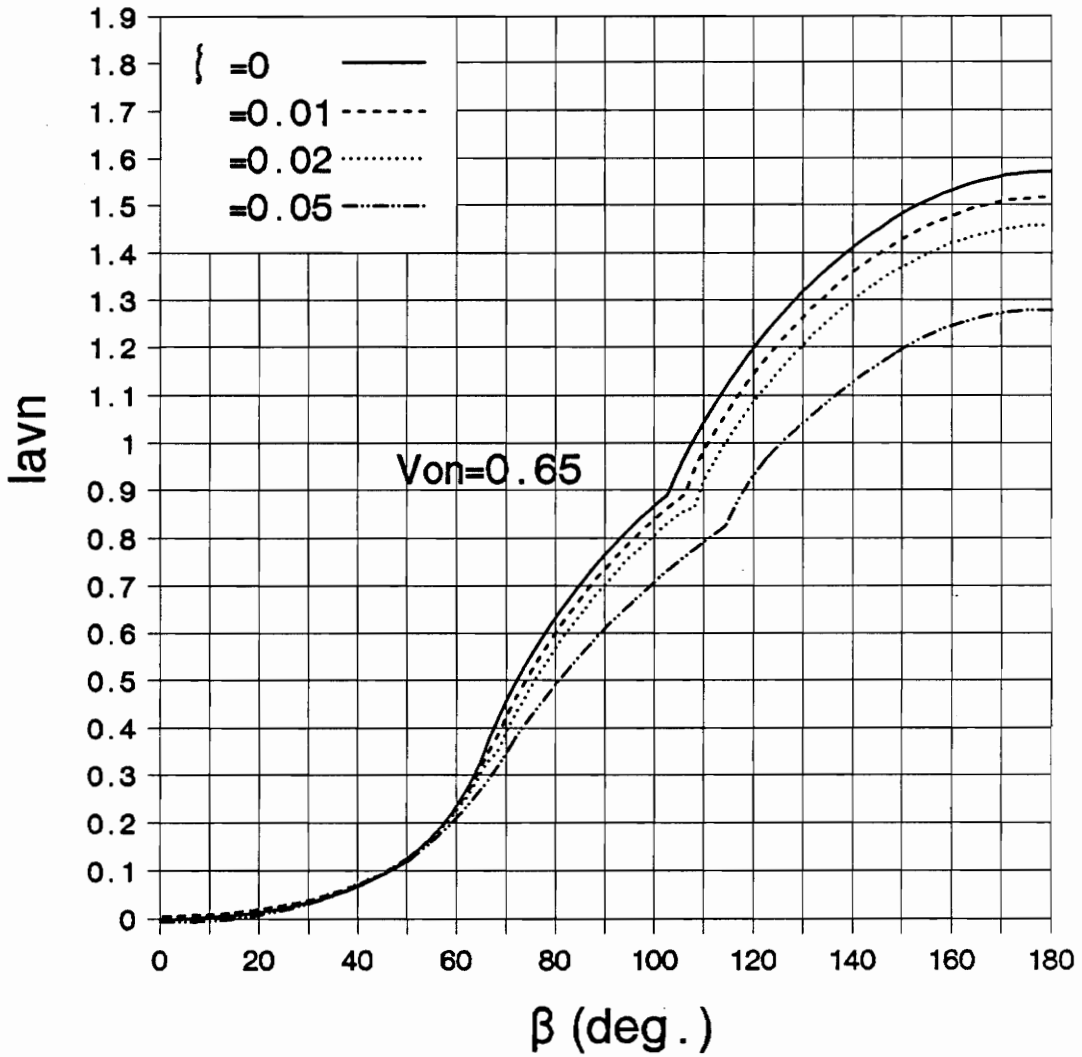


Figure 3.8: Characteristics for different Q values.

Chapter 4

Design considerations

The clamped mode series resonant converter can operate with zero voltage switching or zero current switching. To achieve higher power density, the use of MOSFETs as switches is necessary for high frequency operation. However, high voltage blocking capability is difficult to achieve with MOSFETs and is accompanied with high on-resistance. For the clamped mode series resonant converter, the voltage across the devices is clamped by the supply voltage and this is suitable for an off line application.

4.1 *Design guidelines*

The prototypes were built according to the following specifications.

- input voltage between 200 and 300 volts.
- output voltage 5 volts.
- output power 100 watts.
- operating frequency in the 500 kHz range.

Isolation between primary and secondary is required and is accomplished by using a transformer in series with the resonant tank (and placing the rectifier in the transformer secondary) (Fig. 2.2). The transformer maintains the current through the switches at a reasonable value, thus reducing conduction loss in the devices.

In order to keep the loss in the rectifier as low as possible, the full wave rectifier is constructed using a center tapped secondary for the transformer. Then, the forward drop of only one diode contributes to the losses. To reduce the forward drop, Schottky diodes were used.

Several variations of the bridge are required depending on to the operation region selected. The circuits are presented for each case in the following sections.

The design procedure of the clamped-mode series resonant converter uses the DC characteristics described in Chapter 3. Given the circuit specifications, the operating region for the converter can be selected and the circuit parameters can be determined. The procedure can be summarized as follows:

The load current is normalized,

$$I_{on} = \frac{I_{load} Z_o}{n V_i} \quad (4.1)$$

for full load, high input line and low input line cases gives,

$$I_{onFL}(\max) = \frac{I_{FL} Z_o}{n V_{imin}} \quad (4.2)$$

and

$$I_{onFL}(\min) = \frac{I_{FL} Z_o}{n V_{imax}} \quad (4.3)$$

and for minimum load,

$$I_{onmL}(\max) = \frac{I_{mL} Z_o}{n V_{imin}} \quad (4.4)$$

calculating the ratio between minimum an maximum value for each case:

$$\frac{I_{onFL}(\max)}{I_{onFL}(\min)} = \frac{I_{onmL}(\max)}{I_{onmL}(\min)} = \frac{V_{imax}}{V_{imin}} = \frac{3}{2} \quad (4.5)$$

The output voltage reflected to the primary is normalized as:

$$V_{on}(\text{min}) = \frac{V_o n}{V_{imax}} \quad (4.6)$$

$$V_{on}(\text{max}) = \frac{V_o n}{V_{imin}} \quad (4.7)$$

and the ratio is found,

$$\frac{V_{on}(\text{max})}{V_{on}(\text{min})} = \frac{V_{imax}}{V_{imin}} = \frac{3}{2} \quad (4.8)$$

It is important to note that V_{on} is the normalized voltage reflected to the primary and it includes the forward drop of the rectifying diodes.

Since the DC characteristics define the operation regions as a function of the normalized values, the appropriate choice of transformer ratio (n) and characteristic impedance (Z_o) is determined by the operation region selected.

In the following sections, two designs, one above resonant frequency and the other below resonant frequency, are used to illustrate how to select these parameters.

Two basic cases should be differentiated for the design:

- Regions A and A' with limited load range.
- Regions B and B' that operate from no load to full load.

The cases presented here cover Region A' (above resonant frequency) and Region B (below resonant frequency). The choice of n and Z_o for the regions A and B' would be analogous to the choices for Regions A' and B respectively.

4.1.1 Case below resonant frequency

Two regions of operation are possible below resonant frequency, as discussed in Chapters 2 and 3. In Region A, the four switches are turned off naturally and in region B two switches are turned off naturally and the other two are turned on with zero voltage. Since region A is only possible for a limited load range, region B was selected for the design.

When operating in region B below resonant frequency, the switching conditions for both legs of the bridge are different. In one leg the two switches operate with zero voltage turn-on and in the other leg they operate with zero current turn-off. For the switches that are turned on with zero voltage, no external diodes are needed because their corresponding parallel diodes turn off naturally and capacitors in parallel are used as lossless snubbers. In this case, however, because of the low current values in the switches and the high output capacitance of the MOSFETs, external capacitors were not added. For the switches turned off with zero current, two external diodes are required for each MOSFET. One prevents the internal diode from conducting and the other, a fast recovery diode, conducts when current in the tank reverses and the MOSFET has positive voltage in the gate. The two serial diodes do not have to block the source voltage,

therefore, Schottky diodes with low voltage drop and low blocking voltage (20 V) were used. The final circuit is shown in Fig 4.1.

For ideal components the maximum output power transference capability is obtained operating at resonant frequency. However, operation at resonant frequency is not desirable for the following reasons:

- To operate in Region B deep in CCM, a small turns ratio should be selected. This implies high circulating current in the primary.
- By reducing the current in the primary, the operation of the converter will be in DCM, resulting in high peak currents.
- In DCM, the control to output gain is very low and becomes extremely high when in CCM.
- The current through the rectifier, even with the same average value, would have a higher peak.
- The DC characteristics of the resonant converter are significantly affected by the losses of the resonant tank when operating close to resonant frequency [8], making difficult to determine the DC operating mode.

Considering the devices available and aiming to work in CCM for full load, a normalized operating frequency of $\omega_n = 0.8$ was chosen for the prototype. This

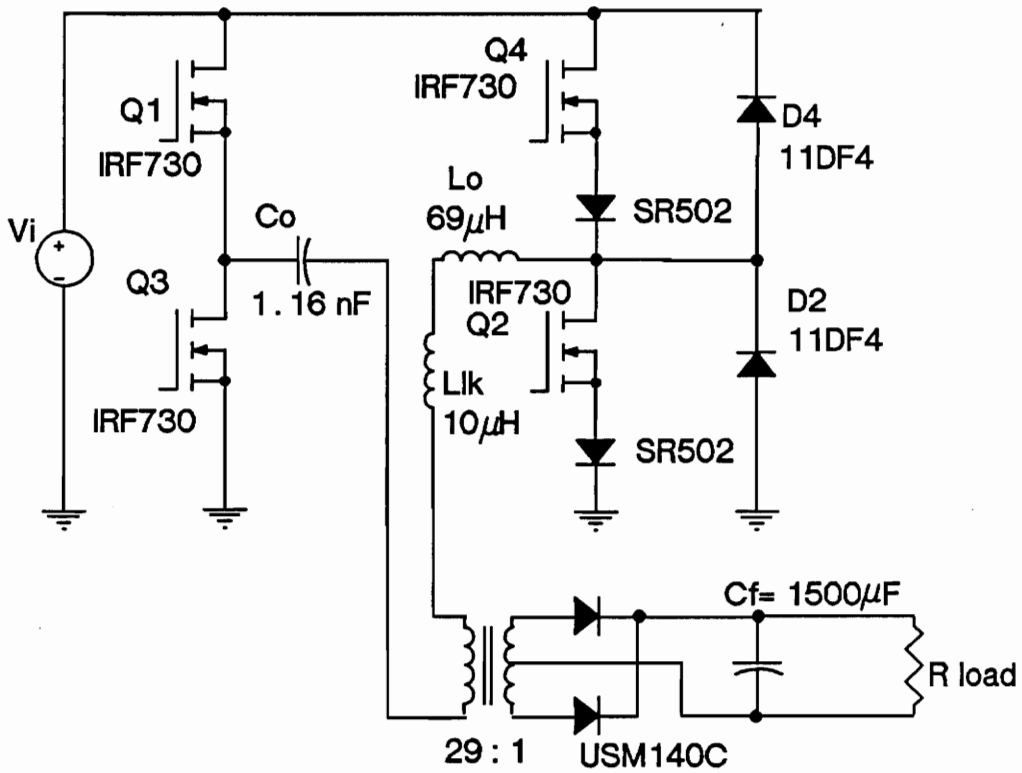


Figure 4.1: Circuit below resonant frequency.

value was considered to provide a good trade-off between conduction losses and attainable output power.

At the selected frequency, $\omega_n = 0.8$, in order to have a range for the control angle between 0° and 150° , a value of $V_{on} = 0.8$ was chosen.

After selection of values for ω_n and $V_{on\max}$, the procedure outlined in the previous section is applied as follows:

- The maximum value of the normalized load current in Region B at $\omega_n = 0.8$ and $V_{on\max} = 0.8$ is $I_{onFL(\max)} = 0.9$

- The maximum and minimum values for the normalized output current and normalized output voltage follow the ratios defined by the equations (4.5) and (4.8) respectively. The minimum normalized values for current and voltage at full load are

$$V_{on}(\min) = 0.55$$

$$I_{onFL}(\min) = 0.6$$

The operating region for this design is depicted in Fig. 4.2. The curve corresponding to full load corresponds to the normalized values of $I_{ON\max}$ for the different input voltages.

The values for the turns ratio of the transformer and the characteristic impedance are calculated as,

$$n = \frac{V_{on\max} 200}{5.6} = 29 \text{ turns} \quad (4.10)$$

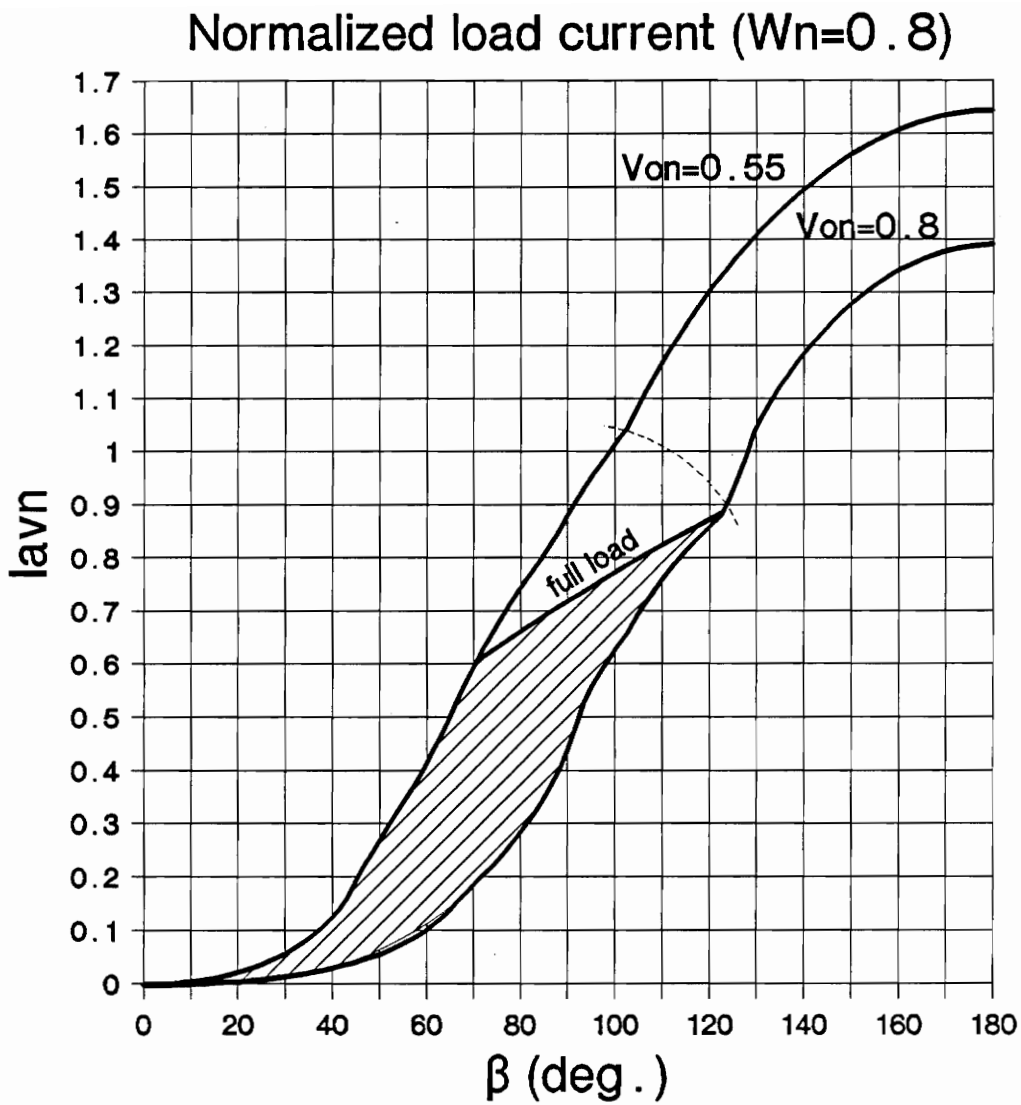


Figure 4.2: Operation region below resonant frequency.

assuming a 0.5 Volt forward drop in the diode and 5.1 Volt output voltage. And

$$Z_o = \frac{I_{onFL_{max}} n 200}{20} = 261 \Omega \quad (4.11)$$

The MOSFETs used are IRF730 which provide a blocking voltage capability of 400 Volts and have a channel resistance of 1 Ω . The external parallel diodes are fast recovery diodes, 11DF4, and the series diodes are Schottky diodes, SR502, (both from International Rectifier).

The values for the resonant tank calculated with the frequency and the characteristic impedance are:

$$C_o = 1.16 \text{ nF}$$

$$L_o = 69 \mu H$$

The transformer leakage inductance was measured at 10 μH , therefore the resonant inductor is,

$$L_o = 69 + 10 = 79 \mu H$$

The resonant frequency and switching frequency have the following values

$$f_o = \frac{1}{2\pi \sqrt{LC}} = 525 \text{ kHz} \quad (4.13)$$

and

$$f_s = f_o \cdot 0.8 = 420 \text{ kHz} \quad (4.14)$$

and the characteristic impedance is

$$Z_o = \sqrt{\frac{L}{C}} = \sqrt{\frac{79 \times 10^{-6}}{1.16 \times 10^{-9}}} = 261 \ \Omega \quad (4.14)$$

The inductor and the transformer were constructed using appropriate cores of P material for the frequency of operation and Litz wire. The inductor is a double 'E' shape core OP43007EC and the transformer is an EC35 with 'E' shape and round central leg (both from Magnetics).

The output filter is a 1500 μ F capacitor implemented with several tantalum capacitors in order to have low ESR. Ten discrete capacitors are used with an ESR at the switching frequency of 70 m Ω each.

4.1.2 Case above resonant frequency

Two regions of operation are possible above resonant frequency, as discussed in Chapters 2 and 3. In this case, region A' was selected, because region B' is very similar to region B below resonant frequency. In region A', the four switches are turned on at zero voltage and no external diodes are required. All diodes in the bridge are turned off naturally when the current reverses. Since the time recovery is not critical, the MOSFETs internal diodes can be used. Lossless snubbers were not used because the output capacitance is large enough for the current levels of operation at the switching frequency. The circuit is presented in Fig 4.3.

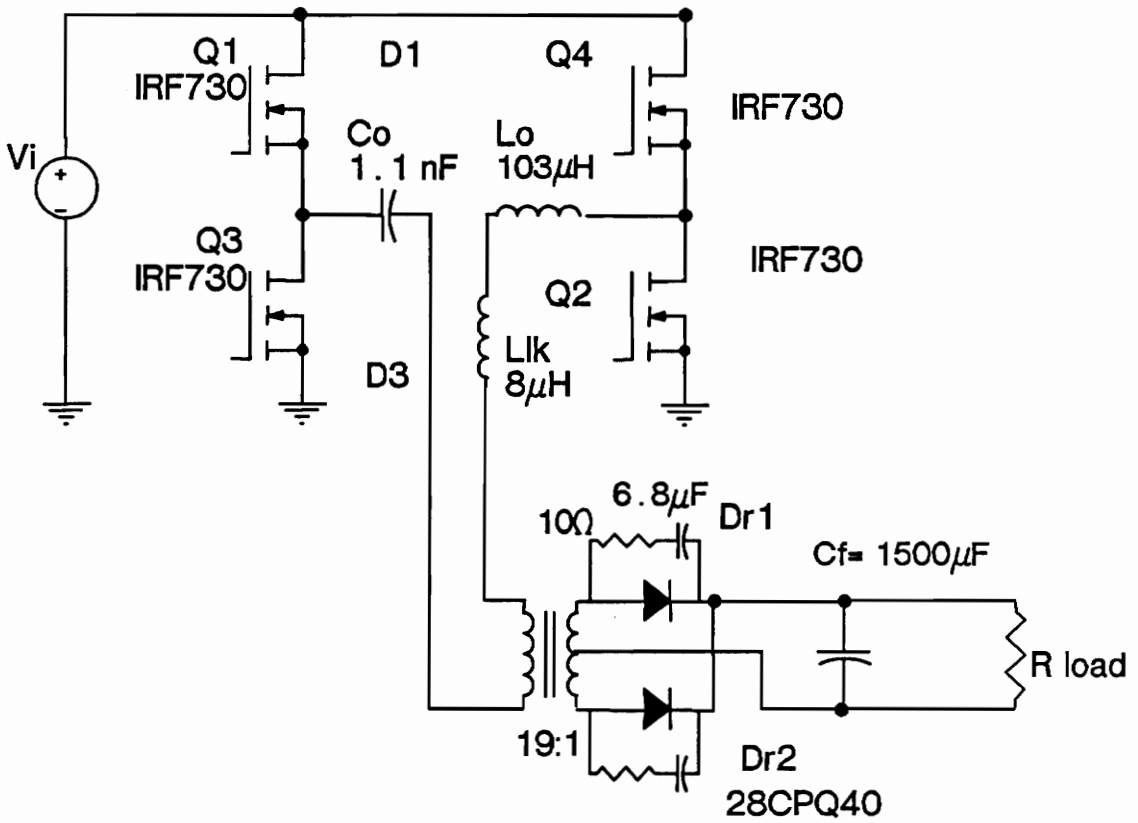


Figure 4.3: Circuit above resonant frequency.

In order to avoid entering into Region B' a minimum value for the normalized output current is one of the design constraints, the switching frequency, it is desirable for this case to be close to the resonant frequency, but to avoid large circulating currents in the primary a trade off choice is made. A feasible value according to the available devices was found to be $\omega_n = 1.2$.

Following the procedure outlined at the beginning of this section, the normalized currents and voltages satisfy eqs (4.5) and (4.8).

Since the maximum β angle attainable with the control logic circuit used is 150 deg. at $\omega_n = 1.2$, the load range is determined as the current range between the boundary with region B' and the values at 150 deg. $V_{on} = 0.5$ was selected as the higher normalized output voltage, because it is the value at which maximum power can be transferred to the load, according to previous studies of series resonant converter [6,9]. The normalized output current for the selected normalized voltage at 150 deg. is $I_{on} = 1.75$, then for high input voltage,

$$V_{on \min} = 0.35$$

and,

$$I_{on \min} = 1.17$$

Since the current limit on the boundary between A' and B' regions is 1.09, operation in mode A' is ensured for high and low line at full load. Figure 4.4 shows the operating region selected and the normalized value of the maximum output load (line labeled full load).

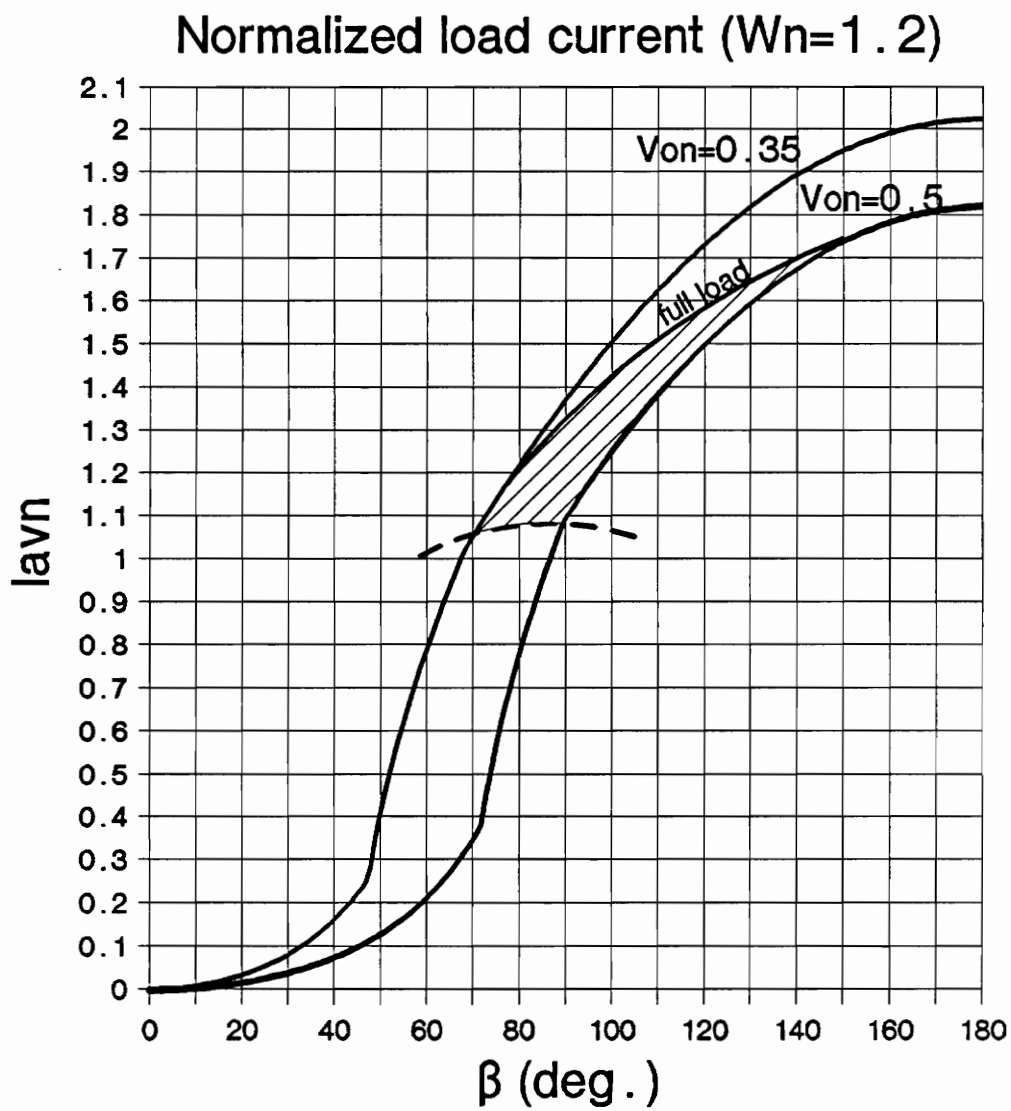


Figure 4.4: Operating region above resonant frequency.

The values of turns ratio and characteristic impedance are calculated using eqs. (4.10) and (4.11), as,

$$n = \frac{V_{on\ max} 200}{5.6} = 18\ turns$$

$$Z_o = \frac{I_{on\ max} n 200}{20} = 306\ \Omega$$

The values used for the resonant tank are $C_o = 1.1\ nF$ and $L_o = 95\ \mu H$. The leakage inductance for the transformer is $8\ \mu H$, therefore, $L_o = 105\ \mu H$, and finally

$$\frac{1}{f_o} = 2\pi \sqrt{LC}$$

$$f_s = f_o 1.2 = 567\ KHz$$

and

$$Z_o = \sqrt{\frac{L}{C}} = 306\ \Omega$$

4.1.3 Control logic and gate driver.

In order to operate the converter at a fixed frequency, the MOSFETs should be activated sequentially. This is done by generating two pairs of complementary square waveforms delayed a variable amount of time. In Fig. 4.5, V_{g1} and V_{g3} (

or V_{g2} and V_{g4}) are complementary and the control parameter is the delay between V_{g1} and V_{g2} (or V_{g3} and V_{g4}).

Ideally, the gate signals can have 50 percent duty ratio, but to avoid a short of the bridge legs, a small delay after the removal of the gate signal is introduced for each device before the turn on of its totem-pole device. In this case, the delay used was 50 nsec (Fig 4.5).

The circuit to implement this is shown in Fig 4.6.

The output of the logic circuit has to be applied to the gates of the MOSFETs. Because the two sources corresponding to Q1 and Q4 are not grounded, isolation is required. A transformer with 1:1 turns ratio and a integrated circuit driver, UC3705, were used. Since the transformer voltage should have an average value of zero, a DC blocking capacitor is placed in series with the primary. The square wave is not exactly symmetrical (positive and negative parts) due to the dead time. The circuit is presented in Fig 4.7.

Since the control of the circuit is accomplished by varying the time when source voltage is applied to the tank, a PWM controller is used. UC3825 was selected for its capability of operation at high frequency. The loop is closed with a simple compensator, since the feedback was not designed to optimize the response and no small signal model was available.

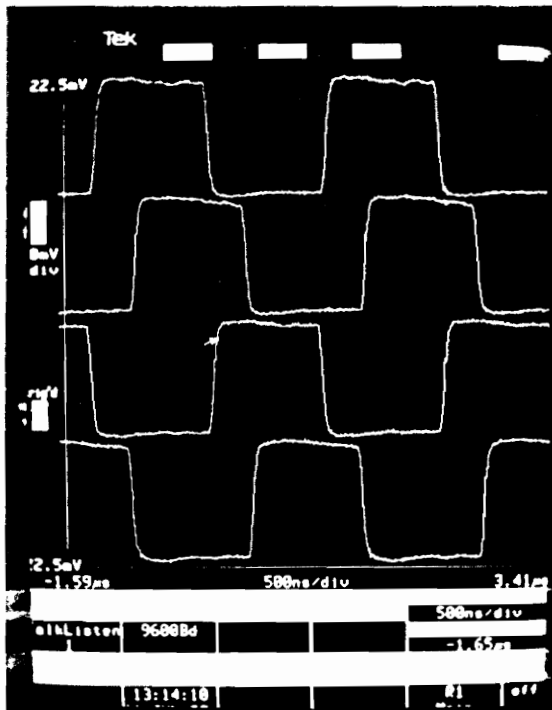


Figure 4.5: Gate voltages.

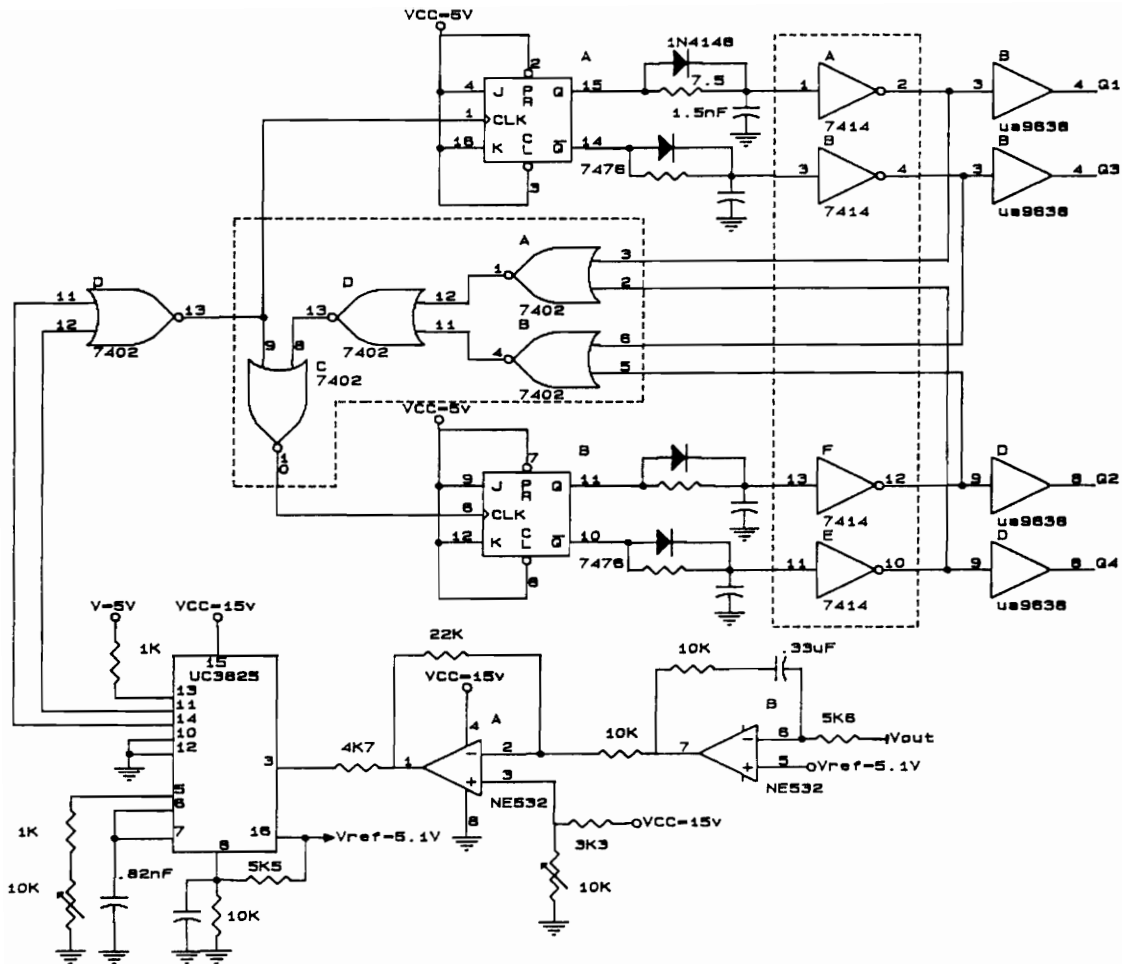


Figure 4.6: Control logic circuit.

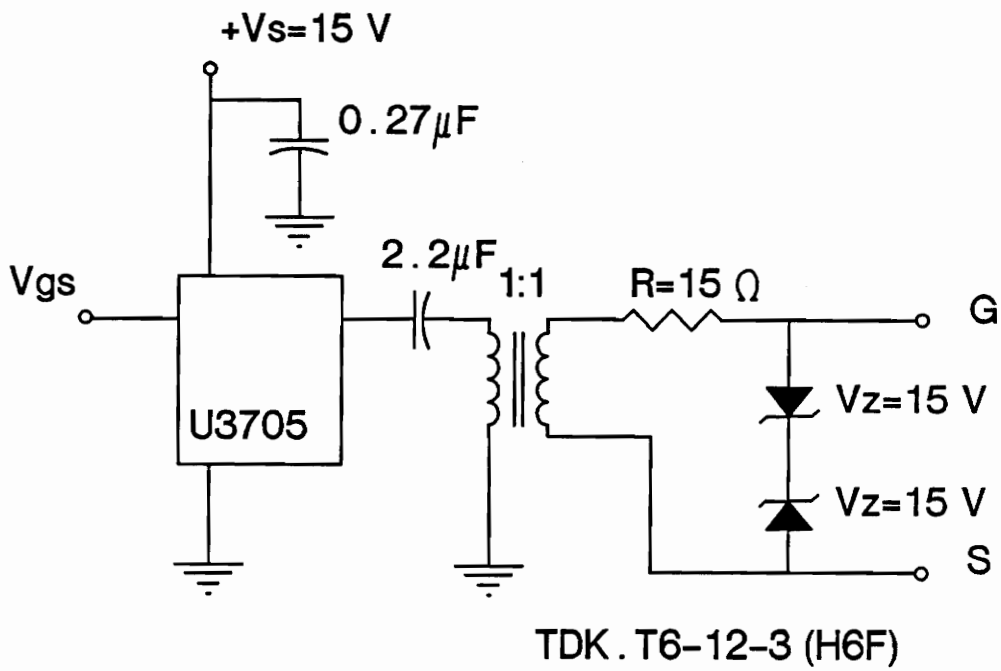


Figure 4.7: Gate driver circuit.

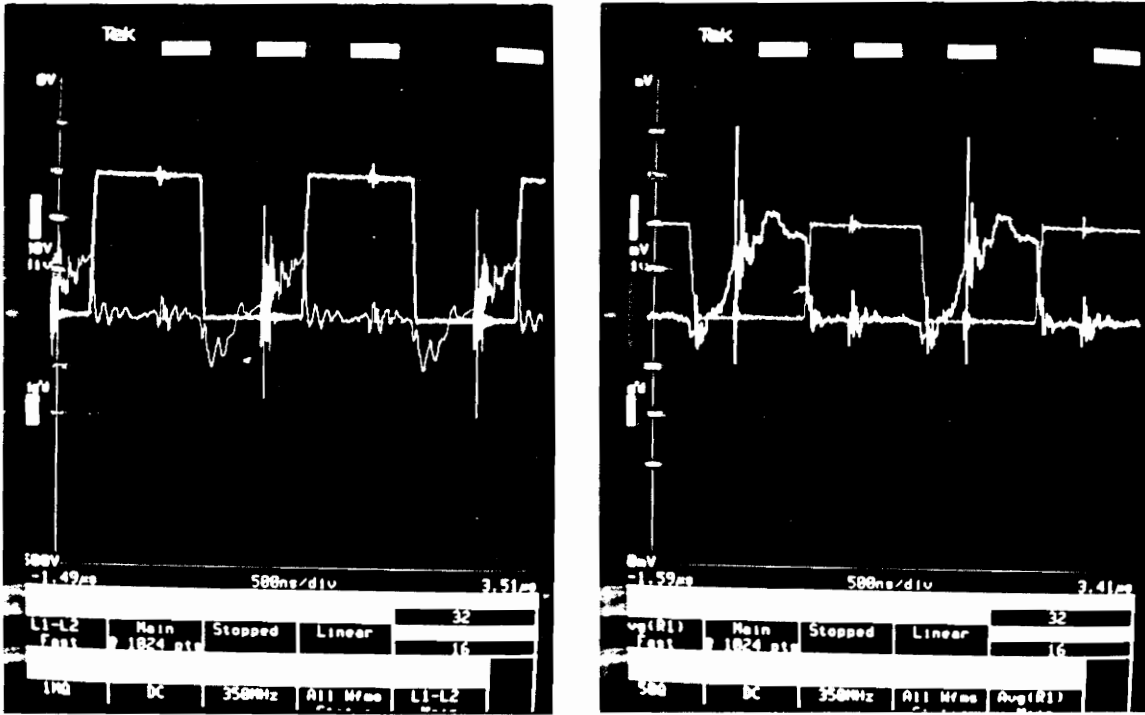
4.2 Performance evaluation

4.2.1 Prototype operating below resonant frequency

The circuit described in 4.1.1 operated for the full load range in the desired region (Region B).

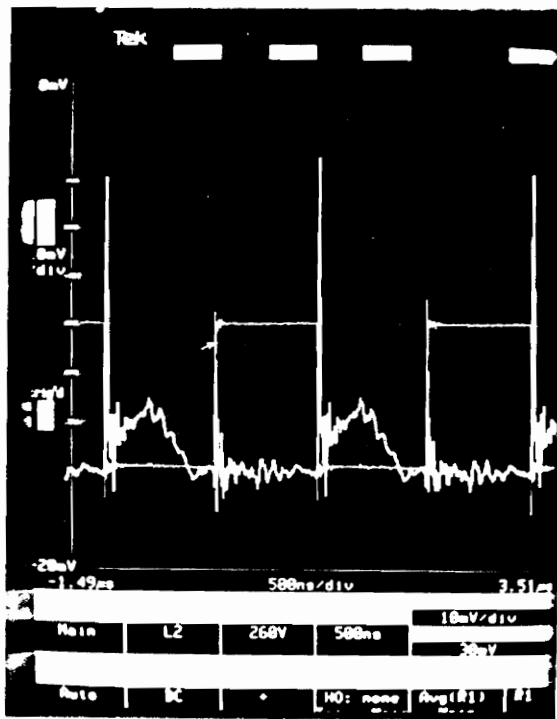
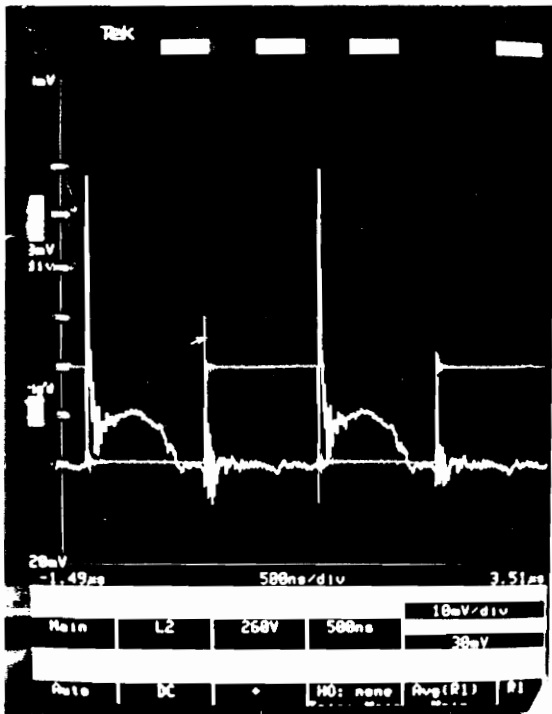
The overall performance was satisfactory, and the zero voltage switched transistors do not show significant voltage overshoot, verifying that the output capacitance ($C_{DS} = 100pF$, $V_{DS} = 25V$) acts sufficiently as snubber during turn off. Figure 4.8 shows the voltage and current waveforms for the devices. The two zero current turned off devices, due to the reverse recovery of the diodes, show more switching loss [5,15,25]. When Q4 (or Q2) is turned on, the source voltage is applied in reverse to the diode D2 (or D4). Then D2 (or D4) starts its recovery process in order to block the reverse voltage. The result of this is that Q4 (or Q2) is turned on when an inrush current to block the diode is flowing through it (Fig. 4.9). The turn on loss for these two devices is significant at the operating frequency and this affects the overall efficiency.

To evaluate the sharing of switching loss among the two pairs of switches, a simulation of the circuit using an accurate model for the MOSFETs [17,18] was developed (Appendix B). The results (Figs 4.10,4.11) show that the turn on losses of the zero current turned off devices account for most of the switching loss. The



(Scale vert.: 100 V/div. 0.5 A/div.)
hor.: 500 nsec/div.)

Figure 4.8: Voltage and current through the switch (0 voltage turn on)



(Scale Vert: 100 V/div . 1 A/div .)
hor .: 500 nsec/div .)

Figure 4.9: Voltage and current through the switch (0 current turn off)

results of the simulation are: Loss for each of the the ZCS devices is 5.2 Watts and for each of the ZVS devices the loss is less than 0.2 Watts.

Another important source of loss is the output rectifier. The forward drop of the diodes was kept low using a high current Schottky rectifier. But, as can be seen in Table 1, almost half of the loss in the converter are due to rectification.

The loss for high input line and low input line is 31 and 43 watts, respectively. This loss is distributed as follows:

For high input line (300 Volts):

- Transformer and resonant tank

$$[(R_t + R_L + R_c) I_{RMS}^2] = 4.0 \text{ Watts}$$

where R_t , R_L , R_c are the equivalent series resistances of every component.

- External diodes

$$2 (V_F I_{RMS}) \frac{t_{DC}}{T_s} = 0.4 \text{ Watts}$$

where V_F is the forward drop of the diodes and t_c and T_s are the conduction times for the diodes and the switching period respectively.

- Rectifying losses

$$V_{FR} I_{oRMS} = 14.3 \text{ Watts}$$

CLAMPED MODE SERIES RES. CONV.

LÖSSES IN Q1 (OR Q3)

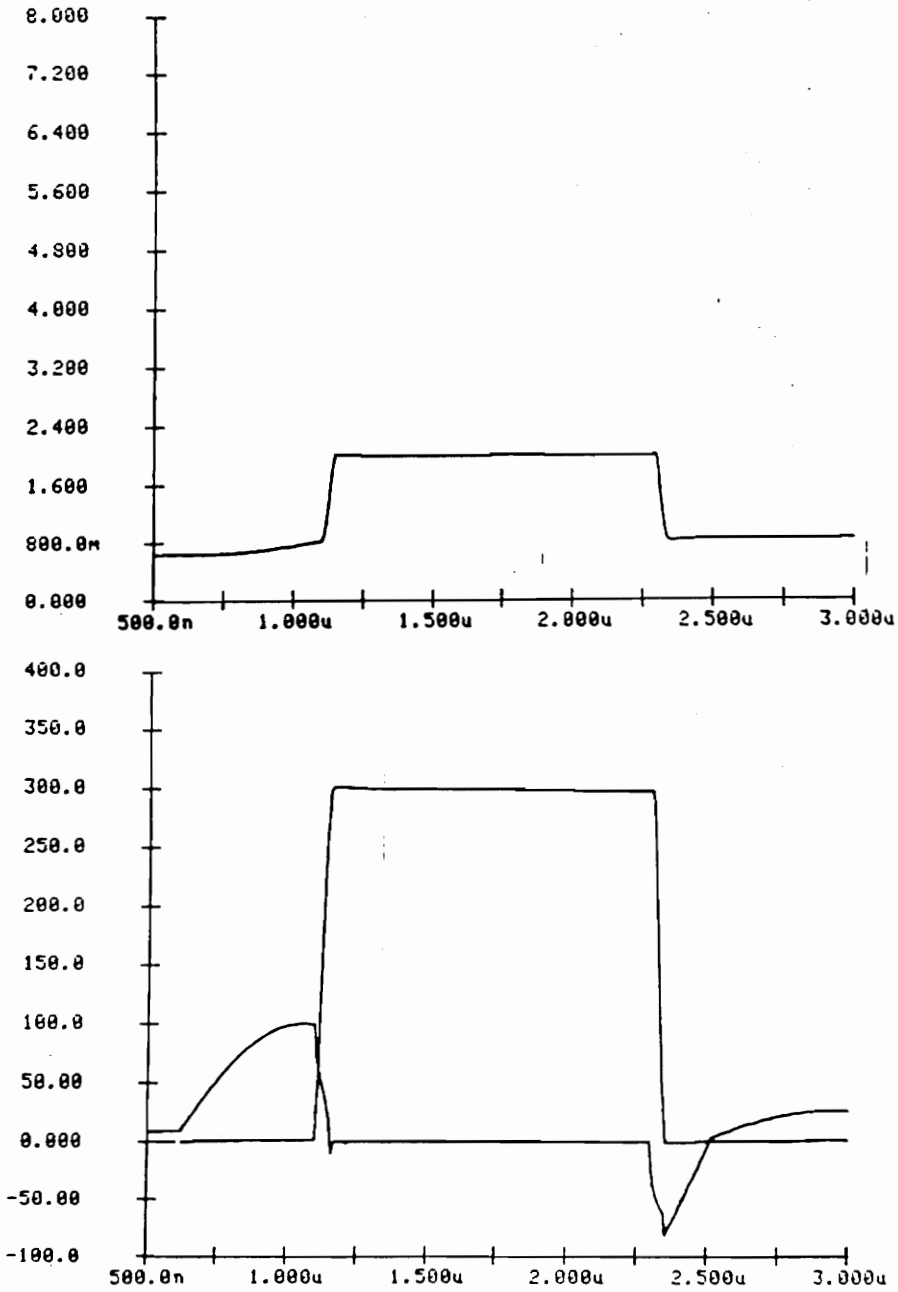


Figure 4.10: Simulated I and V through the switch (0 voltage turn on), and loss.

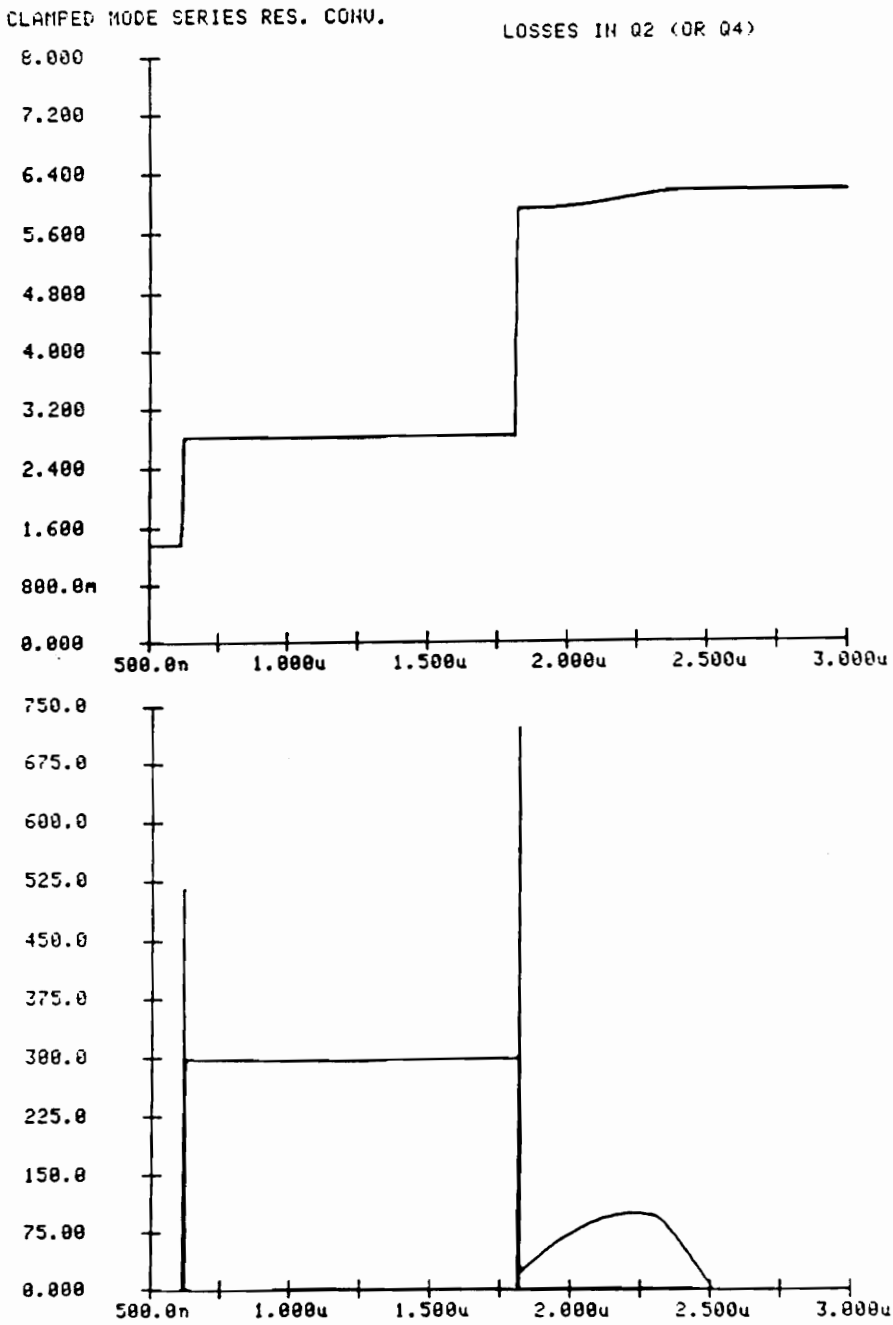


Figure 4.11: Simulated I and V through the switch (0 current turn off), and loss.

- MOSFETs losses
- Conduction losses

$$2 R_{on} I_{LRMS}^2 \frac{t_{Q13}}{T_s} + 2 R_{on} I_{LRMS}^2 \frac{t_{Q24}}{T_s} = 2.2 \text{ Watts}$$

- Switching losses = 16.1 Watts make up the difference. This agrees reasonably well with the simulation results (Figs 4.10,4.11) which show 12 watts of switching loss (5.5 and 0.5 Watts, for zero current and zero voltage respectively).

For low input line :

- Transformer and tank losses = 4. Watts.
- External diodes = 0.2 Watts.
- Rectifier losses = 14.3 Watts.
- MOSFETs loss:
 - Conduction losses = 2.2 Watts.
 - Switching losses = 10.3 Watts.

The fact that switching losses are significant for the overall efficiency makes the high line efficiency lower than the low line one. Although the current through

the tank is the same in both cases, the higher voltage increases the switching losses proportionally (Fig 4.12).

4.2.2 Case above resonant frequency

The circuit was built with the values calculated in Section 4.1.2. As expected the zero voltage turn-on condition for the switches eliminates the time recovery of the diodes, due to natural commutation.

The operating frequency is higher than that of the case below resonant frequency. The overall efficiency is better than the efficiency when the zero voltage condition is not present, but a comparison at the same switching frequency would demonstrate an even better performance for the case above resonance.

The load range was found to be less than expected, according to the ideal model. The tank and switching loss have a damping effect on the resonant tank and the maximum current possible for the low input voltage is reduced. For low line, the maximum load current maintaining regulation is 18 A.

Another effect significant at this frequency is the resonance of the rectifier diodes junction capacitance. Due to this effect, the load range was decreased. This resonance happens in a very low impedance path (secondary of the transformer) and changes the current reflected to the primary significantly, because a circulating current of high frequency is added to the current in the secondary. To attenuate this oscillation, snubber circuits were added to each one of the rectifier diodes, as is common practice, when operating with large current

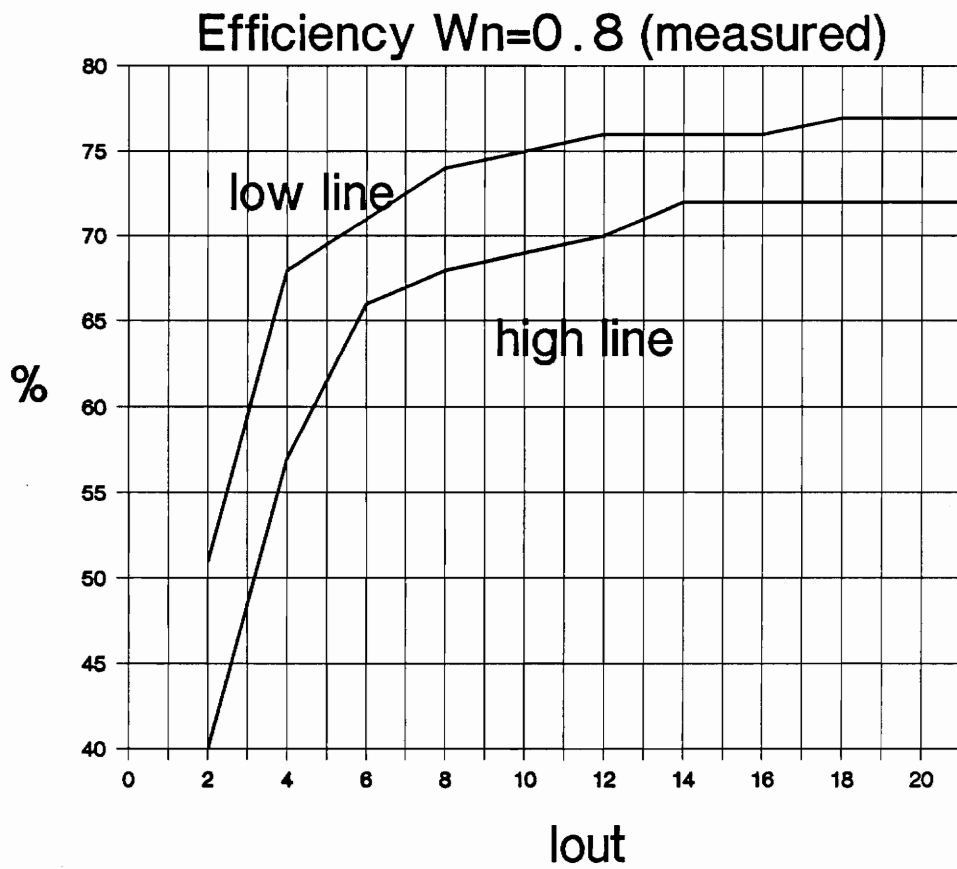


Figure 4.12: Efficiency measurements below resonant frequency

Schottky rectifiers [26]. The penalty on efficiency is negligible, but the overall performance of the converter was more closely correlated with the ideal analysis.

The efficiency of the circuit was measured between full load and the minimum load value that could be regulated. The operation of the circuit was in region A' for the high load but entered region B' and even reached DCM for the lighter loads. Operation in region B' has lower efficiency because the reverse recovery of the diodes increases the switching loss. Operation in region B' was possible because no external capacitors were added and the values of currents when in region B' are below half of the full load for the circuit. The dissipation on the switches was, therefore, below the maximum allowed for the switches.

The measured efficiency for the circuit is matched with calculations using the parameters of the components to provide a better understanding of the different sources of loss and their relative magnitudes.

For low input line (200 Volts), the maximum current delivered at 5.1 Volts is 18 A, and the total loss measured is 23.2 Watts. This loss is distributed as follows:

- Transformer and resonant tank loss

$$R_{eq} I_{Lrms}^2 = 3.0 \text{ Watts}$$

- Output rectifier

$$V_F I_{orms} = 12.33 \text{ Watts}$$

- Conduction losses

$$R_{on} I_{Lrms}^2 \frac{t_{cd}}{T_s} + 2R_{on} I_{Lrms}^2 + I_{Lrms} V_F \frac{t_{cd}}{T_s} = 3.5 \text{ Watts}$$

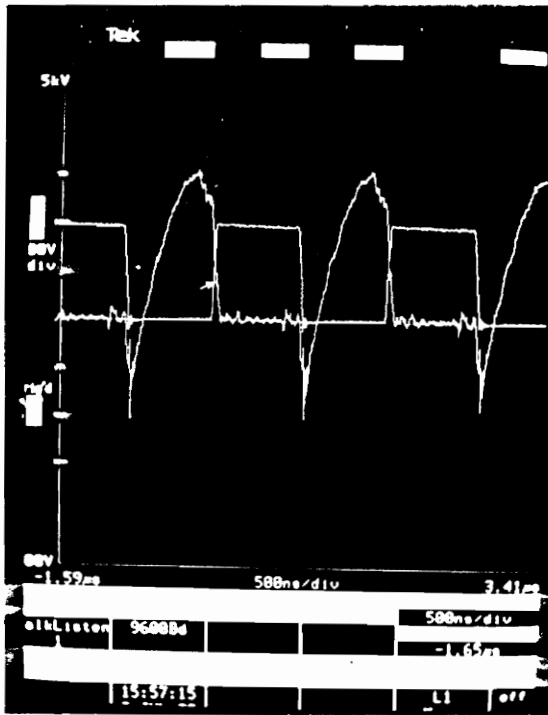
- Switching losses (and others, by difference) = 3.5 Watts

For high input line delivering the same output current, the total loss is 34.2 Watts. The distribution is:

- Transformer and resonant tank loss = 3.0 Watts
- Output rectifier = 12.33 Watts
- Conduction losses = 3.5 Watts
- Rectifier snubber = 1.5
- Switching loss = 13.5 Watts.

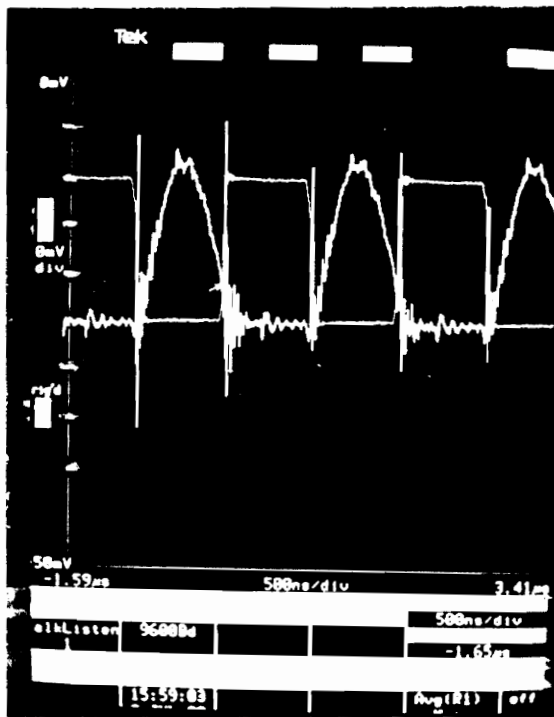
The switching losses are higher than expected. This is because the circuit is not operating with all switches with zero voltage turn on for 18 A output current. Figures 4.13 and 4.14 show the current and voltage in one of the MOSFETs for low and high input line respectively. By increasing the output current for high line, the switching losses are reduced.

In Figure 4.15, current and voltage for any of the four MOSFETs is shown when 25 A is delivered to the load. In the last case, the total power loss is 40.26 Watts and it is distributed as follows:



(Scale vert.: 100 V/div . 0.5 A/div .)
 hor.: 500 nsec/div .)

Figure 4.13: I and V on the switches (low line and $I_{out} = 18 \text{ A}$)



(Scale vert.: 100 V/div. 0.5 A/div.)
 hor.: 500 nsec/div.)

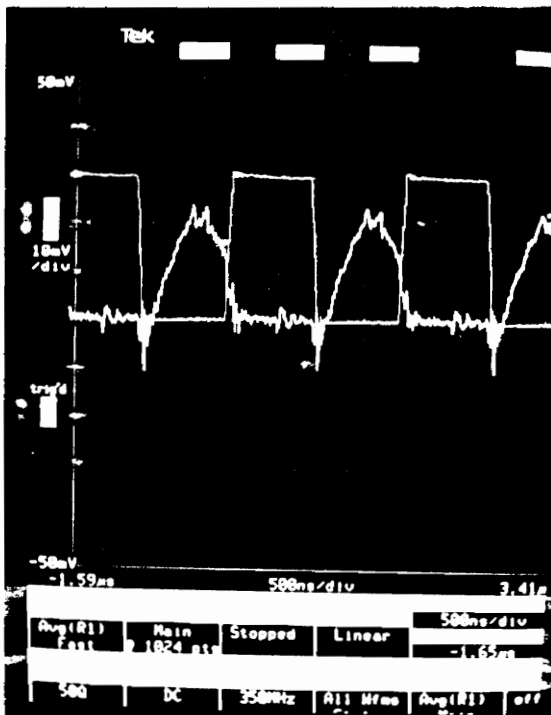
Figure 4.14: I and V on the switches (high line and $I_{out} = 18$ A)

- Transformer and resonant tank = 6.75 Watts
- Conduction loss = 5.1 Watts
- Output rectifier loss = 16.7 Watts
- Rectifier snubbers = 2. Watts
- Switching loss = 9.7 Watts

The reduced value of switching loss verifies the undesirable effect of the loss of zero voltage switching. The 12.5 Watts of switching loss are in good agreement with the proportion of voltages and currents between this case and the low line case.

The problems encountered suggest that an estimate of the losses due to parasitic elements in the tank and turn off is necessary before the final design. This enables use of the model which includes loss to predict the exact load range for the input voltage range required.

The fact that the operation over full load range was possible is because although the efficiency is worst for low loads (in region B'), the total loss is not increased. Figure 4.16 shows the efficiency for low and high input voltage as a function of the load current. Table I compares the results for the case below resonance with the case above resonance.



(Scale Vert: 100 V/div . 1 A/div .)

hor .: 500 nsec/div .)

Figure 4.15: I and V on the switches (high line and $I_{out} = 25\text{ A}$)

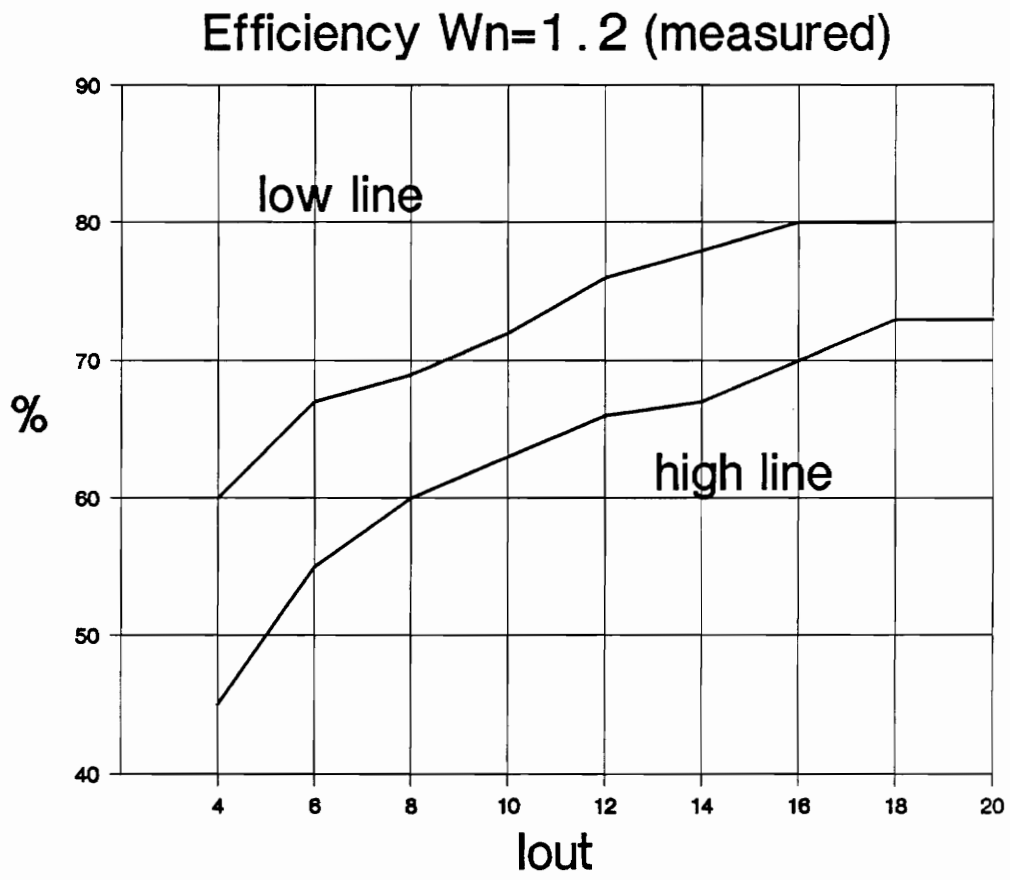


Figure 4.16: Efficiency measurements above resonant frequency

Table 1. Efficiency comparison.

norm. freq.	0.8	0.8	1.2	1.2	1.2	ω_s/ω_o
input voltage	200	300	200	300	300	volts
output current	21.5	21.5	18	18	25	amps
induct. & tr.	4.	4.	3.	3.5	6.75	watts
rectifier	14.3	14.3	12.	12.	16.7	watts
conduction	2.5	2.1	3.5	3.7	5.1	watts
commut.	10.3	16.1	3.5	13.5	9.7	watts
snubber	--	--	1.5	1.5	2.	watts
efficiency	78	72	80	77	77	%

Chapter 5

Verification of the characteristics

The analysis described in Chapters 1 and 2 provides design characteristics for the clamped mode series resonant converter. These characteristics are verified experimentally and by using IG-SPICE simulation.

The efficiencies obtained for the prototypes range between 75 and 80 percent for most of the operating area. Because the prototypes were built to check feasibility of specific application, some deviation is expected with the theoretical results, i.e the output voltage is as low as 5 volts and the isolation transformer has a turns ratio of 18 and 29 above and below resonant frequency, respectively. Nevertheless the agreement with the characteristics shows that all the assumptions for the model are justified, and the accuracy of the characteristics including losses is verified.

5.1 DC characteristics

The experimental points obtained for the characteristics are plotted with the theoretical characteristics (Figs. 5.1 and 5.2). These curves provide current values below the ideal ones as expected. The predicted curves and the experimental results give a reasonable match with curves calculated with damping factors 0.02 and 0.03 for the cases above and below resonant frequency, respectively.

The damping factor associated with the characteristics provides a way to calculate the losses in the converter. Checking the results:

- Above resonant frequency (full load 18 A):

damping factor, $\xi = 0.02$

$$\text{equivalent resistor, } R_{eq} = \frac{Z_o}{1/2\xi} = 12.24\Omega$$

$$\text{tank loss, } I_{L_{rms}}^2 \times R_{eq} = 13.55 \text{ Watts}$$

Adding these losses to the rectifier and snubbers losses results a total loss of 26.05 Watts. The efficiency for this loss is 78 %. This value is in agreement with the expected value between 77 and 80.

- Below resonant frequency (full load 21.5 A)

damping factor $\xi = 0.03$

$$\text{equivalent resistor, } R_{eq} = \frac{Z_o}{1/2\xi} = 15.35 \Omega$$

$$\text{tank loss, } I_{L_{rms}}^2 R_{eq} = 9.1 \text{ Watts}$$

Adding this to the rectifier loss equals a total loss of 23.4 Watts. The value corresponds to an efficiency of 81 %. The actual efficiency is lower due to the nature of the switching loss. Part of the switching loss is due to the current flow in the reverse recovery of the diodes in the bridge. This current does not circulate through the tank so it is modeled by the included series resistor.

Certain differences are observed for low loads below resonant frequency, because the converter is operating in discontinuous conduction at these points and the rectifier diodes capacitance resonates with the leakage inductance of the transformer. As a result some current circulates through the tank and the transformer, causing a larger β angle to be required for the same average current.

5.2 Simulation results

The circuit was simulated using IG-SPICE as is shown in Fig 5.3. The model includes a series resistor with the tank according to the calculations in the former section. A perfect quasi-square wave is applied to the resonant tank and the load is a voltage source of value the output voltage times the turns ratio of the transformer.

Figs. 5.4 to 5.7 show the simulation results and the actual waveforms obtained for the converter. The simulation results agree with the actual waveforms.

When the circuit operates below resonant frequency the current waveform carries noise (Figs. 5.4 and 5.5), because when the two force commutated diodes

Normalized av. current, $\omega_n=0.8$, $\xi=0.03$

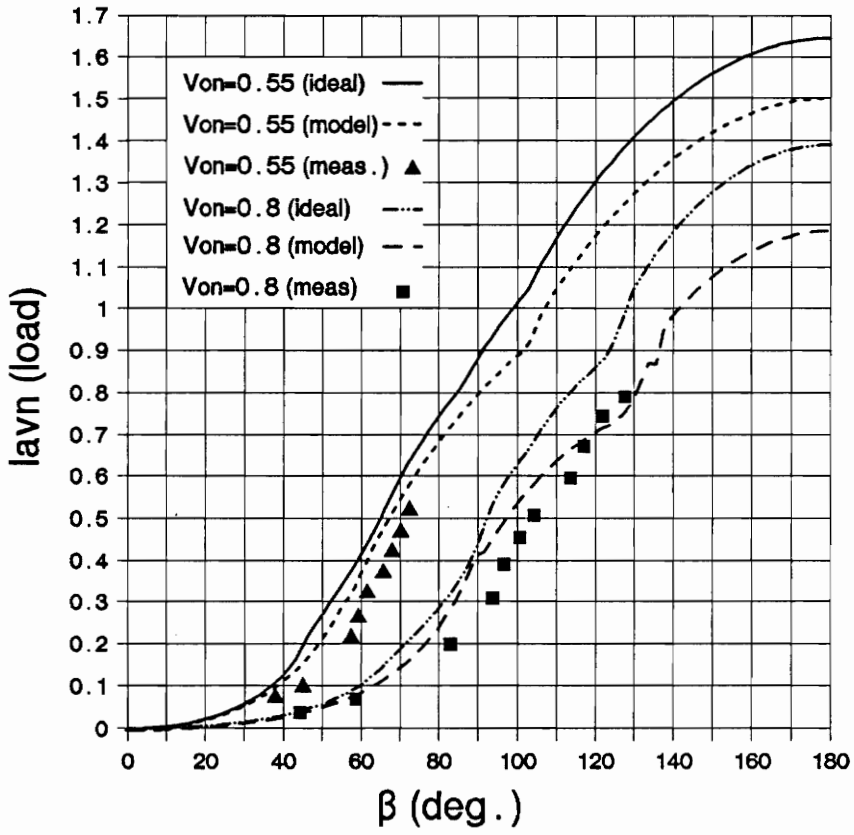


Figure 5.1: DC characteristics and experimental results (below resonant frequency)

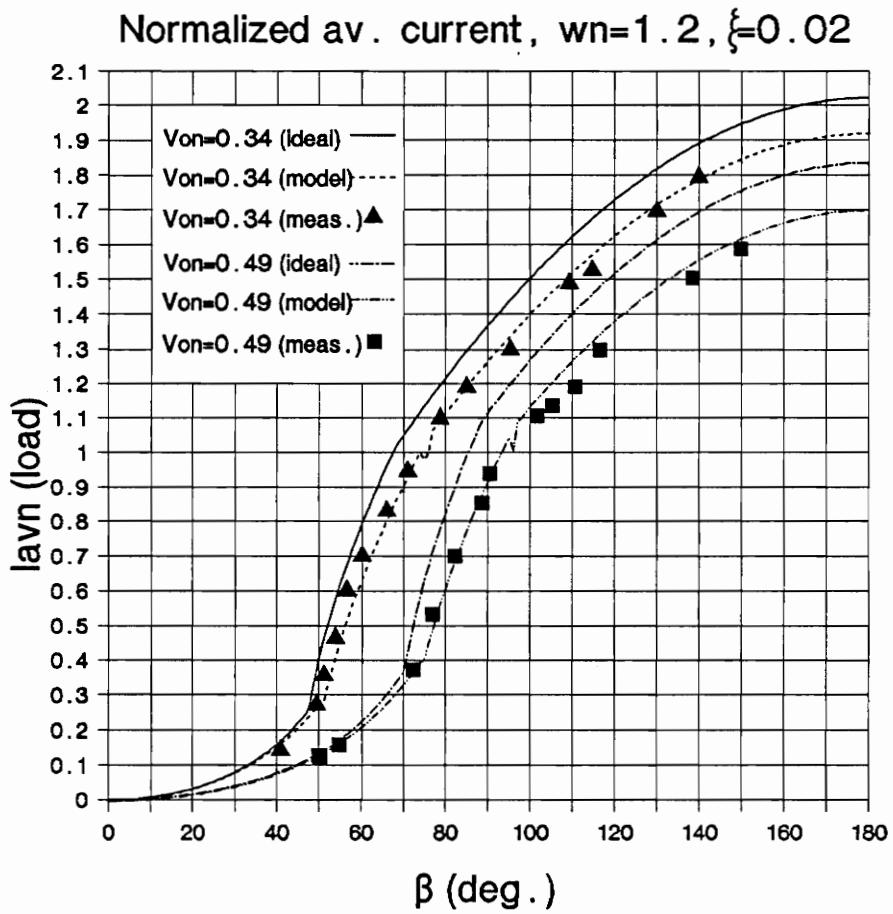


Figure 5.2: DC characteristics and experimental results (above resonant frequency)

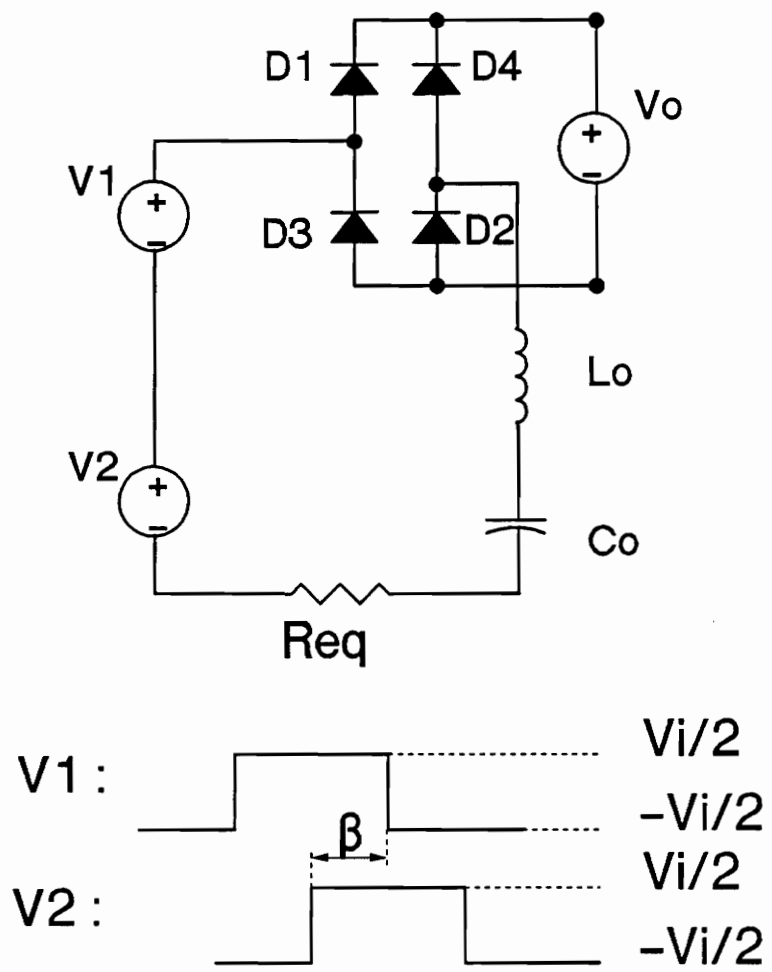
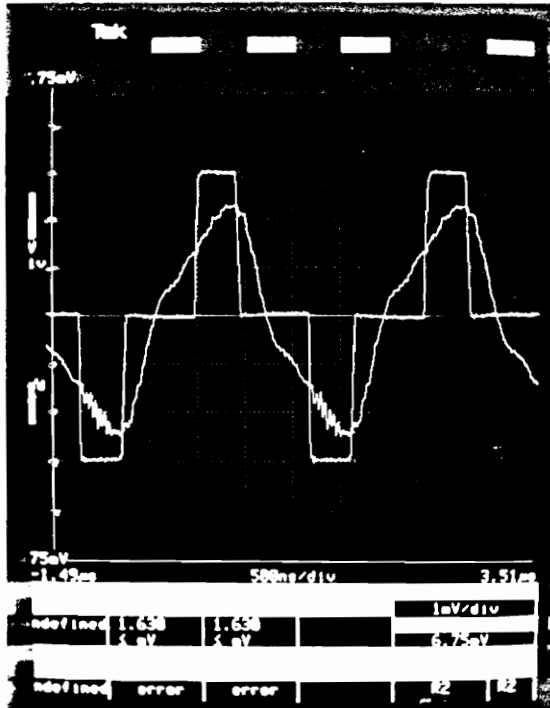
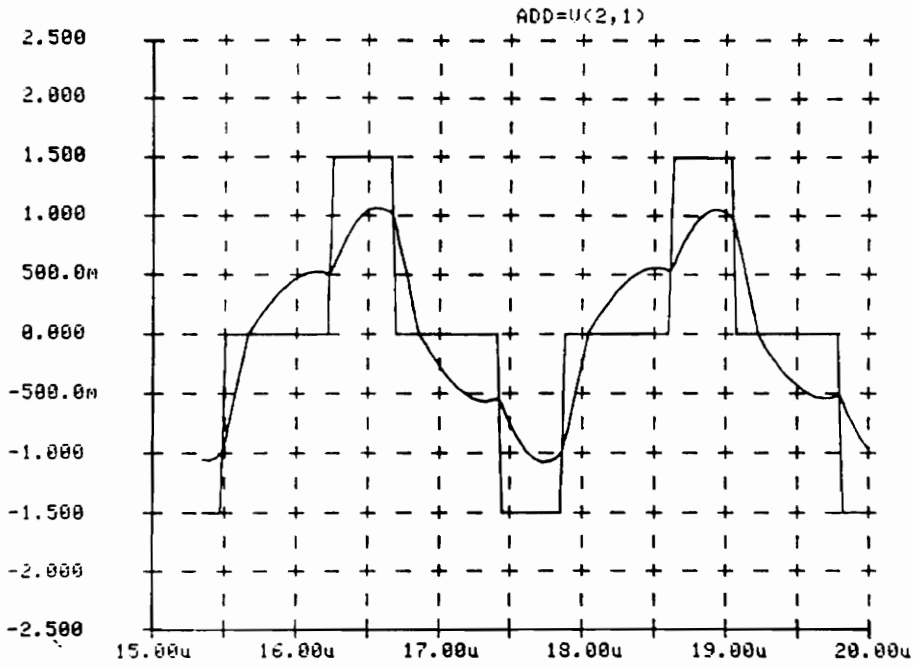


Figure 5.3: Circuit model used for IGSPICE simulation.

go through the reverse recovery transient, a large current goes through the corresponding leg of the bridge. The operating mode and shape of the waveforms, however, is as expected.

When the circuit operates above resonant frequency (Figs. 5.6 and 5.7), all diodes are naturally commutated so the waveforms are clean and closer to the ideal ones. Below resonant frequency, however, an oscillation is superimposed to the current waveform that is caused by the reflected voltage. The output power and low output voltage require the use of Schottky diodes for the output rectifier. These diodes have a relatively large parasitic capacitance which resonates with the leakage inductance of the transformer. The resulting reflected voltage is not a perfect square wave because it contains a high-frequency sinusoidal waveform. This oscillation affects the current in the primary and it is responsible for small differences in the peak values.

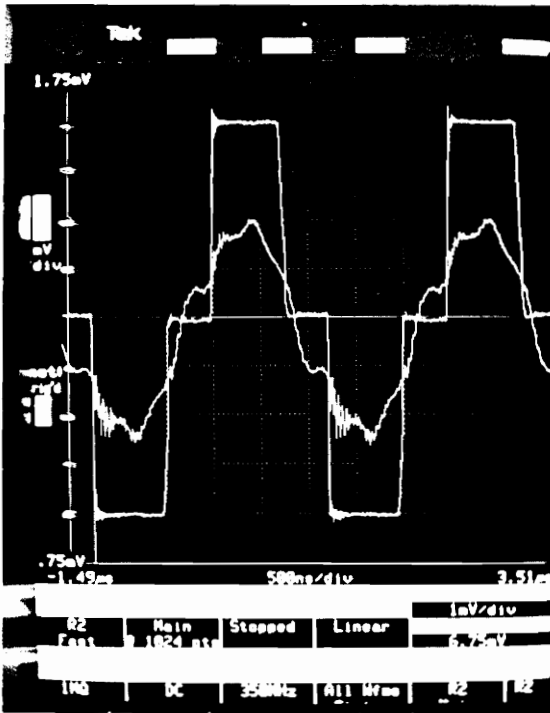
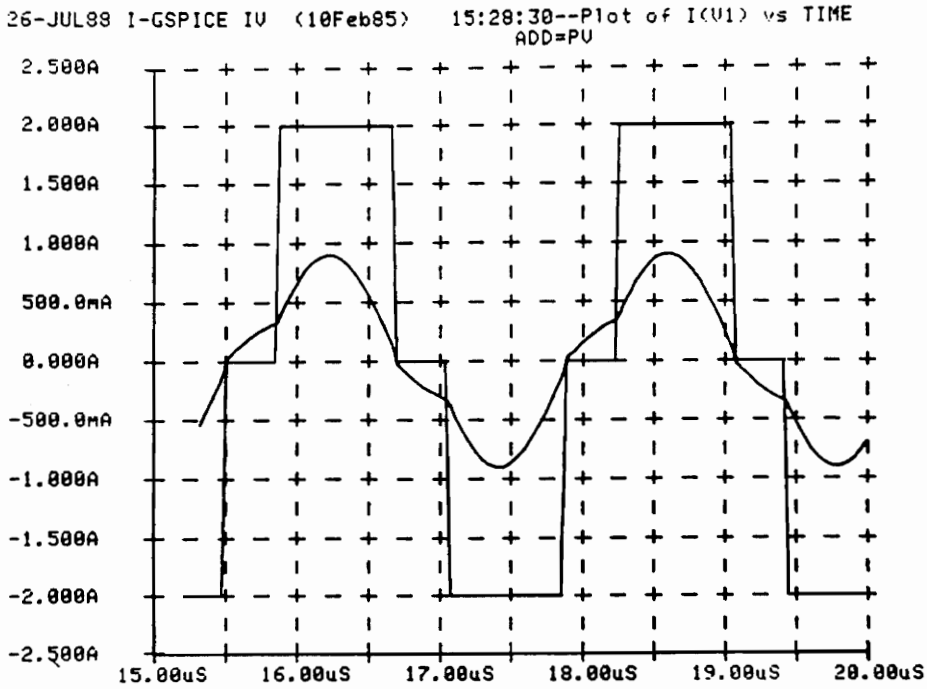
26JUL88 SUPERPLOT (01Jun86) 15:18:00--Plot of I(U1) vs TIME



(Scale vert.: 100 V/div. 0.5 A/div.)

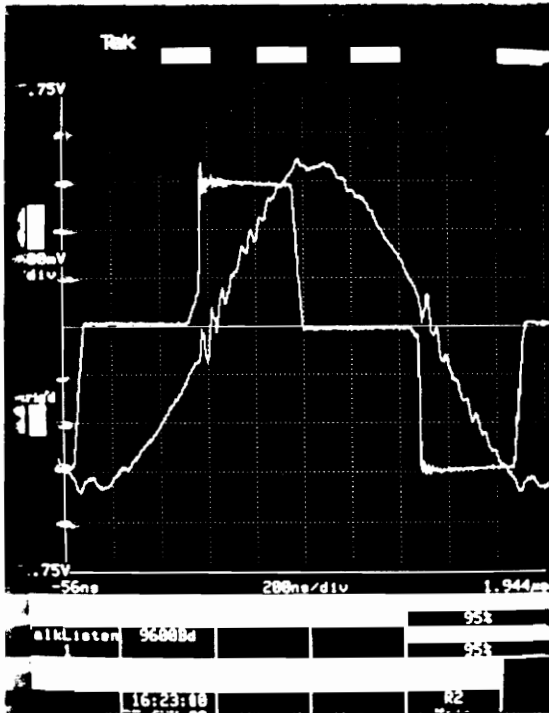
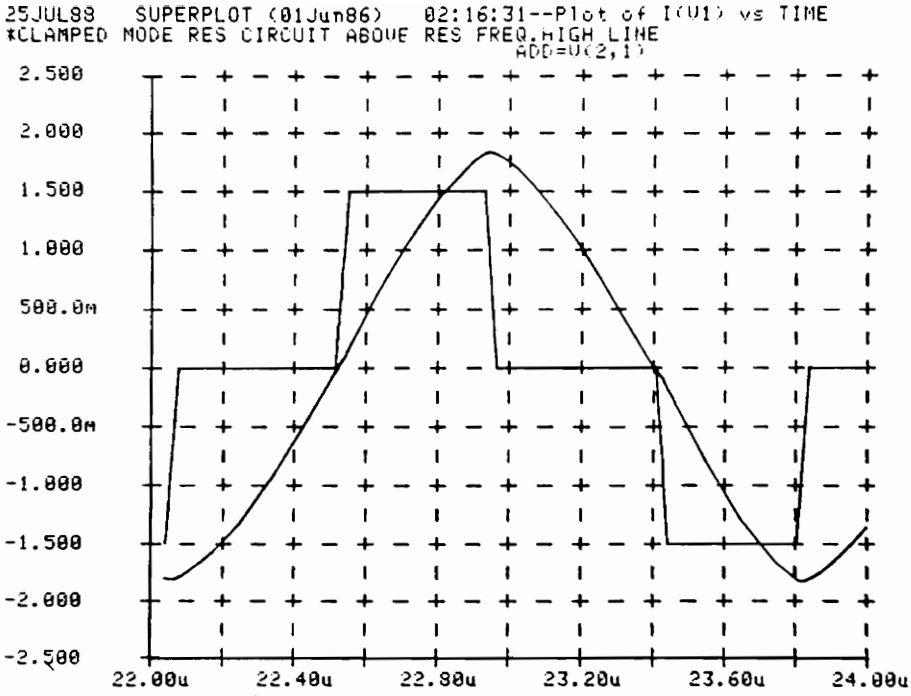
hor.: 500 nsec/div.)

Figure 5.4: Waveforms and IGSPICE simulation, for full load and high line (below resonant frequency).



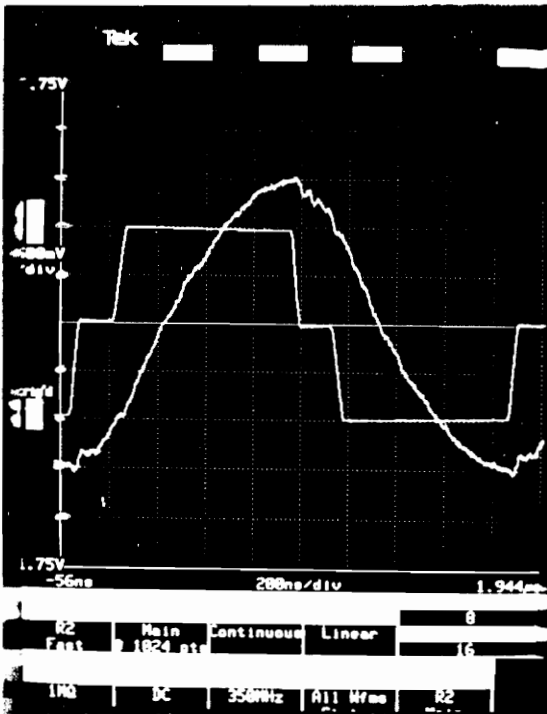
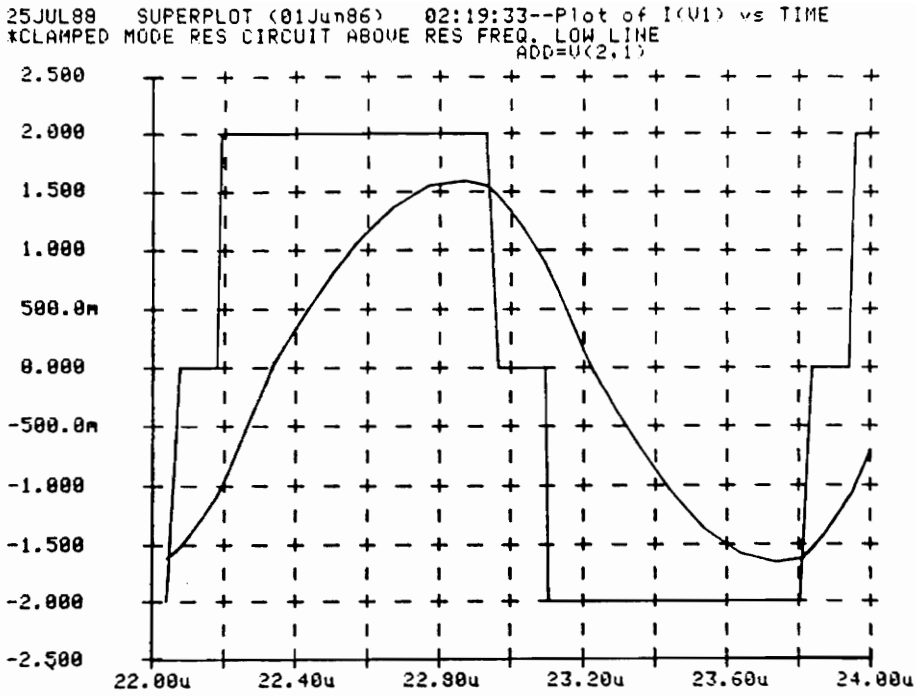
(Scale vert.: 100 V/div. 0.5 A/div.)
hor.: 500 nsec/div.)

Figure 5.5: Waveforms and IGSPICE simulation, for full load and low line (below resonant frequency).



(Scale vert.: 100 V/div. 0.5 A/div.)
hor.: 500 nsec/div.)

Figure 5.6: Waveforms and IGSPICE simulation,for full load and high line (above resonant frequency).



(Scale vert.: 100 V/div. 0.5 A/div.)
hor.: 500 nsec/div.)

Figure 5.7: Waveforms and IGSPICE simulation, for full load and low line (above resonant frequency).

Chapter 6

Conclusions and summary

The feasibility of the clamped-mode series resonant converter (SCR) operating at a fixed frequency was verified experimentally for off line applications.

Operating below resonant frequency, the zero current turn-off operation is not attainable for the whole load range. Consequently, two regions are defined, one with all switches operating with zero current turn-off (region A) and the other where two switches operate with zero current turn-off and two with zero voltage turn-on (region B). In region B, regulation to no load is possible.

Operating above resonant frequency, the zero voltage turn on for all switches is not attainable from no load to full load . Similar to the case below resonance, two regions are defined, one with all switches operating with zero voltage turn on (region A') and the other where two switches operate with zero voltage turn on and the other two switches are operated with zero current turn off (region B').

Design guidelines are described for cases above and below resonant frequency. One prototype was designed and build to operate in region B below resonant frequency and the other prototype to operate in region A' (above resonant frequency).

The switching losses are a major factor considered in performance comparisons between both prototypes. The zero voltage turn on operation for all switches (region A') was proven to be more efficient than when two switches turn on with zero voltage, and the other two turn off with zero current (regions B and B'). The load range, however, in region A' is limited.

The operation with zero current turn off requires the use of external fast recovery diodes and external series blocking diodes to prevent the conduction of the MOSFET's internal diode. Even with this improvement the switching losses are considerably larger than that of the zero voltage turn on case (Region A').

The characteristics generated previously using ideal components were not adequate to assist the design of a practical converter. To provide useful design tools, the converter operation was analyzed including losses in the power circuit. Design guidelines were established using DC characteristics with loss and the design results agree with breadboard performance.

At this point, the clamped mode series resonant converter operation at a fixed frequency has been proved feasible for off-line applications. A comparison of the clamped mode SRC with the parallel resonant converter (PRC) counterpart will be of great interest for future research. Furthermore a converter which combines

both parallel and series resonant converters has been reported recently to obtain improved properties compared to either PRC or SRC.

Appendix A

State plane analysis of the clamped mode series resonant converter including parasitic losses

A.1 Introduction

Previous studies of the clamped mode series resonant converter use the state plane analysis technique to determine the DC characteristics of the converter [11,12]. No studies considering the losses, however, have been reported. The state plane analysis technique has been used to analyze the conventional series resonant converter including loss effect [8,9]. The same method is used here to calculate the DC characteristics for the clamped mode .

A.2 State plane analysis

The state plane analysis applied to the resonant converter has been described in Refs. 7,8 & 9. The approach is based on the trajectories defined in the state plane , inductor current vs. capacitor voltage, for the DC operation of the converter.

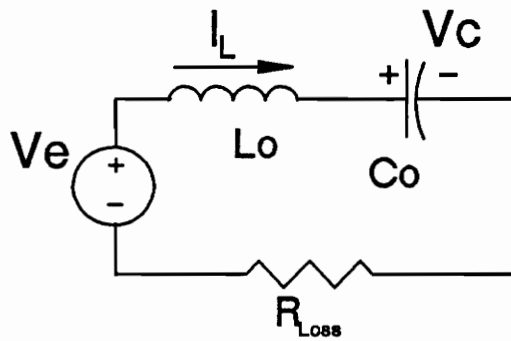
Each topological mode of the converter permits to calculation of the state variables evolution once the boundary condition for the mode is known. In steady state operation, the initial conditions for each mode are determined by the control parameter (at fixed output voltage). The state plane permits to visualization and geometrical determination of the initial conditions for each mode.

The model defined to include the loss effect (Fig. A.1) has been studied in Refs. 8 & 9 for a conventional series resonant converter. The system's state equations are:

$$\begin{bmatrix} \dot{v}_c \\ \dot{i}_l \end{bmatrix} = \begin{bmatrix} 0 & \frac{1}{C} \\ \frac{-1}{L} & \frac{-R}{L} \end{bmatrix} \begin{bmatrix} v_c \\ i_L \end{bmatrix} + \begin{bmatrix} 0 \\ \frac{1}{L} \end{bmatrix} V_e \quad (A.1)$$

with initial conditions defined as

$$\begin{bmatrix} v_c \\ i_L \end{bmatrix}_{t=t_0} = \begin{bmatrix} v_{co} \\ i_{Lo} \end{bmatrix} \quad (A.2)$$



Dev . on	V_e
Q1 Q2	$V_s - V_o$
D1 D2	$V_s + V_o$
Q2 D3	$-V_o$
Q3 D2	$+V_o$
Q3 Q4	$-V_s + V_o$
D3 D4	$-V_s - V_o$
Q4 D1	$+V_o$
Q1 D4	$-V_o$

Figure A.1: Converter model with losses

The following steps are, first to normalize and homogenize the system using the following equations:

$$v'_{cn} = \frac{v_c - v_e}{V_s} \quad (A.3)$$

$$i_{Ln} = \frac{i_L Z_o}{V_s} \quad (A.4)$$

The loss are characterized by:

$$\xi = \frac{R}{2} \sqrt{\frac{C}{L}} \quad (A.5)$$

$$Q = \frac{\omega_o L}{R} = \frac{1}{2\xi} \quad (A.6)$$

With the transformation defined and using polar coordinates such as:

$$\rho = \sqrt{v'^2_{cn} + i^2_{Ln}} \quad (A.7)$$

$$\rho_o = \sqrt{v'^2_{con} + i^2_{Lon}} \quad (A.8)$$

$$\theta = \arctan \left[\frac{-i_{Ln}}{v'_{cn}} \right] \quad (A.9)$$

$$\theta_o = \arctan \left[\frac{-i_{Lon}}{v'_{con}} \right] \quad (A.10)$$

the following solution can be obtained [8,9],

$$\rho = \rho_o \sqrt{\frac{1 - \xi \sin 2\theta_o}{1 - \xi \sin 2\theta}} \exp\left[\frac{-\xi}{\sqrt{1 - \xi^2}} (\phi - \phi_o)\right] \quad (A.11)$$

where

$$\phi = \arctan\left[\frac{-\xi}{\sqrt{1 - \xi^2}} + \frac{\tan \theta}{\sqrt{1 - \xi^2}}\right] \quad (A.11a)$$

and

$$\phi_o = \arctan\left[\frac{-\xi}{\sqrt{1 - \xi^2}} + \frac{\tan \theta_o}{\sqrt{1 - \xi^2}}\right] \quad (A.11b)$$

and

$$\theta = \arctan\left[\xi + \sqrt{1 - \xi^2} \tan(\omega_D t + \phi_o)\right] \quad (A.12)$$

where

$$\omega_d = \omega_o \sqrt{1 - \xi^2} \quad (A.13)$$

These equations show two important facts. The first is that the trajectories are made with segments of spirals instead of circular segments, and the second is that the subtended angle is not proportional to the time. To calculate the equivalent angle proportional to the time, the following equation can be used,

$$\phi = \arctan \left[-\frac{\xi}{\sqrt{1-\xi^2}} + \frac{\tan \theta}{\sqrt{1-\xi^2}} \right] \quad (A.14)$$

The construction of the trajectories can be better understood considering one particular sequence of topological modes. Next sections illustrate the determination of the equilibrium trajectories for the case above resonant frequency.

A.2.1 Equilibrium trajectories above resonant frequency

To illustrate how the trajectories are constructed, consider the case above resonant frequency in the Region A'. The sequence of topological modes (Fig. 2.11 Chapter 2) corresponds to the following values for the source in the model (Fig. A.1):

$V_e = V_s - V_o$, Q1 and Q2 conducting
$V_e = -V_o$, Q2 and D3 conducting
$V_e = -V_s - V_o$, D3 and D4 conducting
$V_e = -V_s + V_o$, Q3 and Q4 conducting
$V_e = V_o$, Q4 and D1 conducting
$V_e = -V_s + V_o$, D1 and D2 conducting

The values for current and voltage are symmetrical with respect to the origin for each half of the cycle. Plotting the trajectory corresponding to each topological mode (Fig. A.2), the inductor current vs. capacitor voltage are spirals centered in $1 - V_{on}$, $-V_{on}$ and $-1 - V_{on}$ respectively. A trajectory formed by three seg-

ments that gives symmetrical maximum and minimum values for the capacitor voltage is the solution (Fig. A.3).

When the β angle is reduced the time conduction of the diodes is reduced until only two segments form the trajectory (Fig. A.4), the β angle corresponding to this trajectory is the boundary angle between regions A' and B'.

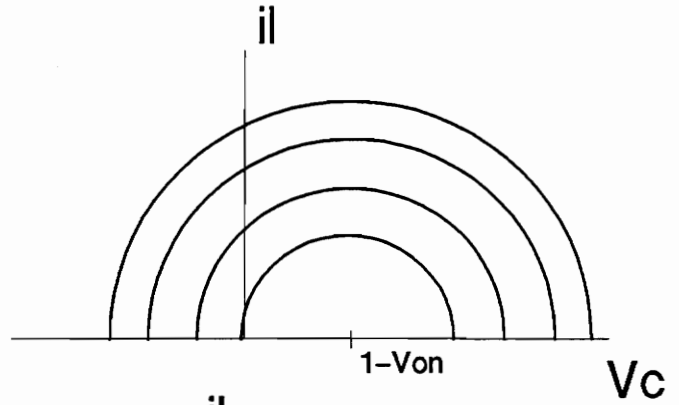
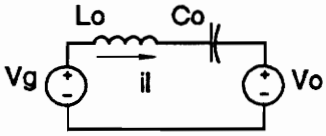
Analogously the trajectories corresponding to the CCM and DCM in region B' can be drawn (Fig. A.6). It can be observed that when the normalized peak capacitor voltage is smaller than V_{on} the trajectory corresponding to CCM in region B' does not exist, then the boundary between Region B' and DCM corresponds to the trajectory depicted in Fig. A.4.

It should be noted in this case that if for the trajectory boundary between Regions A' and B' the normalized peak capacitor voltage is less than V_{on} the converter goes directly from Region A' operation to DCM in region B'.

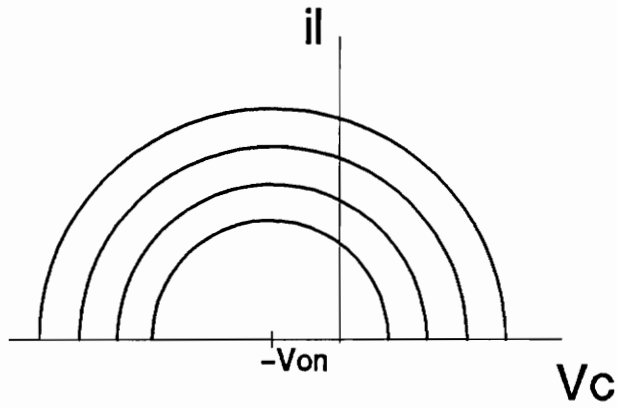
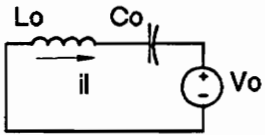
As presented in Chapter 2, two regions of operation are possible above resonant frequency. In the two regions of operation three different sequences (modes of operation) are encountered, this means that three different kinds of equilibrium trajectories have to be considered.

The first step is to calculate the boundaries between the three different modes of operation using this new model. According to f_n and V_{on} of the circuit the continuous conduction mode (CCM) may not be possible in region B'. Figure A.5 shows the limit trajectories for the three possible transitions: Transition from DCM to CCM in region B', transition from CCM to region A' and transition from DCM to region A'.

Q1 and Q2



Q2 and D3



D3 and D4

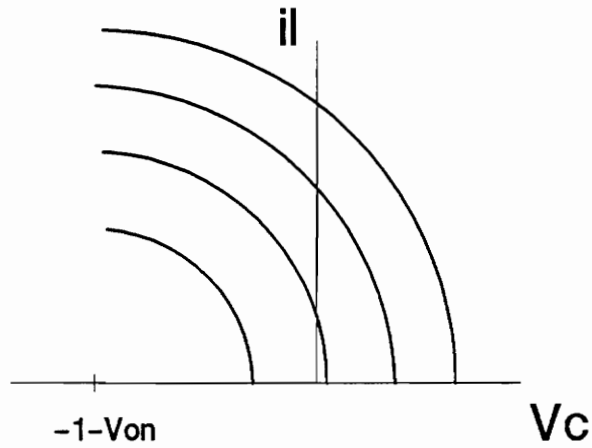
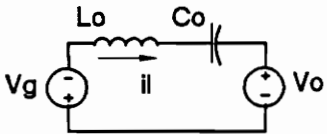


Figure A.2: Trajectories and topological modes for Region A'

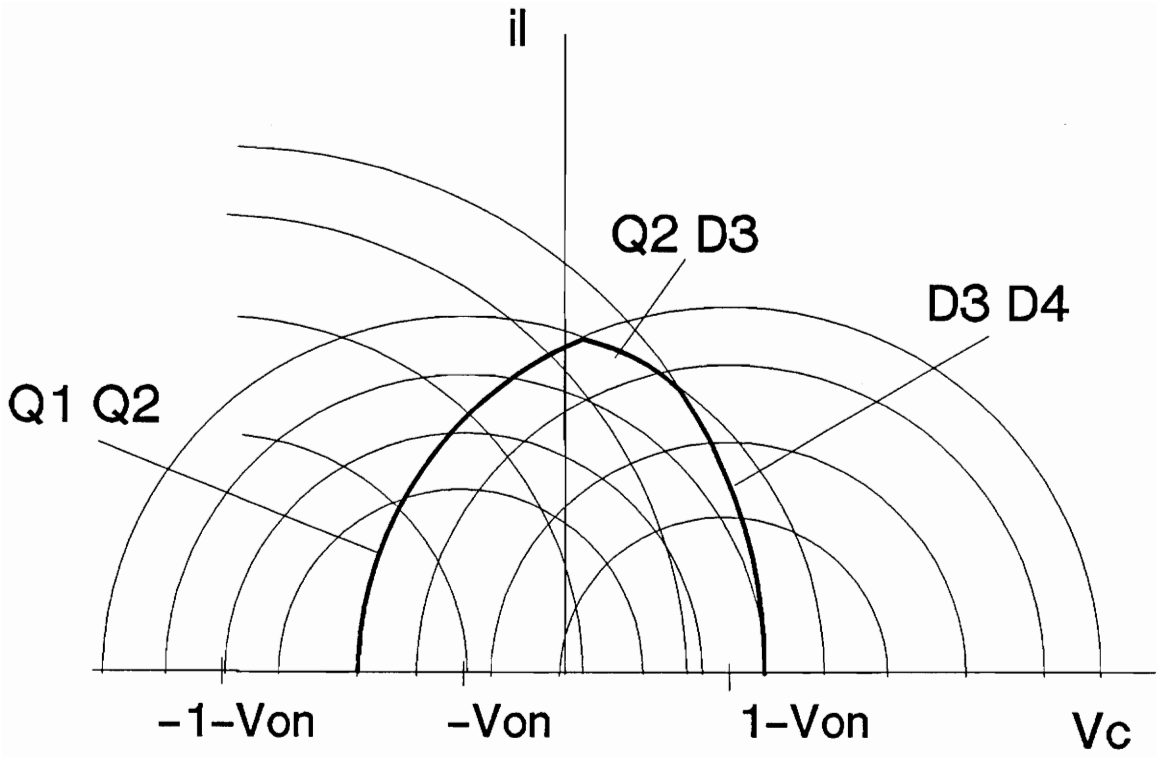


Figure A.3: Trajectories for Region A'

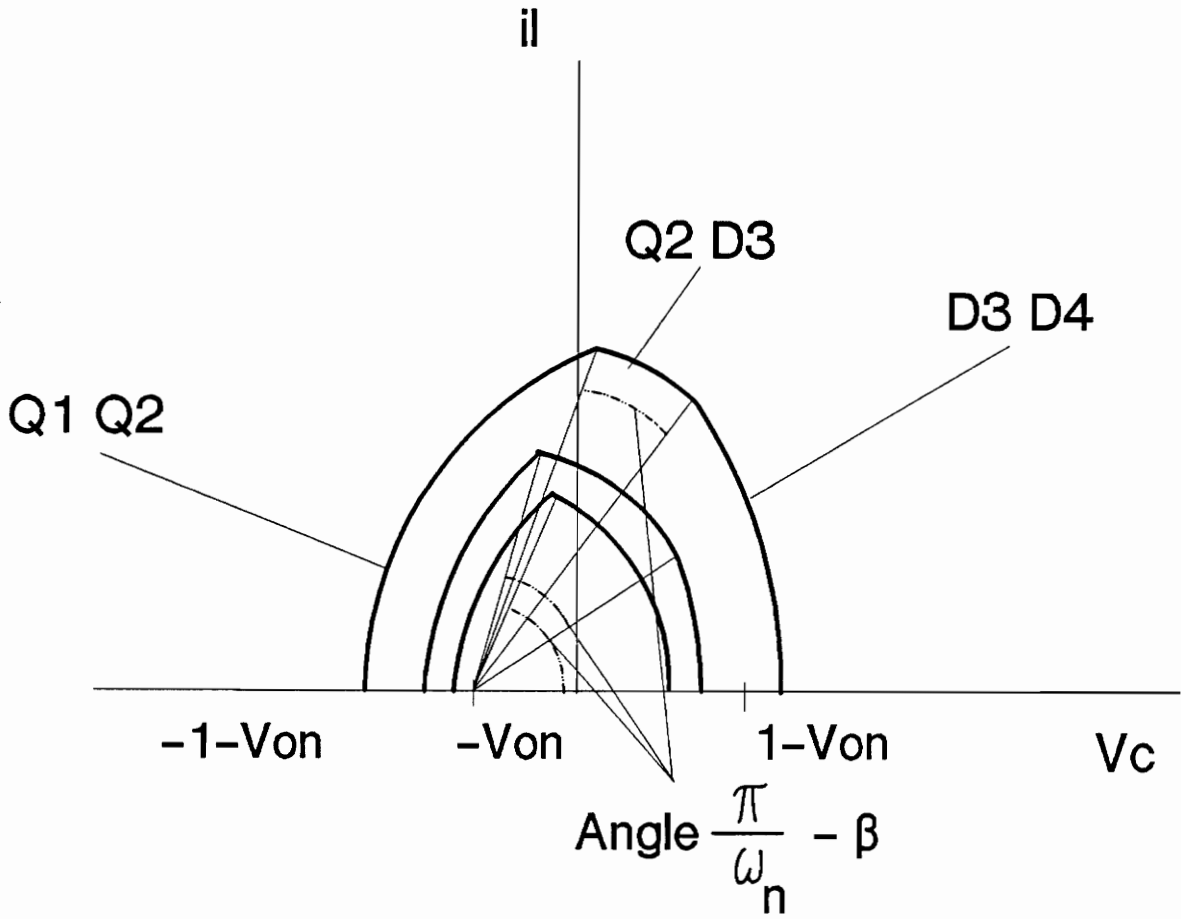


Figure A.4: Boundary trajectory between Region A' and Region B'

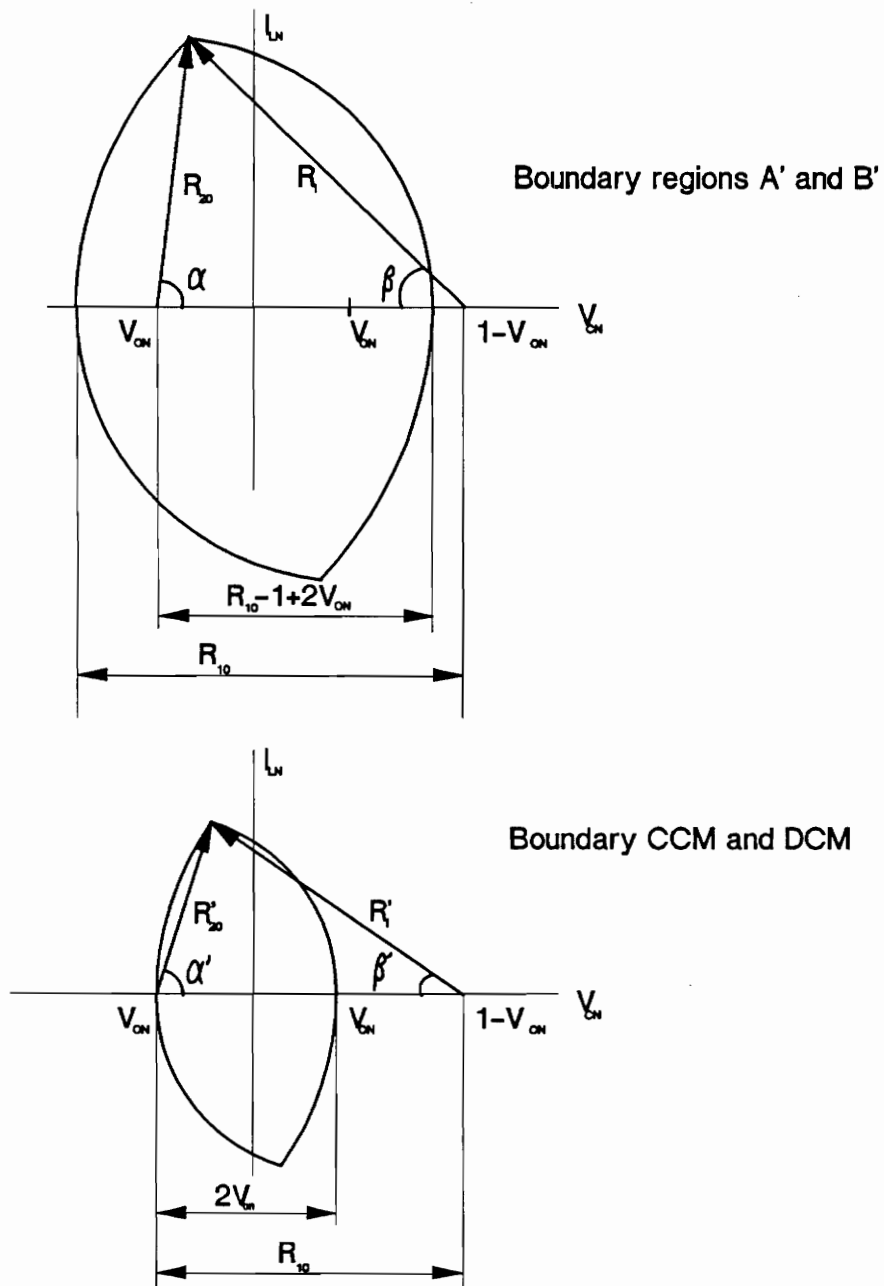


Figure A.5: Boundary trajectories.(Regions A' and B').

Using equations (A.11) and (A.12) together with the geometrical constraints and timing for each case the boundaries are calculated using the following systems of equations:

- Boundary between region B' and region A':

$$\alpha_r + \beta_r = \frac{\pi}{\omega_n}$$

$$R_1 = R_{10} \Phi(\beta_r)$$

$$R_2 = R_{20} \Phi(\alpha_r)$$

$$R_2 = R_{10} - 1 + 2V_{on}$$

$$\cos \beta = \frac{1 + R_1^2 - R_{20}^2}{2R_1}$$

$$\cos \alpha = \frac{1 + R_2^2 - R_1^2}{2R_{20}} \quad (A.15)$$

where α_r and β_r are calculated from the geometrical angles using equation (A.14) and $\Phi(\phi)$ is the damping associated with the trajectory segment radius as defined in equation (A.11).

As seen in Fig. A.5, the transition between DCM and CCM in region B' is only possible when the transition between regions A' and B' occurs with $R_{10} > 1$, otherwise the circuit operation shifts from DCM in region B' to region A' directly.

The boundary equilibrium trajectory between CCM and DCM is shown in Fig. A.5 and, if it exists is determined by the following equations,

$$\alpha'_t + \beta'_t = \frac{\pi}{\omega_n}$$

$$R'_2 = 2V_{on}$$

$$R'_2 = R'_{20} \Phi(\alpha'_t)$$

$$R'_2{}^2 = 2 - 2 \cos \beta'$$

$$\cos \alpha' = \frac{1 + R'_{20}{}^2 - R'_1{}^2}{2R'_{10}}$$

$$1 = R'_{10} \Phi(\beta'_t) \tag{A.16}$$

The boundary between CCM and DCM in region B' provides

$$\omega_{limit} = \frac{\pi}{\alpha'_t + \beta'_t} \tag{A.17}$$

if $\omega_n > \omega_{limit}$, the continuous conduction mode in region B' does not occur.

Once the boundary conditions are determined for ω_n and V_{on} the equilibrium trajectory shape for a given β is known and the set of equations for every case can be used to determine the corresponding values.

The three possible trajectories are shown in fig. A.6, the equations for each case follow:

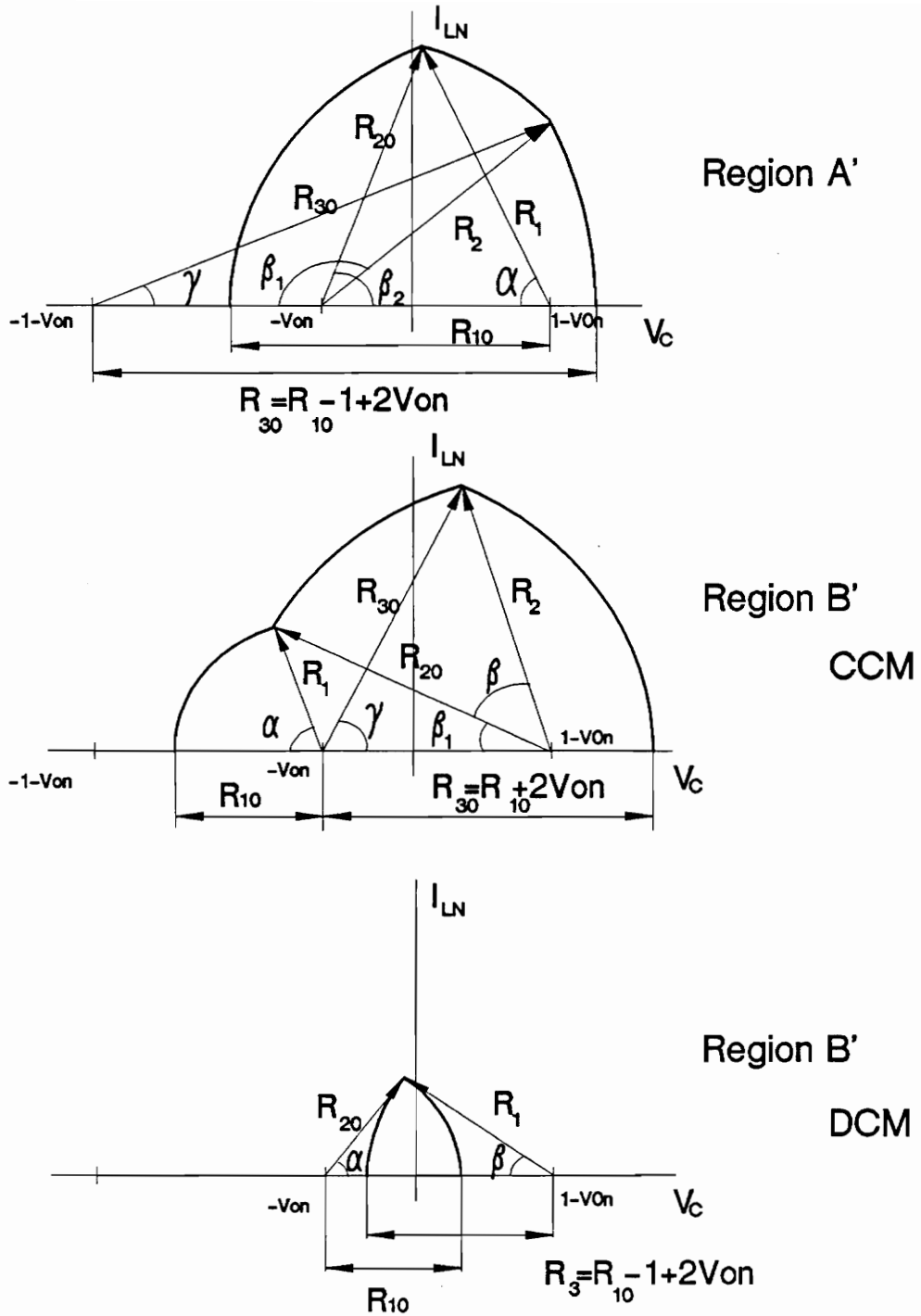


Figure A.6: Space state trajectories.(Regions A' and B').

- Region A', unknowns: $R_{10}, R_1, R_{20}, R_2, R_{30}, R_3, \alpha, \gamma, \beta_1, \beta_2$

$$R_1 = R_{10} \Phi(\alpha_t)$$

$$R_2 = R_{20} \Phi\left(\frac{\pi}{\omega_n} - \beta_t\right)$$

$$R_3 = R_{30} \Phi(\gamma_t)$$

$$\cos \alpha = \frac{1 + R_1^2 - R_{20}^2}{2 R_1}$$

$$\cos \beta_1 = \frac{1 + R_2^2 - R_{30}^2}{2 R_2}$$

$$\cos \beta_2 = \frac{1 + R_{30}^2 - R_2^2}{2 R_{30}}$$

$$\beta_{1t} + \beta_{2t} - \pi = \frac{\pi}{\omega_n} - \beta$$

$$\alpha_t + \gamma_t = \beta_t \tag{A.18}$$

- Region B', continuous conduction mode, unknowns: $R_{10}, R_1, R_{20}, R_2, \alpha, \gamma, \beta_1$

$$R_1 = R_{10} \Phi(\alpha_t)$$

$$R_2 = R_{20} \Phi(\beta_t)$$

$$R_{10} + 2 V_{on} = R_{30} \Phi(\gamma_t)$$

$$\cos(\pi - \alpha) = \frac{1 + R_1^2 - R_{20}^2}{2 R_1}$$

$$\cos \gamma = \frac{1 + R_{30}^2 - R_2^2}{2 R_{30}}$$

$$\cos \beta_1 = \frac{1 + R_{20}^2 - R_1^2}{2 R_{20}}$$

$$\cos(\beta_1 + \beta) = \frac{1 + R_2^2 - R_{30}^2}{2 R_2}$$

$$\alpha_t + \beta_t + \gamma_t = \frac{\pi}{\omega_n} \quad (A.19)$$

- Region B', discontinuous conduction mode , unknowns: $R_{10}, R_1, R_{20}, \gamma, \Phi$.

$$R_1 = R_{10} \Phi(\beta_t)$$

$$R_2 = (R_{10} - 1 + 2V_{on}) \Phi(\gamma_t)$$

$$\cos \beta = \frac{1 + R_1^2 - R_{20}^2}{2 R_1}$$

$$\cos \gamma = \frac{1 + R_{20}^2 - R_1^2}{2 R_{20}}$$

$$\beta_t + \gamma_t + \Phi_t = \frac{\pi}{\omega_n} \quad (A.20)$$

A.2.2 DC characteristics above resonant frequency

Once the equilibrium trajectory parameters are determined, all the parameters for the operating point can be obtained.

The normalized peak voltage of the resonant capacitor can be easily calculated from the trajectory parameters as:

- Region A',

$$V_{cpkn} = R_{10} - 1 + V_{on} \quad (3.21)$$

- Region B', continuous conduction case,

$$V_{cpkn} = R_{20} + V_{on} \quad (A.22)$$

- Region B', discontinuous conduction mode,

$$V_{cpkn} = R_{10} - 1 + V_{on} \quad (A.23)$$

The calculation of the normalized output current is done as follows:

$$I_{L_{av}} = \frac{2}{T} \int_0^{T/2} i_L dt \quad (A.24)$$

since for a capacitor,

$$\int i_L dt = C \Delta V_c \quad (A.25)$$

then adding up the increment of voltage in every trajectory segment,

$$I_{Lav} = \frac{2}{T} C 2 V_{cpk} \quad (A.26)$$

and normalizing,

$$I_{Lavn} = \frac{4 C V_{cpkn} Z_o}{\pi} \omega \sqrt{1 - \xi^2} \omega_n \quad (A.27)$$

hence,

$$I_{Lavn} = \frac{2 V_{cpkn}}{\pi} \omega_n \sqrt{1 - \xi^2} \quad (A.28)$$

For the rest of characteristics that may be needed refer to Refs 8,9,11,26.

A.2.3 Equilibrium trajectories below resonant frequency

Two regions of operation are possible below resonant frequency, considering the switching condition for the devices (Chapter 2). For the cases of interest there is a good analogy with the cases above resonant frequency: One equilibrium trajectory for region A and two for region B (CCM and DCM). Then two transition boundaries are found for every V_{on} and ω_n .

The procedure to calculate the boundaries between the tree modes of operation is analogous to the case above resonant frequency . Using equations (A.11) and (A.12), and the geometrical constraints of the limit trajectories (Fig A.7). The following systems of equations give the boundaries:

- Boundary between regions A and B.

$$\alpha_t + \beta_t = \frac{\pi}{\omega_n}$$

$$\cos(\pi - \beta) = \frac{1 + R_{10}^2 - R_2^2}{2 R_{10}}$$

$$\cos(\pi - \alpha) = \frac{1 R_2^2 - R_{10}^2}{2 R_2}$$

$$R_2 = R_{20} \Phi(\alpha_t)$$

$$R_1 = R_{20} \Phi(\beta_t)$$

$$R_{20} = 1 + R_1 - 2 V_{on} \tag{A.29}$$

where β_t and α_t are calculated from the geometrical angles using equation (A.14).

- Analogously the limit between CCM and DCM is calculated as:

$$\cos \beta = \frac{1 + R_2^2 - R_{10}^2}{2 R_2}$$

$$\cos \alpha = \frac{1 + R_{10}^2 - R_2^2}{2 R_1}$$

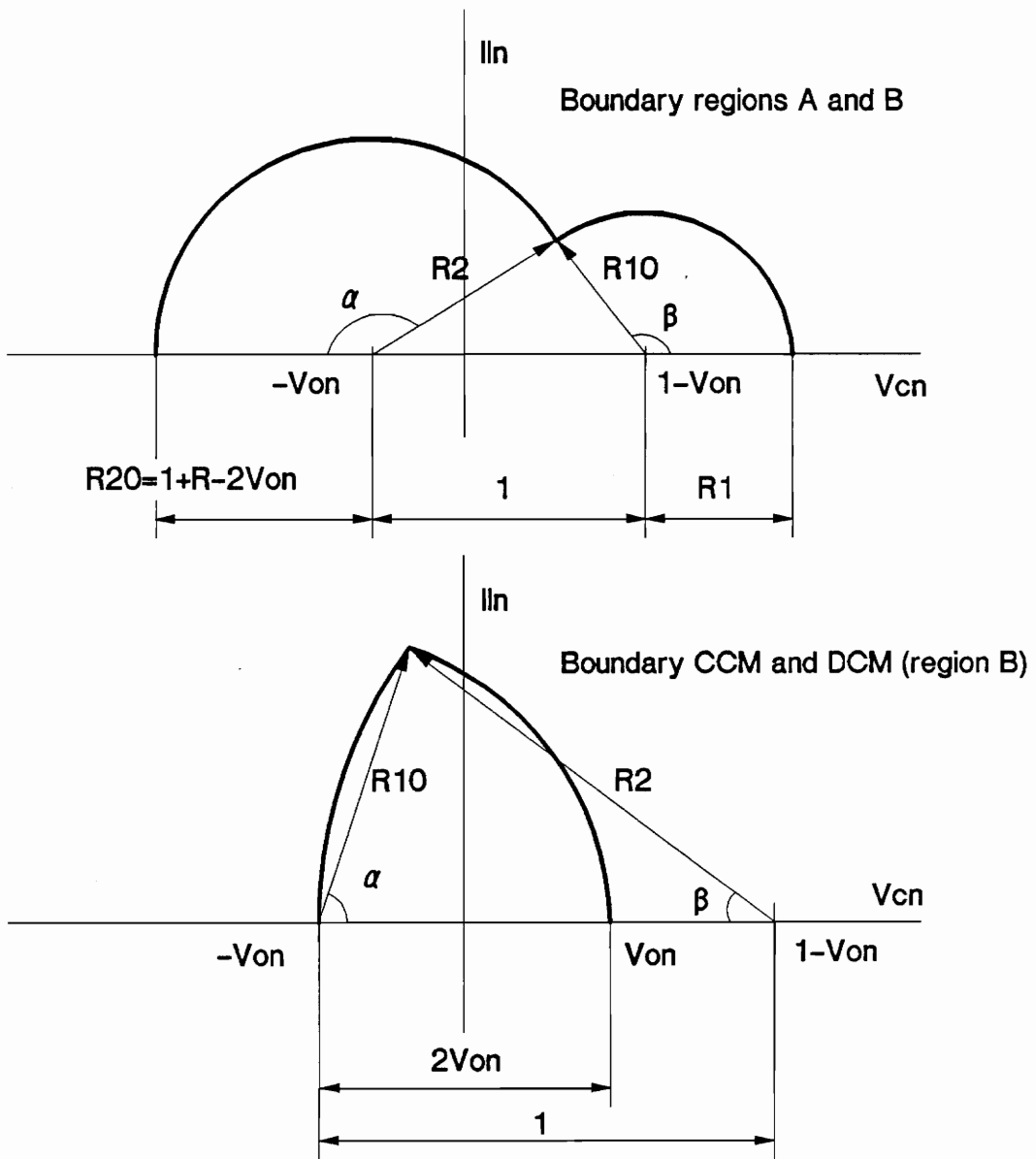


Figure A.7: Boundary trajectories.(Regions A and B).

$$R_1 = R_{10} \Phi(\beta_i)$$

$$R_2 = R_{20} \Phi(\alpha_i)$$

$$R_{20} = 1$$

$$R_2 = 2V_{on} \tag{A.30}$$

Once the boundary conditions are determined , the parameters for every trajectory can be determined, since the corresponding trajectory to a β angle is known (given V_{on}, ω_n). Three trajectories are possible and the notation used in the following formulas is defined in Fig A.8.

The systems of equations for each trajectory are:

- Region A , unknowns : $R_{10}, R_1, R_{20}, R_2, R_{30}, R_3, \alpha, \beta_1, \beta_2, \gamma$

$$R_1 = R_{10} \Phi(\alpha_i)$$

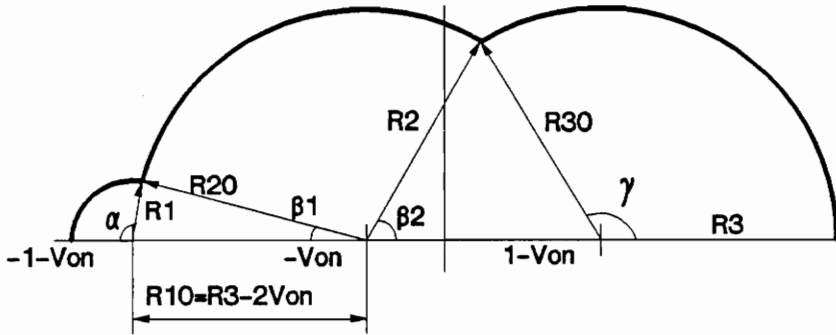
$$R_2 = R_{20} \Phi\left(\frac{\pi}{\omega_n} - \beta_i\right)$$

$$R_3 = R_{30} \Phi(\gamma_i)$$

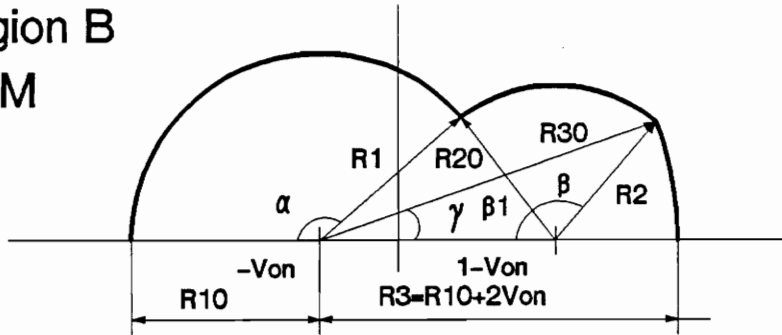
$$R_{10} = R_3 - 2V_{on}$$

$$\cos \alpha = \frac{1 + R_1^2 - R_{20}^2}{2 R_1}$$

Region A



Region B CCM



DCM

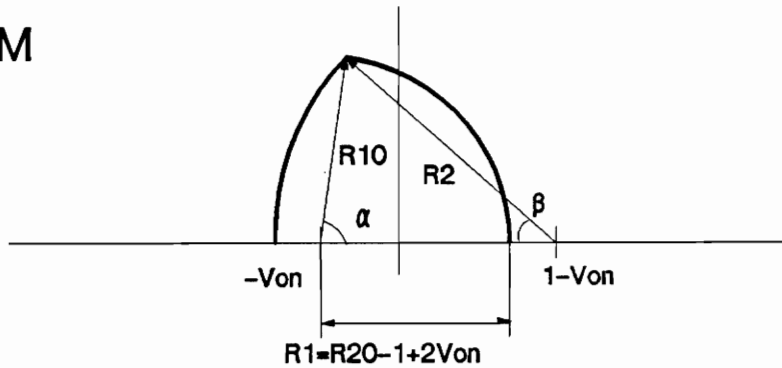


Figure A.8: Space state trajectories.(Regions A and B).

$$\cos \beta_1 = \frac{1 + R_{20}^2 - R_1^2}{2 R_{20}}$$

$$\cos \beta_2 = \frac{1 + R_2^2 - R_{30}^2}{2 R_2}$$

$$\cos(\pi - \gamma) = \frac{1 + R_{30}^2 - R_2^2}{2 R_{30}}$$

$$\beta_t = \alpha_t + \gamma_t$$

$$\pi - \beta_1 - \beta_2 = \frac{\pi}{\omega_n} - \beta_t \quad (A.31)$$

- Region B, CCM, unknowns : $R_{10}, R_1, R_{20}, R_2, R_{30}, R_3, \alpha, \beta_1, \gamma$

$$R_1 = R_{10} \Phi(\alpha_t)$$

$$R_2 = R_{20} \Phi(\beta_t)$$

$$R_3 = R_{30} \Phi(\gamma_t)$$

$$R_3 = R_{10} + 2V_{on}$$

$$\cos(\pi - \alpha) = \frac{1 + R_1^2 - R_{20}^2}{2 R_1}$$

$$\cos(\beta_1 + \beta) = \frac{1 + R_2^2 - R_{30}^2}{2 R_2}$$

$$\cos \beta_1 = \frac{1 + R_{20}^2 - R_1^2}{2 R_{20}}$$

$$\cos \gamma = \frac{1 + R_{30}^2 - R_2^2}{2 R_{30}}$$

$$\alpha_t + \gamma_t + \beta_t = \frac{\pi}{\omega_n} \quad (A.32)$$

- Region B, DCM, unknowns: $R_{10}, R_1, R_{20}, R_2, \alpha, \Phi$.

$$R_1 = R_{10} \Phi(\alpha_t)$$

$$R_2 = R_{20} \Phi(\beta_t)$$

$$R_1 = R_{20} - 1 + 2V_{on}$$

$$\cos \alpha = \frac{1 + R_{10}^2 - R_2^2}{2 R_{10}}$$

$$\cos \beta = \frac{1 + R_2^2 - R_{10}^2}{2 R_2}$$

$$\alpha_t + \beta_t + \Phi = \frac{\pi}{\omega_n} \quad (A.33)$$

Comparing these equations with the ones above resonant frequency it can be seen that although the conduction order for the switches is changed, the geometrical constraints are almost the same due to symmetry.

A.2.4 DC characteristics below resonant frequency

Once the trajectories have been determined, the operating point values can easily be calculated as for the case above resonance. Then analogously the following equations determine the maximum capacitor value for each case:

•Region A :

$$V_{CPKn} = R_3 + 1 - V_{on} \quad (A.34)$$

• Region B (CCM):

$$V_{CPKn} = R_{10} + V_{on} \quad (A.35)$$

•Region B (DCM):

$$V_{CPKn} = R_{20} - 1 + V_{on} \quad (A.36)$$

and the average current can be determined using equation (A.28).

Appendix B

Fortran programs

B.1 Programs to calculate DC characteristics for the ideal case

B.1.1 Case above resonant frequency

```
C#####  
C  
C PROGRAM TO CALCULATE CHARACTERISTICS OF  
C CLAMPED MODE SERIES RESONANT CONVERTER FOR  
C THE IDEAL CASE.  
C *ABOVE RESONANT FREQUENCY.  
C  
C#####  
C
```

```

C  VARIABLES DECLARATION
C
C
INTEGER N,ITMAX,L,I,JUMP,IDMODE
REAL ERRREL
C
REAL FCNA,FCNB,FCNC,FNORM,X1(6),X2(5),X3(3)
REAL XGUESSA(6),XGUESSB(5),XGUESSC(3)
REAL BETA,PI,WN,VBETA,VON,VCPN,W1N
REAL ION,IQAV,IDAV,BETA12,BETA3
REAL A,B
EXTERNAL FCNA,FCNB,FCNC,DNEQNF
C
COMMON RBETA,WN,VON,PI
C
C  DATA INPUT
C
WRITE(5,1000)
1000 FORMAT(/1X,'ENTER PARAMETERS: VON,WN')
READ(5,*) VON,WN
WRITE(19,1001) VON,WN
1001 FORMAT(///1X,'VON = ',E10.4,3X,'WN = ',E10.4)
C
C  CONSTANTS
C
PI = 4.D0*DATAN(1.D0)
ERRREL = 1.E-4
ITMAX = 200
C
X3(1) = 1.D0-VON
X3(2) = PI/WN
X3(3) = 0.D0
IDMODE = 3
N = 3
C

```

```

CALL BOUNDARY(BETA12,BETA3,W1N,R)
C
A = BETA12*180/PI
B = BETA3*180/PI
WRITE(19,102) R,A,B,W1N
102 FORMAT(/1X,'EVALUATED BOUNDARY POINT: ',/2X,'R',15X,'BETA12',10X,
+ 'BETA3',11X,'WN1',/2X,4(E14.8,2X))
C
C MAIN LOOP
C
DO 10 BETA = 0.,180,1.D0
C
RBETA = BETA*PI/(180.D0*WN)
C
C CHECK THE OPERATING MODE
C
IF(W1N.LT.WN.OR.R.LE.1D0) THEN
C ONE TRANSITION
IF(RBETA.LT.BETA12) THEN
JUMP = 1
ELSE
JUMP = 3
ENDIF
ELSE
C TWO TRANSITIONS
IF(RBETA.GE.BETA3) THEN
IF(RBETA.LT.BETA12) THEN
JUMP = 2
ELSE
JUMP = 3
ENDIF
ENDIF
ENDIF
C
GO TO (11,22,33) JUMP
C

```

```

C SOLVE THE SYSTEM FOR THE GIVEN BETA
C
C
C NO TRANSITION C-C
11 DO 15 L=1,3
15 XGUESSC(L)=X3(L)
CALL DNEQNF(FCNC,ERRREL,N,ITMAX,XGUESSC,X3,FNORM)
C
C CALCULATE DESIGN CHARACTERISTICS
C
VCPN = VON + X3(1)-1.D0
ION = 2.D0*VCPN/(PI/WN)
C
GO TO 77
C
C
22 IF(IDMODE.EQ.2) THEN
C NO TRANSITION B-B
DO 16 L=1,5
16 XGUESSB(L)=X2(L)
C
ELSE
C
C TRANSITION C-B
XGUESSB(1)=0.1D0
XGUESSB(2)=X3(1)
XGUESSB(3)=0.D0
XGUESSB(4)=X3(3)
XGUESSB(5)=0.D0
IDMODE=2
N=5
ENDIF
CALL DNEQNF(FCNB,ERRREL,N,ITMAX,XGUESSB,X2,FNORM)
C WRITE(*,*) (X2(LL),LL=1,N)
C

```

C CALCULATE DESIGN CHARACTERISTICS

C

VCPN = VON + X2(1)

ION = 2.D0*VCPN/(PI/WN)

C

GO TO 77

C

33 IF(IDMODE.EQ.1) THEN

C

C NO TRANSITION A-A

DO 17 L=1,6

17 XGUESSA(L) = X1(L)

ELSE

IF(IDMODE.EQ.2) THEN

C

C TRANSITION B-A

XGUESSA(1) = X2(2) + .01

XGUESSA(2) = X2(2) + 2.D0*VON + .01

XGUESSA(3) = BETA3

XGUESSA(4) = 0.1D0

XGUESSA(5) = PI-X2(4)

XGUESSA(6) = X2(4)

ELSE

C

C TRANSITION C-A

XGUESSA(1) = X3(1)

XGUESSA(2) = X3(1) + 2.D0*VON

XGUESSA(3) = 0.D0

XGUESSA(4) = 0.D0

XGUESSA(5) = BETA12

XGUESSA(6) = PI-BETA12

ENDIF

IDMODE = 1

N = 6

ENDIF

```

CALL DNEQNF(FCNA,ERRREL,N,ITMAX,XGUESSA,X1,FNORM)
C
C  CALCULATE DESIGN CHARACTERISTICS
C
VCPN = -1.D0 + VON + X1(1)
ION = 2.D0*VCPN/(PI/WN)
C
C  OUTPUT FOR CHECKING ACCURACY
77  WRITE(5,7777) FNORM,IDMODE
7777 FORMAT(/1X,1E11.4,2X,1I1)
C
C
C  DATA OUTPUT
C
WRITE(15,2000) BETA,VCPN
WRITE(16,2000) BETA,ION
C  WRITE(17,2000) BETA,IQAV
C  WRITE(18,2000) BETA,IDAVN
2000 FORMAT(1X,2(E10.4,1X))
10  CONTINUE
C
STOP
END
C#####
C
C  SUBROUTINE TO DEFINE THE HOMOGENEOUS
C  NONLINEAR SYSTEM.ON MODE A.(REGION A')
C
C#####
C
SUBROUTINE FCNA(X,F,N)
C
C  VARIABLES DECLARATION
C
COMMON RBETA,WN,VON,PI
C

```

```

INTEGER N,I
REAL X(N),F(N)
REAL RBETA,WN,VON,PI,RTEMP,R2
C
C
C  MAIN PROGRAM
C
C  VARIABLES DEFINITION:
C  X(1)= R      ;INITIAL GUESS FOR FIRST RADIUS
C  X(2)= R1     ;INITIAL VALUE FOR 2ND ARC
C  X(3)= ALFA
C  X(4)= GAMMA
C  X(5)= BETA1
C  X(6)= BETA2
C
C  X(3)= DABS(X(3))
C  X(4)= DABS(X(4))
C  X(5)= DABS(X(5))
C  X(6)= DABS(X(6))
C
C  MAIN PROGRAM
C
C  F(1)= RBETA-X(3)-X(4)
C
C  RTEMP = (PI/WN)-RBETA
C  F(2)= X(5) + X(6)-PI-RTEMP
C
C  F(3)= 1.D0 + X(1)*X(1)-X(2)*X(2)-2.D0*X(1)*COS(X(3))
C
C  R2 = X(1)+ 2.D0*VON
C
C  F(4)= 1.D0-X(2)*X(2) + R2*R2-2.D0*R2*COS(X(4))
C
C  F(5)= 1.D0 + X(2)*X(2)-R2*R2-2.D0*X(2)*COS(X(5))
C

```

```

F(6) = 1.D0 + X(2)*X(2)-X(1)*X(1)-2.D0*X(2)*COS(X(6))
C
  RETURN
  END
C#####
C
C  SUBROUTINE TO DEFINE THE HOMOGENEOUS
C  NONLINEAR SYSTEM.ON MODE B.(REGION B' CCM)
C
C#####
C
  SUBROUTINE FCNB(X,F,N)
C
C  VARIABLES DECLARATION
C
  COMMON RBETA,WN,VON,PI
C
  INTEGER N,I
  REAL X(N),F(N)
  REAL RBETA,WN,VON,PI,RTEMP
C
C
C  MAIN PROGRAM
C
C  VARIABLES DEFINITION:
C  X(1) = R    ;INITIAL GUESS FOR FIRST RADIUS
C  X(2) = R1   ;INITIAL VALUE FOR 2ND ARC
C  X(3) = ALFA
C  X(4) = GAMMA
C  X(5) = BETA1
C
C  MAIN PROGRAM
C
  X(3) = DABS(X(3))
  X(4) = DABS(X(4))
  X(5) = DABS(X(5))

```

```

F(1)= X(3)+ X(4)+ RBETA-(PI/WN)
C
F(2)= 1.D0 + X(1)*X(1)-X(2)*X(2)+ 2.D0*X(1)*DCOS(X(3))
C
RTEMP= X(1)+ 2.D0*VON
F(3)= 1.D0 + RTEMP*RTEMP-X(2)*X(2)-2.D0*RTEMP*DCOS(X(4))
C
F(4)= 1.D0 + X(2)*X(2)-X(1)*X(1)-2.D0*X(2)*DCOS(X(5))
C
F(5)= 1.D0 + X(2)*X(2)-RTEMP*RTEMP-2.D0*X(2)*DCOS(X(5)+ RBETA)
C
RETURN
END
C#####
C
C SUBROUTINE TO DEFINE THE HOMOGENEOUS
C NONLINEAR SYSTEM.ON MODE C.(REGION B' DCM)
C
C#####
C
C SUBROUTINE FCNC(X,F,N)
C
C VARIABLES DECLARATION
C
COMMON RBETA,WN,VON,PI
C
INTEGER N,I
REAL X(N),F(N)
REAL RBETA,WN,VON,PI,RTEMP
C
C
C MAIN PROGRAM
C
C VARIABLES DEFINITION:
C X(1)= R ;INITIAL GUESS FOR FIRST RADIUS

```

```

C X(2) = PHI ;NON CONDUCTION ANGLE
C X(3) = GAMMA
C
C MAIN PROGRAM
C
X(3) = DABS(X(3))
X(2) = DABS(X(2))
C
F(1) = RBETA + X(3) + X(2) - (PI/ WN)
C
RTEMP = X(1) - 1.D0 + 2.D0 * VON
F(2) = 1.D0 + X(1) * X(1) - RTEMP * RTEMP - 2.D0 * X(1) * DCOS(RBETA)
C
F(3) = 1.D0 + RTEMP * RTEMP - X(1) * X(1) - 2.D0 * RTEMP * DCOS(X(3))
C
RETURN
END
C#####
C
C PROGRAM TO CALCULATE BOUNDARY
C FOR THE IDEAL TANK. ABOVE RESONANT FREQ.
C
C#####
C
SUBROUTINE BOUNDARY(BETA12,BETA3,W1N,R)
C
REAL X(2),FCBOUND,XG(2),ERRREL, FNORM,VON,PI
REAL BETA12,BETA3,W1N,ALFA3,R
INTEGER L,ITMAX,N
EXTERNAL FCBOUND,DNEQNF
C
COMMON RBETA,WN,VON,PI
C
ITMAX = 200
N = 2

```

```

ERRREL = 1.D-5
C
BETA3 = DACOS(1.D0-2.D0*VON**2.D0)
ALPHA3 = DACOS(VON)
W1N = PI/(ALPHA3 + BETA3)
C
C
WRITE(5,101)
101 FORMAT(/1X,'ENTER INITIAL GUESS FOR BOUNDARY:R,ALPHA')
READ(5,*) (XG(L),L = 1,N)
CALL DNEQNF(FCBOUND,ERRREL,N,ITMAX,XG,X,FNORM)
C
WRITE(5,103) FNORM
103 FORMAT(/1X,'FNORM = ',1E10.4)
C
BETA12 = X(2)
R = X(1)
C
C
RETURN
END
C
C#####
C
SUBROUTINE FCBOUND(X,F,N)
C
COMMON RBETA,WN,VON,PI
C
INTEGER N
REAL X(N),F(N),A,VON
C
A = X(1)-1.D0 + 2.D0*VON
F(1) = 1.D0 + X(1)*X(1)-A*A-2.D0*X(1)*DCOS(X(2))
C
F(2) = 1.D0 + A*A-X(1)*X(1)-2.D0*A*DCOS(PI/WN-X(2))
C

```

```
RETURN
END
```

B.1.2 Case below resonant frequency

```
C#####
C
C PROGRAM TO CALCULATE CHARACTERISTICS OF
C CLAMPED MODE SERIES RESONANT CONVERTER FOR
C THE IDEAL CASE.
C
C *BELOW RESONANT FREQUENCY
C
C#####
C
C VARIABLES DECLARATION
C
C
C INTEGER N,ITMAX,L,I,JUMP,IDMODE
REAL ERRREL
C
REAL FCNA,FCNB,FCNC,FNORM,X1(6),X2(5),X3(3)
REAL XGUESSA(6),XGUESSC(5),XGUESSF(3)
REAL BETA,PI,WN,VBETA,VON,VCPN,WN1
REAL ION,IQAV,IDAV,BETA12,BETA36
REAL A,B,R13
EXTERNAL FCNA,FCNB,FCNC,DNEQNF
C
COMMON VBETA,WN,VON,PI
C
C DATA INPUT
C
WRITE(5,1000)
1000 FORMAT(/1X,'ENTER PARAMETERS: VON,WN')
```

```

READ(5,*) VON,WN
WRITE(17,1001) VON,WN
1001 FORMAT(///1X,'VON = ',E10.4,3X,'WN = ',E10.4)
C
C  CONSTANTS
C
PI = 4.D0*DATAN(1.D0)
ERRREL = 1.E-5
ITMAX = 200
C
X3(1) = 1.D0-VON
X3(2) = PI/WN
X3(3) = 0.D0
IDMODE = 3
N = 3
C
CALL BOUNDARY(BETA13,BETA36,R13)
C
A = BETA13*180./PI
B = BETA36*180./PI
WRITE(17,102) R13,A,B
102 FORMAT(/1X,'EVALUATED BOUNDARY POINT:',/2X,'R',15X,'BETA12',10X,
+ 'BETA36',/2X,3(E14.8,2X))
C
C  MAIN LOOP
C
DO 10 BETA = 0.,180,1.D0
C
RBETA = BETA*PI/(180.D0*WN)
C
C  CHECK THE OPERATING MODE
C
C  TRANSITION F TO C
IF(RBETA.LT.BETA36) THEN
    JUMP = 1

```

```

ELSE
C  TRANSITION C TO A
    IF(RBETA.GE.BETA13) THEN
        JUMP=3
    ELSE
        JUMP=2
    ENDIF
ENDIF
C
GO TO (11,22,33) JUMP
C
C  SOLVE THE SYSTEM FOR THE GIVEN BETA
C
C
C  NO TRANSITION F-F
11 DO 15 L=1,3
15 XGUESSF(L)=X3(L)
    CALL DNEQNF(FCNC,ERRREL,N,ITMAX,XGUESSF,X3,FNORM)
C
C  CALCULATE DESIGN CHARACTERISTICS
C
VCPN=VON+X3(1)-1.D0
ION=2.D0*VCPN/(PI/WN)
C
GO TO 77
C
C
22 IF(IDMODE.EQ.2) THEN
C  NO TRANSITION C-C
    DO 16 L=1,5
16 XGUESSC(L)=X2(L)
C
ELSE
C
C  TRANSITION F-C
XGUESSC(1)=X3(1)+0.1

```

```

XGUESSC(2) = 0.1
XGUESSC(3) = (PI-RBETA)/2.-0.1
XGUESSC(4) = X3(3)
XGUESSC(5) = 0.
IDMODE = 2
N = 5
ENDIF
CALL DNEQNF(FCNB,ERRREL,N,ITMAX,XGUESSC,X2,FNORM)
C
C  CALCULATE DESIGN CHARACTERISTICS
C
VCPN = VON + X2(2)
ION = 2.D0*VCPN/(PI/WN)
C
GO TO 77
C
33 IF(IDMODE.EQ.1) THEN
C
C  NO TRANSITION A-A
DO 17 L = 1,6
17 XGUESSA(L) = X1(L)
ELSE
C
C  TRANSITION C-A
XGUESSA(1) = X2(1) + 0.1
XGUESSA(2) = X2(2) - 0.1
XGUESSA(3) = 0.01
XGUESSA(4) = BETA13
XGUESSA(5) = 0.
XGUESSA(6) = PI - X2(4) - 0.01
ENDIF
IDMODE = 1
N = 6
C
CALL DNEQNF(FCNA,ERRREL,N,ITMAX,XGUESSA,X1,FNORM)
C

```

```

C  CALCULATE DESIGN CHARACTERISTICS
C
  VCPN = 1.D0-VON + X1(1)
  ION = 2.D0*VCPN/(PI/WN)
C
C  OUTPUT FOR CHECKING ACCURACY
77  WRITE(5,*) FNORM
C
C
C  DATA OUTPUT
C
  WRITE(15,2000) BETA,VCPN
  WRITE(16,2000) BETA,ION
2000  FORMAT(1X,2(E10.4,1X))
10  CONTINUE
C
  STOP
  END
C#####
C
C  SUBROUTINE TO DEFINE THE HOMOGENEOUS
C  NONLINEAR SYSTEM.ON MODE A.(REGION A)
C
C#####
C
  SUBROUTINE FCNA(X,F,N)
C
C  VARIABLES DECLARATION
C
  COMMON RBETA,WN,VON,PI
C
  INTEGER N,I
  REAL X(N),F(N)
  REAL RBETA,WN,VON,PI,RTEMP,R2
C
C

```

```

C MAIN PROGRAM
C
C VARIABLES DEFINITION:
C X(1)= R ;INITIAL GUESS FOR FIRST RADIUS
C X(2)= R1 ;INITIAL VALUE FOR 2ND ARC
C X(3)= ALFA
C X(4)= GAMMA
C X(5)= BETA1
C X(6)= BETA2
C
C X(3)= DABS(X(3))
C X(4)= DABS(X(4))
C X(5)= DABS(X(5))
C X(6)= DABS(X(6))
C
C MAIN PROGRAM
C
C F(1)= RBETA-X(3)-X(4)
C
C F(2)= RBETA + PI-X(5)-X(6)-(PI/WN)
C
C R2 = X(1)-2.D0*VON
C
C F(3)= 1.D0 + X(1)*X(1)-X(2)*X(2) + 2.D0*X(1)*DCOS(X(4))
C
C F(4)= 1.D0 + R2*R2-X(2)*X(2) + 2.D0*R2*DCOS(X(3))
C
C F(5)= 1.D0 + X(2)*X(2)-R2*R2-2.D0*X(2)*DCOS(X(5))
C
C F(6)= 1.D0 + X(2)*X(2)-X(1)*X(1)-2.D0*X(2)*DCOS(X(6))
C
C RETURN
C END
C#####
C
C SUBROUTINE TO DEFINE THE HOMOGENEOUS

```

```

C  NONLINEAR SYSTEM.ON MODE C.(REGION B CCM)
C
C#####
C
C      SUBROUTINE FCNB(X,F,N)
C
C  VARIABLES DECLARATION
C
C      COMMON RBETA,WN,VON,PI
C
C      INTEGER N,I
C      REAL X(N),F(N)
C      REAL RBETA,WN,VON,PI,RTEMP
C
C
C
C  MAIN PROGRAM
C
C  VARIABLES DEFINITION:
C  X(1)=R      ;INITIAL GUESS FOR FIRST RADIUS
C  X(2)=R1     ;INITIAL VALUE FOR 2ND ARC
C  X(3)=ALFA
C  X(4)=GAMMA
C  X(5)=BETA1
C
C  MAIN PROGRAM
C
C      X(3)=DABS(X(3))
C      X(4)=DABS(X(4))
C      X(5)=DABS(X(5))
C
C      F(1)=X(3)+X(4)+RBETA-(PI/WN)
C
C      F(2)=1.D0+X(2)*X(2)-X(1)*X(1)+2.D0*X(2)*DCOS(X(3))
C
C      RTEMP=X(2)+2.D0*VON

```

```

F(3) = 1.D0 + RTEMP*RTEMP-X(1)*X(1)-2.D0*RTEMP*DCOS(X(4))
C
F(4) = 1.D0 + X(1)*X(1)-X(2)*X(2)-2.D0*X(1)*DCOS(X(5))
C
F(5) = 1.D0 + X(1)*X(1)-RTEMP*RTEMP-2.D0*X(1)*DCOS(X(5) + RBETA)
C
RETURN
END
C#####
C
C  SUBROUTINE TO DEFINE THE HOMOGENEOUS
C  NONLINEAR SYSTEM.ON MODE F.(REGION B DCM)
C
C#####
C
C  SUBROUTINE FCNC(X,F,N)
C
C  VARIABLES DECLARATION
C
COMMON RBETA,WN,VON,PI
C
INTEGER N,I
REAL X(N),F(N)
REAL RBETA,WN,VON,PI,RTEMP
C
C
C  MAIN PROGRAM
C
C  VARIABLES DEFINITION:
C  X(1) = R    ;INITIAL GUESS FOR FIRST RADIUS
C  X(2) = PHI  ;NON CONDUCTION ANGLE
C  X(3) = ALFA
C
C  MAIN PROGRAM
C
X(3) = DABS(X(3))

```

```

X(2) = DABS(X(2))
C
F(1) = RBETA + X(3) + X(2) - (PI/WN)
C
RTEMP = X(1) - 1.D0 + 2.D0 * VON
F(2) = 1.D0 + X(1) * X(1) - RTEMP * RTEMP - 2.D0 * X(1) * DCOS(RBETA)
C
F(3) = 1.D0 + RTEMP * RTEMP - X(1) * X(1) - 2.D0 * RTEMP * DCOS(X(3))
C
RETURN
END
C#####
C
C PROGRAM TO CALCULATE BOUNDARY
C FOR THE IDEAL TANK. BELOW RESONANT FREQ.
C (FOR MODES 1,3,6)
C
C#####
C
SUBROUTINE BOUNDARY(BETA13,BETA36,R)
C
REAL X(3),FCBOUND,XG(3),ERRREL,FNORM,VON,PI
REAL BETA13,BETA36,DELTA,R
INTEGER L,ITMAX,N
EXTERNAL FCBOUND,DNEQNF
C
COMMON RBETA,WN,VON,PI
C
ITMAX = 200
N = 3
ERRREL = 1.D-5
C
C BOUNDARY BETWEEN 3 AND 6
C

```

```

BETA36 = DACOS(1.D0-2.D0*VON**2.D0)
C
C
WRITE(5,101)
101 FORMAT(/1X,'ENTER INITIAL GUESS FOR BOUNDARY:R,ALPHA,BETA1')
READ(5,*) (XG(L),L=1,N)
CALL DNEQNF(FCBOUND,ERRREL,N,ITMAX,XG,X,FNORM)
C
WRITE(5,103) FNORM
103 FORMAT(/1X,'FNORM = ',1E10.4)
C
BETA13 = X(3)
R = X(1)
C
C
RETURN
END
C
C#####
C
SUBROUTINE FCBOUND(X,F,N)
C
COMMON RBETA,WN,VON,PI
C
INTEGER N
REAL X(N),F(N),A,VON
C
C VARIABLES DESCRIPTION
C
C X(1) = R
C X(2) = PSI
C X(3) = DELTA
C
C X(3) = DABS(X(3))
C X(2) = DABS(X(2))
C

```

```

A = X(1) + 1.D0 - 2.D0 * VON
F(1) = 1.D0 + X(1) * X(1) - A * A + 2.D0 * X(1) * DCOS(X(3))
C
F(2) = 1.D0 + A * A - X(1) * X(1) + 2.D0 * A * DCOS(X(2))
C
F(3) = WN - (PI / (X(2) + X(3)))
C
RETURN
END

```

B.2 Programs to calculate DC characteristics for the case including loss

B.2.1 Case above resonant frequency

```

C#####
C
C PROGRAM TO CALCULATE CHARACTERISTICS OF
C CLAMPED MODE SERIES RESONANT CONVERTER FOR
C A NONIDEAL TANK.
C *Case above resonant frequency
C
C#####
C
C VARIABLES DECLARATION
C
C INTEGER N,ITMAX,L,MODE
C REAL ERREL,ION,PSI,VON,WN,PI,BETA,RBETA,WD,TS
C

```

```

REAL FCNC, FNORM
REAL XA(10), XB(8), XC(6)
REAL XGUESSA(10), XGUESSB(8), XGUESSC(6)
REAL BETA12, BETA13, W1N, RB
EXTERNAL FCNA, FCNB, FCNC, DNEQNF, BOUNDARY
C
COMMON RBETA, PSI, WN, VON, PI
C
C DATA INPUT
C
WRITE(5,1000)
1000 FORMAT(/1X,'ENTER PARAMETERS: VON,PSI,WN')
READ(5,*) VON,PSI,WN
C
C CONSTANTS
C
PI = 4.D0 * DATAN(1.D0)
ERREL = 1.D-5
ITMAX = 200
C
C DETERMINE BOUNDARIES
C
CALL BOUNDARY(BETA12, BETA13, W1N, RB)
C
N = 6
MODE = 1
C
C INITIAL GUESS
C
XC(1) = 1.01D0 - VON
XC(2) = 1.D0 - VON
XC(3) = VON + 0.01D0
XC(4) = VON + .005D0

XC(5) = 0.01

```

```

XC(6)=PI/WN
C
WRITE(5,1001)
1001 FORMAT(/1X,'INITIAL GUESS FOR C MODE:R10,R1,R20,GAMMA,PHI')
WRITE(5,*) (XC(L),L= 1,N)
C
C MAIN LOOP
C
DO 10 BETA = 0.D0,180.D0,1.D0
C
RBETA = BETA*PI/(180.D0*WN)
C
C SOLVE THE SYSTEM FOR THE GIVEN BETA
C
C
C CHECK THE OPERATING MODE
C
IF(W1N.LT.WN.OR.RB.LE.1.D0) THEN
C ONE TRANSITION
IF(RBETA.LT.BETA12) THEN
JUMP = 1
C GO TO MODE C
ELSE
JUMP = 3
C GO TO MODE A
ENDIF
ELSE
C TWO TRANSITIONS
IF(RBETA.GE.BETA13) THEN
IF(RBETA.LT.BETA12) THEN
JUMP = 2
C GO TO MODE B
ELSE
JUMP = 3
C GO TO MODE A
ENDIF
ENDIF

```

```

        ENDIF
ENDIF
C
GO TO (11,22,33) JUMP
C
C SOLVE THE SYSTEM FOR THE GIVEN BETA
C
11 DO 111 LL=1,N
111 XGUESSC(LL)=XC(LL)
C
CALL DNEQNF(FCNC,ERREL,N,ITMAX,XGUESSC,XC,FNORM)
C
C OUTPUT FOR CHECKING ACCURACY
WRITE(5,333) FNORM,BETA,MODE
333 FORMAT(1X,2E11.4,2X,1I1)
C
C CALCULATE DESIGN CHARACTERISTICS MODE C
C
VCPN = -1.D0 + VON + XC(1)
ION = 2.D0*VCPN/(PI/WN)
C IQAVN = X(1)/(2.D0*WD*TS)
C IDAVN = (2.D0*VCPN-X(1)*(1.D0-COS(X(4))))/(2.D0*WD*TS)
C
GO TO 777
C
C MODE B
C
22 IF(MODE.EQ.2) THEN
C
C NO TRANSITION
DO 55 L=1,N
55 XGUESSB(L)=XB(L)
C
ELSE
C
C TRANSITION FROM MODE C

```

```

MODE=2
N=8
XGUESSB(1)=0.2
XGUESSB(2)=0.2
XGUESSB(3)=XC(1)+0.2
XGUESSB(4)=XC(2)+0.2
XGUESSB(5)=2.D0*VON+0.2
XGUESSB(6)=0.1
XGUESSB(7)=XC(4)+0.1
XGUESSB(8)=0.1
WRITE(5,5555) (XGUESSB(LLL),LLL=1,N)
C READ(5,*) (XGUESSB(LLL),LLL=1,N)
C
ENDIF
C
C
CALL DNEQNF(FCNB,ERREL,N,ITMAX,XGUESSB,XB,FNORM)
C
C OUTPUT FOR CHECKING ACCURACY
WRITE(5,333) FNORM,BETA,MODE
C
C CALCULATE DESIGN CHARACTERISTICS MODE B
C
VCPN = VON + XB(1)
ION = 2.D0*VCPN/(PI/WN)
C IQAVN = X(1)/(2.D0*WD*TS)
C IDAVN = (2.D0*VCPN-X(1)*(1.D0-COS(X(4))))/(2.D0*WD*TS)
C
GO TO 777
C MODE A
C
33 IF(MODE.EQ.3) THEN
C
C NO TRANSITION

```

```

DO 66 L=1,N
66  XGUESSA(L)=XA(L)
C
ELSE
C
N=10
  IF(MODE.EQ.1) THEN
C    TRANSITION FROM MODE C
XGUESSA(1)=XC(1)+0.1
XGUESSA(2)=XC(2)+0.1
XGUESSA(3)=XC(3)+0.1
XGUESSA(4)=XC(1)-1.D0+2.D0*VON+0.1
XGUESSA(5)=XC(1)+2.D0*VON
XGUESSA(6)=XC(1)+2.D0*VON
XGUESSA(7)=RBETA
XGUESSA(8)=0.01
XGUESSA(9)=PI-0.01
XGUESSA(10)=XC(5)+0.01
C
ELSE
C
C    TRANSITION FROM MODE B
XGUESSA(1)=XB(3)+0.1
XGUESSA(2)=XB(4)+0.1
XGUESSA(3)=XB(5)+0.1
XGUESSA(4)=XB(1)+2.D0*VON+0.1
XGUESSA(5)=XB(3)+2.D0*VON+0.1
XGUESSA(6)=XB(3)+2.D0*VON+0.1
XGUESSA(7)=BETA12+0.1
XGUESSA(8)=0.1
XGUESSA(9)=3.14
XGUESSA(10)=XB(7)+0.001
ENDIF
C
5555 FORMAT(/1X,'SUGGESTED GUESS',/1X,5E11.4,/1X,5E11.4)

```

```

WRITE(5,5555) (XGUESSA(LLL),LLL = 1,N)
C READ(5,*) (XGUESSA(LLL),LLL = 1,N)
C
MODE=3
C
ENDIF
C
C
CALL DNEQNF(FCNA,ERREL,N,ITMAX,XGUESSA,XA,FNORM)
C
C OUTPUT FOR CHECKING ACCURACY
WRITE(5,333) FNORM,BETA,MODE
C
C CALCULATE DESIGN CHARACTERISTICS MODE A
C
VCPN = -1.D0 + VON + XA(1)
ION = 2.D0*VCPN/(PI/WN)
C IQAVN = X(1)/(2.D0*WD*TS)
C IDAVN = (2.D0*VCPN-X(1)*(1.D0-COS(X(4))))/(2.D0*WD*TS)
C
C DATA OUTPUT
C
C WRITE(15,2000) BETA,VCPN
777 WRITE(16,2000) BETA,ION
C WRITE(17,2000) BETA,IQAV
C WRITE(18,2000) BETA,IDAVN
2000 FORMAT(1X,2(E10.4,1X))
10 CONTINUE
C
STOP
END
C#####
C
C SUBROUTINE TO DEFINE THE HOMOGENEOUS
C NONLINEAR SYSTEM.FOR MODE A.(Region A')
C

```

```

C#####
C
C   SUBROUTINE FCNA(X,F,N)
C
C   VARIABLES DECLARATION
C
C   COMMON RBETA,PSI,WN,VON,PI
C
C   INTEGER N
C   REAL X(N),F(N)
C   REAL RBETA,PSI,WN,VON,PI,A,B,C,D,FC
C   REAL PHI0,PHI1,PHI3,PHIPI
C   REAL TEMP,TEMP1,TEMP3,TEMP4
C   REAL TEMPB1,TEMPB2
C
C   MAIN PROGRAM
C
C   VARIABLES DEFINITION:
C   X(1)= R10   ;INITIAL VALUE FOR 1ST ARC
C   X(2)= R1    ;FINAL   " " " "
C   X(3)= R20   ;INITIAL VALUE FOR 2ND ARC
C   X(4)= R2    ;FINAL   " " " "
C   X(5)= R30   ;INITIAL VALUE FOR 3RD ARC
C   X(6)= R3    ;FINAL   " " " "
C   X(7)= ALFA
C   X(8)= GAMMA
C   X(9)= BETA1
C   X(10)= BETA2
C
C   X(7)= DABS(X(7))
C   X(8)= DABS(X(8))
C   X(9)= DABS(X(9))
C   X(10)= DABS(X(10))
C
C   PARAMETERS
C

```

```
B = DSQRT(1.D0-PSI*PSI)
```

```
A = -PSI/B
```

```
C
```

```
C = 1.D0-PSI*DSIN(0.D0)
```

```
D = 1.D0-PSI*DSIN(2.D0*X(7))
```

```
FC = DSQRT(C/D)
```

```
C
```

```
PHI0 = DATAN(A)
```

```
IF(DABS(X(7)-PI/2.D0).LT.1.D-7) THEN
```

```
PHI1 = PI/2.D0
```

```
ELSE
```

```
PHI1 = DATAN(A + DTAN(X(7))/B)
```

```
IF(PHI1.LT.0.D0) THEN
```

```
PHI1 = PI + PHI1
```

```
ENDIF
```

```
ENDIF
```

```
F(1) = X(2)-X(1)*FC*DEXP(A*(PHI1-PHI0))
```

```
C
```

```
C = 1.D0-PSI*DSIN(2.D0*(PI-X(10)))
```

```
D = 1.D0-PSI*DSIN(2.D0*X(9))
```

```
FC = DSQRT(C/D)
```

```
C
```

```
F(2) = X(4)-X(3)*FC*DEXP(A*((PI/WN)-RBETA))
```

```
C
```

```
C = 1.D0-PSI*DSIN(2.D0*(PI-X(8)))
```

```
D = 1.D0-PSI*DSIN(2.D0*PI)
```

```
FC = DSQRT(C/D)
```

```
IF(DABS(X(8)-PI/2.D0).LT.1.D-8) THEN
```

```
PHI3 = PI/2.D0
```

```
ELSE
```

```
PHI3 = DATAN(A + DTAN(PI-X(8))/B)
```

```
IF(PHI3.LT.0.D0) THEN
```

```
PHI3 = PI + PHI3
```

```
ENDIF
```

```
ENDIF
```

```
PHIPI = PI + DATAN(A)
```

```

F(3) = X(6)-X(5)*FC*DEXP(A*(PHIPI-PHI3))
C
F(4) = 1.D0 + X(2)*X(2)-X(3)*X(3)-2.D0*X(2)*DCOS(X(7))
C
F(5) = 1.D0 + X(4)*X(4)-X(5)*X(5)-2.D0*X(4)*DCOS(X(9))
C
F(6) = 1.D0 + X(5)*X(5)-X(4)*X(4)-2.D0*X(5)*DCOS(X(8))
C
F(7) = 1.D0 + X(3)*X(3)-X(2)*X(2)-2.D0*X(3)*DCOS(X(10))
C
F(8) = X(6)-X(1)-2.D0*VON
C
IF(DABS(X(9)-(PI/2.D0)).LT.1.D-7) THEN
  TEMPB1 = PI/2.D0
ELSE
  TEMPB1 = DATAN(A + DTAN(X(9)/B))
IF(TEMPB1.LT.0.D0) THEN
  TEMPB1 = PI + TEMPB1
ENDIF
ENDIF
TEMPB1 = TEMPB1-PHI0
IF(DABS(X(10)-(PI/2.D0)).LT.1.D-7) THEN
  TEMPB2 = PI/2.D0
ELSE
  TEMPB2 = DATAN(A + DTAN(PI-X(10)/B))
IF(TEMPB2.LT.0.D0) THEN
  TEMPB2 = PI + TEMPB2
ENDIF
ENDIF
TEMPB2 = PHIPI-TEMPB2
F(9) = TEMPB1 + TEMPB2-PI-(PI/WN) + RBETA
C
TEMP1 = PHI1-PHI0
TEMP2 = PHIPI-PHI3
F(10) = TEMP1 + TEMP2-RBETA
C

```

```

RETURN
END
C#####
C
C  SUBROUTINE TO DEFINE THE HOMOGENEOUS
C  NONLINEAR SYSTEM.MODE B.(Region B' CCM)
C
C#####
C
C  SUBROUTINE FCNB(X,F,N)
C
C  VARIABLES DECLARATION
C
C  COMMON RBETA,PSI,WN,VON,PI
C
C  INTEGER N
C  REAL X(N),F(N),TEMP,TEMP1,TEMP2
C  REAL RBETA,PSI,WN,VON,PI,A,B,C,D,FC
C  REAL PHI0,PHI1,PHI2,PHIPI
C
C  DESCRIPTION
C
C  X(1)= R10
C  X(2)= R1
C  X(3)= R20
C  X(4)= R2
C  X(5)= R30  "R3 = R10 + 2V0N"
C  X(6)= ALPHA
C  X(7)= GAMMA
C  X(8)= BETA1
C
C
C  PARAMETERS
C
C  X(6) = DABS(X(6))
C  X(7) = DABS(X(7))

```

```

X(8) = DABS(X(8))
C
B = DSQRT(1.D0-PSI*PSI)
A = -PSI/B
C
TEMP = RBETA + DTAN(A + DTAN(X(8))/B)
IF(DABS(TEMP-(PI/2.D0)).LT.1.D-5) THEN
TEMP = PI/2.D0
ELSE
TEMP = DATAN(PSI + B*DTAN(TEMP))
ENDIF
IF(TEMP.LT.0.D0) TEMP = PI + TEMP
C
F(1) = 1.D0 + X(2)*X(2)-X(3)*X(3) + 2.D0*X(2)*DCOS(X(6))
F(2) = 1.D0 + X(5)*X(5)-X(4)*X(4)-2.D0*X(5)*DCOS(X(7))
F(3) = 1.D0 + X(3)*X(3)-X(2)*X(2)-2.D0*X(3)*DCOS(X(8))
F(4) = 1.D0 + X(4)*X(4)-X(5)*X(5)-2.D0*X(4)*DCOS(TEMP)
C
PHI0 = DATAN(A)
IF(DABS(X(8)-(PI/2.D0)).LT.1.D-5) THEN
PHI1 = PI/2.D0
ELSE
PHI1 = DATAN(A + DTAN(X(8))/B)
ENDIF
IF(DABS(X(7)-(PI/2.D0)).LT.1.D-5) THEN
PHI2 = PI/2.D0
ELSE
PHI2 = DATAN(A + DTAN(PI-X(7))/B)
ENDIF
IF(PHI2.LT.0.D0) PHI2 = PI + PHI2
PHIPI = PI + DATAN(A)
TEMP1 = PHIPI-PHI2
IF(DABS(X(6)-(PI/2.D0)).LT.1.D-5) THEN
TEMP2 = PI/2.D0
ELSE
TEMP2 = DATAN(A + (DTAN(X(6))/B))

```

```

ENDIF
TEMP2 = TEMP2 - PHI0
C
C = 1.D0
D = 1.D0 - PSI * DSIN(2.D0 * X(6))
FC = DSQRT(C/D)
F(5) = X(2) - X(1) * FC * DEXP(A * TEMP2)
C
C = 1.D0 - PSI * DSIN(2.D0 * X(8))
D = 1.D0 - PSI * DSIN(2.D0 * (TEMP))
FC = DSQRT(C/D)
F(6) = X(4) - X(3) * FC * DEXP(A * RBETA)
C
C = 1.D0 - PSI * DSIN(2.D0 * (PI - X(7)))
D = 1.D0
FC = DSQRT(C/D)
F(7) = (X(1) + 2.D0 * VON) - X(5) * FC * DEXP(A * TEMP1)
C
F(8) = TEMP1 + TEMP2 + RBETA - (PI / WN)
RETURN
END
C#####
C
C SUBROUTINE TO DEFINE THE HOMOGENEOUS
C NONLINEAR SYSTEM. MODE C. (Region B' DCM)
C
C#####
C
SUBROUTINE FCNC(X,F,N)
C
C VARIABLES DECLARATION
C
COMMON RBETA,PSI,WN,VON,PI
C
INTEGER N
REAL X(N),F(N),TEMP,TEMP1,TEMP2,TEMP3

```

```

REAL RBETA,PSI,WN,VON,PI,A,B,C,D,FC
C
C DESCRIPTION
C
C X(1)= R10
C X(2)= R1
C X(3)= R20
C X(4)= R2
C X(5)= GAMMA
C X(6)= PHI ;NON-CONDUCTION ANGLE
C
C
C PARAMETERS
C
X(5)= DABS(X(5))
X(6)= DABS(X(6))
C
B = DSQRT(1.D0-PSI*PSI)
A = -PSI/B
C
TEMP = DATAN(PSI + B*DTAN(RBETA))
IF(TEMP.LT.0.D0) TEMP = PI + TEMP
F(1) = 1.D0 + X(2)*X(2)-X(3)*X(3)-2.D0*X(2)*DCOS(TEMP)
C
F(2) = 1.D0 + X(3)*X(3)-X(2)*X(2)-2.D0*X(3)*DCOS(X(5))
C
TEMP1 = DATAN(A + (DTAN(PI-X(5))/B))
IF(TEMP1.LT.0.D0) TEMP1 = PI + TEMP1
TEMP3 = PI + DATAN(A)
TEMP2 = TEMP3-TEMP1
F(3) = RBETA + TEMP2 + X(6)-(PI/WN)
C
C = 1.D0-PSI*DSIN(0.D0)
D = 1.D0-PSI*DSIN(2.D0*TEMP)
FC = DSQRT(C/D)

```

```

F(4) = X(2)-X(1)* FC*DEXP(A*RBETA)
C
C = 1.D0-PSI*DSIN(2.D0*(PI-X(5)))
D = 1.D0
FC = DSQRT(C/D)
F(5) = X(1)-1.D0 + 2.D0*VON-X(4)
F(6) = X(4)-X(3)*FC*DEXP(A*TEMP2)
C
RETURN
END
C#####
C
C PROGRAM TO CALCULATE MODES BOUNDARIES OF
C CLAMPED MODE SERIES RESONANT CONVERTER FOR
C A NONIDEAL TANK.
C
C#####
C
SUBROUTINE BOUNDARY(BETA12,BETA13,W1N,R)
C ALL OUTPUT VARIABLES
C INPUT THROUGH THE COMMON
C ALL ANGLES TIME PROPORTIONAL AND RADIANS VALUE
C
C VARIABLES DECLARATION
C
INTEGER N,ITMAX,II
REAL ERREL,ION,PSI,WN,R
REAL A,B,BETA13,ALFA,W1N,BETA12
REAL FBOUNDBC,FNORM,X(6),XGUESS(6),XGUESSB(4),XB(4)
REAL FBOUNDAB
C
EXTERNAL FBOUNDAB,DNEQNF,FBOUNDBC
C
COMMON RBETA,PSI,WN,VON,PI
C
C

```

```

C  CONSTANTS
C
PI = 4.D0*DATAN(1.D0)
ERREL = 1.D-5
ITMAX = 100
C
C  DATA INPUT
C
WRITE(19,2003)
2003 FORMAT(///1X,'BOUNDARY CONDITIONS FOR: ',/1X,24('='))
WRITE(19,1001) VON,PSI,WN
1001 FORMAT(/1X,'VON = ',E10.4,2X,'PSI = ',E10.4,2X,'WN = ',E10.4)
C
N = 4
C
WRITE(5,1005)
1005 FORMAT(/1X,'ENTER INITIAL GUESS BOUNDARY 13:R1,R2,BETA,ALFA')
READ(5,*) (XGUESSB(L),L = 1,N)
WRITE(5,*) (XGUESSB(L),L = 1,N)
C
CALL DNEQNF(FBOUNDBC,ERREL,N,ITMAX,XGUESSB,XB,FNORM)
C
WRITE(5,*) FNORM
WRITE(19,2001) (XB(L),L = 1,N)
2001 FORMAT(///1X,'R1',9X,'R2',9X,'BETA13',6X,'ALFA',/1X,44('-'),
+ /1X,4(E10.4,1X))
B = DSQRT(1.D0-PSI*PSI)
A = -PSI/B
BETA13 = DATAN(A + (DTAN(XB(3))/B))
IF(BETA13.LT.0.D0) BETA13 = PI + BETA13
BETA13 = BETA13-DATAN(A)
ALFA = DATAN(A + DTAN(PI-X(4))/B)
IF(ALFA.LT.0.D0) ALFA = PI + ALFA
ALFA = PI + DATAN(A)-ALFA
WIN = PI/(ALFA + BETA13)

```

```

WRITE(19,2002) BETA13,W1N
2002 FORMAT(/1X,'BETA13 = ',E10.4,/1X,'W1N = ',E10.4)
C
N = 6
C
WRITE(5,1002)
1002 FORMAT(/1X,'ENTER INITIAL GUESS BOUND.12:R10,R1,R20,R2,ALFA,BETA')
READ(5,*) (XGUESS(L),L = 1,N)
WRITE(5,*) (XGUESS(L),L = 1,N)
C
C MAIN LOOP
C
C
C SOLVE THE SYSTEM FOR THE GIVEN BETA
C
CALL DNEQNF(FBOUNDAB,ERREL,N,ITMAX,XGUESS,X,FNORM)
C
C OUTPUT FOR CHECKING ACCURACY
WRITE(5,*) FNORM
C
C DATA OUTPUT
C
WRITE(19,2000) (X(L),L = 1,N)
2000 FORMAT(/1X,'R10',8X,'R1',9X,'R20',8X,'R2',9X,'ALFA',7X
+,'BETA12',7X,/1X,66('-',/1X,6(E10.4,1X))
C
BETA12 = DATAN(A + (DTAN(X(6)))/B)
IF(BETA12.LT.0.D0) BETA12 = PI + BETA12
BETA12 = BETA12-DATAN(A)
R = X(1)
WRITE(19,2004) BETA12
2004 FORMAT(/1X,'BETA12 = ',E10.4)
C
RETURN
END
C#####

```

```

C
C  SUBROUTINE TO DEFINE THE HOMOGENEOUS
C  NONLINEAR SYSTEM.BOUNDARY A-B.
C
C#####
C
C  SUBROUTINE FBOUNDAB(X,F,N)
C
C  VARIABLES DECLARATION
C
COMMON RBETA,PSI,WN,VON,PI
C
INTEGER N
REAL X(N),F(N),PSI,WN,VON,PI
REAL A,B,C,D,FC
REAL PHI0,PHI1,PHI2,PHI3
REAL TIMEA,TIMEB
C
C  MAIN PROGRAM
C
C  VARIABLES DEFINITION:
C  X(1)= R10  ;INITIAL GUESS FOR FIRST RADIUS
C  X(2)= R1   ;FINAL  VALUE FOR 1ST ARC
C  X(3)= R20  ;INITIAL  "  " 2ND  "
C  X(4)= R2   ;FINAL  "  " 2ND  "
C  X(5)= ALFA
C  X(6)= BETA
C
C  PARAMETERS
C
B = DSQRT(1.D0-PSI*PSI)
A = -PSI/B
C
C  MAIN PROGRAM
C
F(1) = 1.D0 + X(2)*X(2)-X(3)*X(3)-2.D0*X(2)*DCOS(X(6))

```

```

F(2) = 1.D0 + X(3)*X(3)-X(2)*X(2)-2.D0*X(3)*DCOS(X(5))
C
PHI0 = DATAN(A + DTAN(0.0)/B)
IF(DABS(X(6)-(PI/2.D0)).LT.1.E-5) THEN
PHI1 = PI/2.D0
ELSE
PHI1 = DATAN(A + DTAN(X(6))/B)
ENDIF
IF(PHI1.LT.0.D0) PHI1 = PI + PHI1
IF(DABS(X(5)-(PI/2.D0)).LT.1.D-5) THEN
PHI2 = PI/2.D0
ELSE
PHI2 = DATAN(A + DTAN(PI-X(5))/B)
ENDIF
IF(PHI2.LT.0.D0) PHI2 = PI + PHI2
PHI3 = PI-DATAN(A)
TIMEA = PHI3-PHI2
TIMEB = PHI1-PHI0
F(3) = TIMEA + TIMEB-(PI/WN)
C
C = 1.D0-PSI*DSIN(2.D0*0.D0)
D = 1.D0-PSI*DSIN(2.D0*X(6))
FC = DSQRT(C/D)
F(4) = X(2)-X(1)*FC*DEXP(A*TIMEB)
C
C = 1.D0-PSI*DSIN(2.D0*(PI-X(5)))
D = 1.D0-PSI*DSIN(2.D0*PI)
FC = DSQRT(C/D)
F(5) = X(4)-X(3)*FC*DEXP(A*TIMEA)
C
F(6) = X(1)-X(4)-1.D0 + 2.D0*VON
C
RETURN
END
C#####
C

```

```

C  SUBROUTINE TO DEFINE THE HOMOGENEOUS
C  NONLINEAR SYSTEM.BOUNDARY B-C.
C
C#####
C
C  SUBROUTINE FBOUNDBC(X,F,N)
C
C  VARIABLES DECLARATION
C
COMMON RBETA,PSI,WN,VON,PI
C
INTEGER N
REAL X(N),F(N),PSI,WN,VON,PI
REAL A,B,C,D,FC
REAL PHI0,PHI1,PHI2,PHI3,PHI4
C
C  MAIN PROGRAM
C
C  VARIABLES DEFINITION:
C  X(1)= R1    ;FIRST RADIUS AFTER BETA13
C  X(2)= R2    ;FINAL " " ALFA3
C  X(3)= BETA13 ;BETA13
C  X(4)= ALFA3 ;ALFA3
C
C  PARAMETERS
C
B = DSQRT(1.D0-PSI*PSI)
A = -PSI/B
C
C  MAIN PROGRAM
C
F(1)= 1.D0 + X(1)*X(1)-X(2)*X(2)-2.D0*X(1)*DCOS(X(3))
F(2)= 1.D0 + (2.D0*VON)**2.D0-X(1)*X(1)-4.D0*VON*DCOS(X(4))
C
C
PHI0 = DATAN(A + DTAN(0.0)/B)

```

```

IF((X(3)-PI),LE.1.E-8) THEN
PHI1 = X(3)
ELSE
PHI1 = DATAN(A + DTAN(X(3))/B)
ENDIF
C = 1.D0-PSI*DSIN(2.D0*0.D0)
D = 1.D0-PSI*DSIN(2.D0*X(3))
FC = DSQRT(C/D)
F(3) = X(1)-FC*DEXP(A*(PHI1-PHI0))
C
IF(DABS(X(4)-(PI/2.D0)),LE.1.E-8) THEN
PHI3 = PI/2.D0
ELSE
PHI3 = DATAN(A + DTAN(PI-X(4))/B)
ENDIF
IF(PHI3.LE.0.D0) PHI3 = PI + PHI3
PHI4 = PI + DATAN(A)
C = 1.D0-PSI*DSIN(2.D0*(PI-X(4)))
D = 1.D0-PSI*DSIN(2.D0*PI)
FC = DSQRT(C/D)
F(4) = (2.D0*VON)-X(2)*FC*DEXP(A*(PHI4-PHI3))
C
C
RETURN
END

```

B.2.2 Case below resonant frequency

```

C#####
C
C PROGRAM TO CALCULATE CHARACTERISTICS OF
C CLAMPED MODE SERIES RESONANT CONVERTER FOR
C A NONIDEAL TANK.
C *CASE BELOW RESONANT FREQUENCY

```

```

C
C#####
C
C  VARIABLES DECLARATION
C
C  INTEGER N,ITMAX,L,MODE,JUMP
C  REAL ERREL,ION,PSI,VON,WN,PI,BETA,RBETA,WD,TS
C
C  REAL FNORM
C  REAL XA(10),XC(8),XF(6),XB(7)
C  REAL XGUESSA(10),XGUESSC(8),XGUESSF(6),XGUESSB(7)
C  REAL BETA12,BETA13,W1N,WNC,BETABA
C  EXTERNAL FCNA,FCNB,FCNC,FCNF,DNEQNF,BOUNDARY
C
C  COMMON RBETA,PSI,WN,VON,PI
C
C  DATA INPUT
C
C  WRITE(5,1000)
1000 FORMAT(/1X,'ENTER PARAMETERS: VON,PSI,WN')
C  READ(5,*) VON,PSI,WN
C
C  CONSTANTS
C
C  PI = 4.D0*DATAN(1.D0)
C  ERREL = 1.D-4
C  ITMAX = 200
C
C  DETERMINE BOUNDARIES
C
C  CALL BOUNDARY(BETA12,BETA13,W1N,WNC,BETABA)
C
C  WRITE(5,*) BETABA,BETA12
C  READ(5,*) BETABA,BETA12
C
C  N = 6

```

```

MODE= 1
C
C  INITIAL GUESS
C
XF(1)=1.01D0-VON
XF(2)=1.D0-VON
XF(3)= VON + 0.01D0
XF(4)= VON + .005D0

XF(5)=0.01
XF(6)= PI/WN
C
WRITE(5,1001)
1001 FORMAT(/1X,'INITIAL GUESS FOR C MODE:R10,R1,R20,GAMMA,PHI')
WRITE(5,*) (XF(L),L= 1,N)
C
C  MAIN LOOP
C
DO 10 BETA =0.D0,180.D0,2.D0
C
RBETA = BETA*PI/(180.D0*WN)
C
C  SOLVE THE SYSTEM FOR THE GIVEN BETA
C
C
C  CHECK THE OPERATING MODE
C
IF(RBETA.GE.BETA13) THEN
  IF(WN.GE.WNC) THEN
    IF(RBETA.LE.BETA12) THEN
      JUMP = 2
C      GO TO MODE C
    ELSE
      JUMP = 3
C      GO TO MODE A
    ENDIF
  ENDIF

```

```

ELSE
  IF(RBETA.LE.BETA12) THEN
    JUMP=2
C    GO TO MODE C
  ELSE
    IF(RBETA.LE.BETABA) THEN
      JUMP=4
C    GO TO MODE B
    ELSE
      JUMP=3
C    GO TO MODE A
    ENDIF
  ENDIF
ENDIF
ELSE
  JUMP=1
ENDIF
C
GO TO (11,22,33,44) JUMP
C
C SOLVE THE SYSTEM FOR THE GIVEN BETA
C
11 DO 111 LL=1,N
111 XGUESSF(LL)=XF(LL)
C
CALL DNEQNF(FCNF,ERREL,N,ITMAX,XGUESSF,XF,FNORM)
C
C OUTPUT FOR CHECKING ACCURACY
WRITE(5,333) FNORM,BETA,MODE
333 FORMAT(1X,2E11.4,2X,1I1)
C
C CALCULATE DESIGN CHARACTERISTICS MODE F
C
VCPN = -1.D0 + VON + XF(1)
ION = 2.D0*VCPN/(PI/WN)
C IQAVN = X(1)/(2.D0*WD*TS)

```

```

C   IDAVN = (2.D0*VCPN-X(1)*(1.D0-COS(X(4))))/(2.D0*WD*TS)
C
C   GO TO 777
C
C   MODE C
C
22  IF(MODE.EQ.2) THEN
C
C     NO TRANSITION
C     DO 55 L = 1,N
55  XGUESSC(L) = XC(L)
C
C     ELSE
C
C     TRANSITION FROM MODE F
C     MODE = 2
C     N = 8
C     XGUESSC(1) = 0.
C     XGUESSC(2) = 0.
C     XGUESSC(3) = XF(3) + 0.01
C     XGUESSC(4) = XF(4) + 0.01
C     XGUESSC(5) = XF(1) + 0.01
C     XGUESSC(6) = 1.
C     XGUESSC(7) = XF(5) + 0.01
C     XGUESSC(8) = 0.
C     WRITE(5,555) (XGUESSC(LLL),LLL = 1,N)
C   READ(5,*) (XGUESSC(LLL),LLL = 1,N)
C
C   ENDIF
C
C
C   CALL DNEQNF(FCNC,ERREL,N,ITMAX,XGUESSC,XC,FNORM)
C
C   OUTPUT FOR CHECKING ACCURACY
C   WRITE(5,333) FNORM,BETA,MODE
C

```

```

C   CALCULATE DESIGN CHARACTERISTICS MODE C
C
      VCPN = VON + XC(1)
      ION = 2.D0*VCPN/(PI/WN)
C   IQAVN = X(1)/(2.D0*WD*TS)
C   IDAVN = (2.D0*VCPN-X(1)*(1.D0-COS(X(4))))/(2.D0*WD*TS)
C
      GO TO 777
C   MODE A
C
33  IF(MODE.EQ.3) THEN
C
      NO TRANSITION
      DO 66 L = 1,N
66  XGUESSA(L) = XA(L)
C
      ELSE
C
      N = 10
      IF(MODE.EQ.4) THEN
C   TRANSITION FROM MODE B
      XGUESSA(1) = 0.
      XGUESSA(2) = 0.
      XGUESSA(3) = XB(1) + 0.1
      XGUESSA(4) = XB(2) + 0.1
      XGUESSA(5) = XB(3) + 0.1
      XGUESSA(6) = XB(4) + 0.1
      XGUESSA(7) = 0.
      XGUESSA(8) = BETABA + 0.01
      XGUESSA(9) = 0.
      XGUESSA(10) = PI - XB(5) + 0.01
C
      ELSE
C
C   TRANSITION FROM MODE C
      XGUESSA(1) = 0.

```

```

XGUESSA(2)=0.
XGUESSA(3)=XC(1)+0.01
XGUESSA(4)=XC(2)+0.01
XGUESSA(5)=XC(3)+0.01
XGUESSA(6)=XC(4)+0.01
XGUESSA(7)=0.1
XGUESSA(8)=BETABA+0.1
XGUESSA(9)=0.1
XGUESSA(10)=PI-XC(6)
ENDIF
C
5555 FORMAT(/1X,'SUGGESTED GUESS',/1X,5E11.4,/1X,5E11.4)
      WRITE(5,5555) (XGUESSA(LLL),LLL=1,N)
C   READ(5,*) (XGUESSA(LLL),LLL=1,N)
C
      MODE=3
C
      ENDIF
C
C
      CALL DNEQNF(FCNA,ERREL,N,ITMAX,XGUESSA,XA,FNORM)
C
C   OUTPUT FOR CHECKING ACCURACY
      WRITE(5,*) (XA(L),L=1,N)
      WRITE(5,333) FNORM,BETA,MODE
C
C   CALCULATE DESIGN CHARACTERISTICS MODE A
C
      VCPN=1.D0-VON+XA(6)
      ION=2.D0*VCPN/(PI/WN)
C   IQAVN=X(1)/(2.D0*WD*TS)
C   IDAVN=(2.D0*VCPN-X(1)*(1.D0-COS(X(4))))/(2.D0*WD*TS)
C
      GO TO 777
C
C   MODE B

```

```

C
44  IF(MODE.EQ.4) THEN
C
C    NO TRANSITION
      DO 77 L= 1,N
77  XGUESSB(L)= XB(L)
C
      ELSE
C
      N=7
      MODE=4
C    TRANSITION FROM MODE C
      XGUESSB(1)= XC(1)+0.01
      XGUESSB(2)= XC(2)+0.01
      XGUESSB(3)= XC(3)+0.01
      XGUESSB(4)= XC(4)+0.01
      XGUESSB(5)= XC(6)+0.01
      XGUESSB(6)= BETA12+0.01
      XGUESSB(7)= 0.01
      ENDIF
C
      CALL DNEQNF(FCNB,ERREL,N,ITMAX,XGUESSB,XB,FNORM)
C
C    OUTPUT FOR CHECKING ACCURACY
      WRITE(5,333) FNORM,BETA,MODE
      WRITE(5,*) (XB(L),L= 1,N)
C
C    CALCULATE DESIGN CHARACTERISTICS MODE B
C
      VCPN = VON + XB(1)
      ION = 2.D0*VCPN/(PI/WN)
C
C    DATA OUTPUT
C
777  WRITE(16,2000) BETA,ION
2000  FORMAT(1X,2(E10.4,1X))

```

```

C
10 CONTINUE
C
STOP
END
C#####
C
C SUBROUTINE TO DEFINE THE HOMOGENEOUS
C NONLINEAR SYSTEM.FOR MODE A.(REGION A)
C
C#####
C
SUBROUTINE FCNA(X,F,N)
C
C VARIABLES DECLARATION
C
COMMON RBETA,PSI,WN,VON,PI
C
INTEGER N
REAL X(N),F(N)
REAL RBETA,PSI,WN,VON,PI,A,B,C,D,FC
REAL PHI0,PHI1,PHI3,PHIPI
REAL TEMP,TEMP1,TEMP3,TEMP4
REAL TEMPB1,TEMPB2
C
C MAIN PROGRAM
C
C VARIABLES DEFINITION:
C X(1)= R10 ;INITIAL VALUE FOR 1ST ARC
C X(2)= R1 ;FINAL " " " "
C X(3)= R20 ;INITIAL VALUE FOR 2ND ARC
C X(4)= R2 ;FINAL " " " "
C X(5)= R30 ;INITIAL VALUE FOR 3RD ARC
C X(6)= R3 ;FINAL " " " "
C X(7)= ALFA
C X(8)= GAMMA

```

```

C   X(9) = BETA1
C   X(10) = BETA2
C
      X(7) = DABS(X(7))
      X(8) = DABS(X(8))
      X(9) = DABS(X(9))
      X(10) = DABS(X(10))
C
C   PARAMETERS
C
      B = DSQRT(1.D0-PSI*PSI)
      A = -PSI/B
C
      C = 1.D0-PSI*DSIN(0.D0)
      D = 1.D0-PSI*DSIN(2.D0*X(7))
      FC = DSQRT(C/D)
C
      PHI0 = DATAN(A)
      IF(DABS(X(7)-PI/2.D0).LT.1.D-7) THEN
        PHI1 = PI/2.D0
      ELSE
        PHI1 = DATAN(A + DTAN(X(7))/B)
      IF(PHI1.LT.0.D0) THEN
        PHI1 = PI + PHI1
      ENDIF
      ENDIF
      F(1) = X(2)-X(1)*FC*DEXP(A*(PHI1-PHI0))
C
      C = 1.D0-PSI*DSIN(2.D0*X(9))
      D = 1.D0-PSI*DSIN(2.D0*(PI-X(10)))
      FC = DSQRT(C/D)
C
      F(2) = X(4)-X(3)*FC*DEXP(A*((PI/WN)-RBETA))
C
      C = 1.D0-PSI*DSIN(2.D0*(PI-X(8)))
      D = 1.D0-PSI*DSIN(2.D0*PI)

```

```

FC = DSQRT(C/D)
IF(DABS(X(8)-PI/2.D0).LT.1.D-8) THEN
PHI3 = PI/2.D0
ELSE
PHI3 = DATAN(A + DTAN(PI-X(8))/B)
IF(PHI3.LT.0.D0) THEN
PHI3 = PI + PHI3
ENDIF
ENDIF
PHIPI = PI + DATAN(A)
F(3) = X(6)-X(5)*FC*DEXP(A*(PHIPI-PHI3))
C
F(4) = 1.D0 + X(2)*X(2)-X(3)*X(3) + 2.D0*X(2)*DCOS(X(7))
C
F(5) = 1.D0 + X(4)*X(4)-X(5)*X(5)-2.D0*X(4)*DCOS(X(10))
C
F(6) = 1.D0 + X(5)*X(5)-X(4)*X(4) + 2.D0*X(5)*DCOS(X(8))
C
F(7) = 1.D0 + X(3)*X(3)-X(2)*X(2)-2.D0*X(3)*DCOS(X(9))
C
F(8) = X(6)-X(1)-2.D0*VON
C
IF(DABS(X(9)-(PI/2.D0)).LT.1.D-7) THEN
TEMPB1 = PI/2.D0
ELSE
TEMPB1 = DATAN(A + DTAN(X(9)/B))
IF(TEMPB1.LT.0.D0) THEN
TEMPB1 = PI + TEMPB1
ENDIF
ENDIF
IF(DABS(X(10)-(PI/2.D0)).LT.1.D-7) THEN
TEMPB2 = PI/2.D0
ELSE
TEMPB2 = DATAN(A + DTAN(PI-X(10))/B)
IF(TEMPB2.LT.0.D0) THEN
TEMPB2 = PI + TEMPB2

```

```

ENDIF
ENDIF
F(9)=TEMPB2-TEMPB1-(PI/WN)+RBETA
C
TEMP1 = PHI1-PHI0
TEMP2 = PHIPI-PHI3
F(10)=TEMP1 +TEMP2-RBETA
C
RETURN
END
C#####
C
C  SUBROUTINE TO DEFINE THE HOMOGENEOUS
C  NONLINEAR SYSTEM.MODE C.(REGION B CCM)
C
C#####
C
SUBROUTINE FCNC(X,F,N)
C
C  VARIABLES DECLARATION
C
COMMON RBETA,PSI,WN,VON,PI
C
INTEGER N
REAL X(N),F(N),TEMP,TEMP1,TEMP2
REAL RBETA,PSI,WN,VON,PI,A,B,C,D,FC
REAL PHI0,PHI1,PHI2,PHIPI
C
C  DESCRIPTION
C
C  X(1)= R10
C  X(2)= R1
C  X(3)= R20
C  X(4)= R2
C  X(5)= R30  "R3 = R10+2V0N"
C  X(6)= ALPHA

```

```

C  X(7)=  GAMMA
C  X(8)=  BETA1
C
C
C  PARAMETERS
C
  X(6)= DABS(X(6))
  X(7)= DABS(X(7))
  X(8)= DABS(X(8))
C
  B = DSQRT(1.D0-PSI*PSI)
  A = -PSI/B
C
  PHI0 = DATAN(A)
  IF(DABS(X(8)-(PI/2.D0)).LT.1.D-5) THEN
  PHI1 = PI/2.D0
  ELSE
  PHI1 = DATAN(A + DTAN(X(8))/B)
  ENDIF
  IF(PHI1.LT.0.D0) PHI1 = PI + PHI1
  IF(DABS(X(7)-(PI/2.D0)).LT.1.D-5) THEN
  PHI2 = PI/2.D0
  ELSE
  PHI2 = DATAN(A + DTAN(PI-X(7))/B)
  ENDIF
  IF(PHI2.LT.0.D0) PHI2 = PI + PHI2
  PHIPI = PI + DATAN(A)
  TEMP1 = PHIPI-PHI2
  IF(DABS(X(6)-(PI/2.D0)).LT.1.D-5) THEN
  TEMP2 = PI/2.D0
  ELSE
  TEMP2 = DATAN(A + (DTAN(X(6))/B))
  ENDIF
  IF(TEMP2.LT.0.D0) TEMP2 = PI + TEMP2
  TEMP2 = TEMP2-PHI0
C

```

```

TEMP = RBETA ÷ PHI1
IF(DABS(TEMP-(PI/2.D0)).LT.1.D-5) THEN
TEMP = PI/2.D0
ELSE
TEMP = DATAN(PSI + B*DTAN(TEMP))
ENDIF
IF(TEMP.LT.0.D0) TEMP = PI + TEMP
C
F(1) = 1.D0 + X(2)*X(2)-X(3)*X(3) + 2.D0*X(2)*DCOS(X(6))
F(2) = 1.D0 + X(5)*X(5)-X(4)*X(4)-2.D0*X(5)*DCOS(X(7))
F(3) = 1.D0 + X(3)*X(3)-X(2)*X(2)-2.D0*X(3)*DCOS(X(8))
F(4) = 1.D0 + X(4)*X(4)-X(5)*X(5)-2.D0*X(4)*DCOS(TEMP)
C
C
C = 1.D0
D = 1.D0-PSI*DSIN(2.D0*X(6))
FC = DSQRT(C/D)
F(5) = X(2)-X(1)*FC*DEXP(A*TEMP2)
C
C = 1.D0-PSI*DSIN(2.D0*X(8))
D = 1.D0-PSI*DSIN(2.D0*(TEMP))
FC = DSQRT(C/D)
F(6) = X(4)-X(3)*FC*DEXP(A*RBETA)
C
C = 1.D0-PSI*DSIN(2.D0*(PI-X(7)))
D = 1.D0
FC = DSQRT(C/D)
F(7) = (X(1) + 2.D0*VON)-X(5)*FC*DEXP(A*TEMP1)
C
F(8) = TEMP1 + TEMP2 + RBETA-(PI/WN)
RETURN
END
C#####
C
C SUBROUTINE TO DEFINE THE HOMOGENEOUS
C NONLINEAR SYSTEM.MODE F.(REGION B DCM)

```

```

C
C#####
C
  SUBROUTINE FCNF(X,F,N)
C
C  VARIABLES DECLARATION
C
  COMMON RBETA,PSI,WN,VON,PI
C
  INTEGER N
  REAL X(N),F(N),TEMP,TEMP1,TEMP2,TEMP3
  REAL RBETA,PSI,WN,VON,PI,A,B,C,D,FC
C
C  DESCRIPTION
C
C  X(1)= R10
C  X(2)= R1
C  X(3)= R20
C  X(4)= R2
C  X(5)= GAMMA
C  X(6)= PHI ;NON-CONDUCTION ANGLE
C
C
C  PARAMETERS
C
  X(5)= DABS(X(5))
  X(6)= DABS(X(6))
C
  B = DSQRT(1.D0-PSI*PSI)
  A = -PSI/B
C
  TEMP = DATAN(PSI + B*DTAN(RBETA))
  IF(TEMP.LT.0.D0) TEMP = PI + TEMP
  F(1) = 1.D0 + X(2)*X(2)-X(3)*X(3)-2.D0*X(2)*DCOS(TEMP)
C

```

```

F(2) = 1.D0 + X(3)*X(3)-X(2)*X(2)-2.D0*X(3)*DCOS(X(5))
C
TEMP1 = DATAN(A + (DTAN(PI-X(5))/B))
IF(TEMP1.LT.0.D0) TEMP1 = PI + TEMP1
TEMP3 = PI + DATAN(A)
TEMP2 = TEMP3-TEMP1
F(3) = RBETA + TEMP2 + X(6)-(PI/WN)
C
C = 1.D0-PSI*DSIN(0.D0)
D = 1.D0-PSI*DSIN(2.D0*TEMP)
FC = DSQRT(C/D)
F(4) = X(2)-X(1)* FC*DEXP(A*RBETA)
C
C = 1.D0-PSI*DSIN(2.D0*(PI-X(5)))
D = 1.D0
FC = DSQRT(C/D)
F(5) = X(1)-1.D0 + 2.D0*VON-X(4)
F(6) = X(4)-X(3)*FC*DEXP(A*TEMP2)
C
RETURN
END
C#####
C
C SUBROUTINE TO DEFINE THE HOMOGENEOUS
C NONLINEAR SYSTEM.MODE B.(REGION A DCM)
C
C#####
C
C SUBROUTINE FCNB(X,F,N)
C
C VARIABLES DECLARATION
C
COMMON RBETA,PSI,WN,VON,PI
C
INTEGER N
REAL X(N),F(N),TEMP,PHI0,PHI1,PHI2,PHIPI

```

```

REAL RBETA,PSI,WN,VON,PI,A,B,C,D,FC
C
C DESCRIPTION
C
C X(1)= R10
C X(2)= R1
C X(3)= R20
C X(4)= R2
C X(5)= ALPHA
C X(6)= BETA1
C X(7)= PHI ;NON-CONDUCTION ANGLE
C
C
C PARAMETERS
C
X(5)= DABS(X(5))
X(6)= DABS(X(6))
X(7)= DABS(X(7))
C
B = DSQRT(1.D0-PSI*PSI)
A = -PSI/B
C
F(1) = 1.D0 + X(2)*X(2)-X(3)*X(3) + 2.D0*X(2)*DCOS(X(5))
F(2) = 1.D0 + X(3)*X(3)-X(2)*X(2) + 2.D0*X(3)*DCOS(X(6))
C
PHI0 = DATAN(A)
PHI1 = DATAN(A + (DTAN(X(5))/B))
IF(PHI1.LT.0.D0) PHI1 = PI + PHI1
C = 1.D0-PSI*DSIN(0.D0)
D = 1.D0-PSI*DSIN(2.D0*X(5))
FC = DSQRT(C/D)
F(3) = X(2)-X(1)* FC*DEXP(A*(PHI1-PHI0))
C
C = 1.D0-PSI*DSIN(2.D0*(PI-X(6)))
D = 1.D0
FC = DSQRT(C/D)

```

```

PHI2 = DATAN(A + DTAN(PI-X(6))/B)
IF(PHI2.LT.0.D0) PHI2 = PI + PHI2
PHIPI = PI + DATAN(A)
F(4) = X(4)-X(3)*FC*DEXP(A*(PHIPI-PHI2))
C
F(5) = (PHI1-PHI0) + RBETA-PI/WN
C
F(6) = RBETA-X(7)-(PHIPI-PHI2)
C
F(7) = X(1)-X(4)-1.D0 + 2.D0*VON
C
RETURN
END
C
C#####
C
C PROGRAM TO CALCULATE MODES BOUNDARIES OF
C CLAMPED MODE SERIES RESONANT CONVERTER FOR
C A NONIDEAL TANK.
C
C#####
C
SUBROUTINE BOUNDARY(BETA12,BETA13,W1N,WNC,BETABA)
C ALL OUTPUT VARIABLES
C INPUT THROUGH THE COMMON
C ALL ANGLES TIME PROPORTIONAL AND RADIANS VALUE
C
C VARIABLES DECLARATION
C
INTEGER N,ITMAX,II
REAL ERREL,ION,PSI,WN,WNC
REAL A,B,BETA13,ALFA,W1N,BETA12,ALPHA3,BETABA
REAL FBOUNDFC,FNORM,X(6),XGUESS(6),XGUESSC(4),XC(4)
REAL FBOUNDBA,FBOUNDCA
C

```

```

EXTERNAL FBOUNDBA,DNEQNF,FBOUNDCA,FBOUNDFC
C
COMMON RBETA,PSI,WN,VON,PI
C
C
C  CONSTANTS
C
PI = 4.D0*DATAN(1.D0)
ERREL = 1.D-5
ITMAX = 100
C
C  DATA INPUT
C
WRITE(19,2003)
2003 FORMAT(///1X,'BOUNDARY CONDITIONS FOR: ',/1X,24('='))
WRITE(19,1001) VON,PSI,WN
1001 FORMAT(/1X,'VON = ',E10.4,2X,'PSI = ',E10.4,2X,'WN = ',E10.4)
C
N = 4
C
WRITE(5,1005)
1005 FORMAT(/1X,'ENTER INITIAL GUESS BOUNDARY 13:R1,R2,BETA,ALFA')
READ(5,*) (XGUESSC(L),L = 1,N)
WRITE(5,*) (XGUESSC(L),L = 1,N)
C
CALL DNEQNF(FBOUNDFC,ERREL,N,ITMAX,XGUESSC,XC,FNORM)
C
WRITE(5,*) FNORM
WRITE(19,2001) (XC(L),L = 1,N)
2001 FORMAT(//1X,'R1',9X,'R2',9X,'BETA13',6X,'ALFA',/1X,44('-'),
+ /1X,4(E10.4,1X))
B = DSQRT(1.D0-PSI*PSI)
A = -PSI/B
BETA13 = DATAN(A + (DTAN(XC(3))/B))
IF(BETA13.LT.0.D0) BETA13 = PI + BETA13
BETA13 = BETA13-DATAN(A)

```

```

ALFA = DATAN(A + DTAN(PI-X(4))/B)
IF(ALFA.LT.0.D0) ALFA = PI + ALFA
ALFA = PI + DATAN(A)-ALFA
W1N = PI/(ALFA + BETA13)
WRITE(19,2002) BETA13,W1N
2002 FORMAT(/1X,'BETA13 = ',E10.4,/1X,'W1N = ',E10.4)
C
N = 6
C
WRITE(5,1002)
1002 FORMAT(/1X,'ENTER INITIAL GUESS BOUND.12:R10,R1,R20,R2,ALFA,BETA')
READ(5,*) (XGUESS(L),L = 1,N)
WRITE(5,*) (XGUESS(L),L = 1,N)
C
C MAIN LOOP
C
C
C SOLVE THE SYSTEM FOR THE GIVEN BETA
C
CALL DNEQNF(FBOUNDCA,ERREL,N,ITMAX,XGUESS,X,FNORM)
C
C OUTPUT FOR CHECKING ACCURACY
WRITE(5,*) FNORM
C
C DATA OUTPUT
C
WRITE(19,2000) (X(L),L = 1,N)
2000 FORMAT(/1X,'R10',8X,'R1',9X,'R20',8X,'R2',9X,'ALFA',7X
+,'BETA12',7X,/1X,66('-'),/1X,6(E10.4,1X))
C
BETA12 = DATAN(A + (DTAN(PI-X(6))/B))
IF(BETA12.LT.0.D0) BETA12 = PI + BETA12
BETA12 = PI + DATAN(A)-BETA12
WRITE(19,2004) BETA12
2004 FORMAT(/1X,'BETA12 = ',E10.4)
N = 4

```

```

CALL DNEQNF(FBOUNDBA,ERREL,N,ITMAX,XGUESSC,X,FNORM)
WRITE(5,*) FNORM
C
WRITE(19,2005) (X(L),L = 1,N)
2005 FORMAT(/1X,'R1',9X,'R2',9X,'BETABA',6X,'ALFA',/1X,44('-'),
+ /1X,4(E10.4,1X))
C
BETABA = DATAN(A + DTAN(PI-X(4))/B)
IF(BETABA.LT.0.) BETABA = PI + BETABA
BETABA = PI + DATAN(A)-BETABA
ALPHA3 = DATAN(A + (DTAN(X(3))/B))
IF(ALPHA3.LT.0.) ALPHA3 = PI + ALPHA3
ALPHA3 = ALPHA3-DATAN(A)
WNC = PI/(ALPHA3 + BETABA)
C
IF(WN.GE.WNC) THEN
BETABA = BETA12
ENDIF
C
WRITE(19,2006) BETABA,WNC
2006 FORMAT(/1X,'BETABA = ',E10.4,/1X,'WNC = ',E10.4)
C
RETURN
END
C#####
C
C SUBROUTINE TO DEFINE THE HOMOGENEOUS
C NONLINEAR SYSTEM.BOUNDARY NATURAL COMMUTATION.
C
C#####
C
SUBROUTINE FBOUNDCA(X,F,N)
C
C VARIABLES DECLARATION
C

```

```

COMMON RBETA,PSI,WN,VON,PI
C
INTEGER N
REAL X(N),F(N),PSI,WN,VON,PI
REAL A,B,C,D,FC
REAL PHI0,PHI1,PHI2,PHI3
REAL TIMEA,TIMEB
C
C MAIN PROGRAM
C
C VARIABLES DEFINITION:
C X(1)= R10 ;INITIAL GUESS FOR FIRST RADIUS
C X(2)= R1 ;FINAL VALUE FOR 1ST ARC
C X(3)= R20 ;INITIAL " " 2ND "
C X(4)= R2 ;FINAL " " 2ND "
C X(5)= ALFA
C X(6)= BETA
C
X(5)= DABS(X(5))
X(6)= DABS(X(6))
C PARAMETERS
C
B = DSQRT(1.D0-PSI*PSI)
A = -PSI/B
C
C MAIN PROGRAM
C
F(1) = 1.D0 + X(3)*X(3)-X(2)*X(2) + 2.D0*X(3)*DCOS(X(6))
F(2) = 1.D0 + X(2)*X(2)-X(3)*X(3) + 2.D0*X(2)*DCOS(X(5))
C
PHI0 = DATAN(A + DTAN(0.0)/B)
IF(DABS(X(6)-(PI/2.D0)).LT.1.E-5) THEN
PHI1 = PI/2.D0
ELSE
PHI1 = DATAN(A + DTAN(PI-X(6))/B)
ENDIF

```

```

IF(PHI1.LT.0.D0) PHI1 = PI + PHI1
IF(DABS(X(5)-(PI/2.D0)).LT.1.D-5) THEN
PHI2 = PI/2.D0
ELSE
PHI2 = DATAN(A + DTAN(X(5))/B)
ENDIF
IF(PHI2.LT.0.D0) PHI2 = PI + PHI2
PHI3 = PI + DATAN(A)
TIMEA = PHI2-PHI0
TIMEB = PHI3-PHI1
F(3)=TIMEA + TIMEB-(PI/WN)
C
C = 1.D0-PSI*DSIN(2.D0*0.D0)
D = 1.D0-PSI*DSIN(2.D0*X(5))
FC = DSQRT(C/D)
F(4) = X(2)-X(1)*FC*DEXP(A*TIMEA)
C
C = 1.D0-PSI*DSIN(2.D0*(PI-X(6)))
D = 1.D0-PSI*DSIN(2.D0*PI)
FC = DSQRT(C/D)
F(5) = X(4)-X(3)*FC*DEXP(A*TIMEB)
C
F(6) = X(4)-X(1) + 1.D0-2.D0*VON
C
RETURN
END
C#####
C
C  SUBROUTINE TO DEFINE THE HOMOGENEOUS
C  NONLINEAR SYSTEM.BOUNDARY F-C.(DCM-CCM IN REGION B)
C
C#####
C
C  SUBROUTINE FBOUNDFC(X,F,N)
C

```

```

C  VARIABLES DECLARATION
C
COMMON RBETA,PSI,WN,VON,PI
C
INTEGER N
REAL X(N),F(N),PSI,WN,VON,PI
REAL A,B,C,D,FC
REAL PHI0,PHI1,PHI2,PHI3,PHI4
C
C  MAIN PROGRAM
C
C  VARIABLES DEFINITION:
C  X(1)= R1      ;FIRST RADIUS AFTER BETA13
C  X(2)= R2      ;FINAL " " ALFA3
C  X(3)= BETA13  ;BETA13
C  X(4)= ALFA3   ;ALFA3
C
C  PARAMETERS
C
B = DSQRT(1.D0-PSI*PSI)
A = -PSI/B
C
C  MAIN PROGRAM
C
F(1) = 1.D0 + X(1)*X(1)-X(2)*X(2)-2.D0*X(1)*DCOS(X(3))
F(2) = 1.D0 + (2.D0*VON)**2.D0-X(1)*X(1)-4.D0*VON*DCOS(X(4))
C
C
PHI0 = DATAN(A + DTAN(0.0)/B)
IF((X(3)-PI).LE.1.E-8) THEN
PHI1 = X(3)
ELSE
PHI1 = DATAN(A + DTAN(X(3))/B)
ENDIF
C = 1.D0-PSI*DSIN(2.D0*0.D0)
D = 1.D0-PSI*DSIN(2.D0*X(3))

```

```

FC = DSQRT(C/D)
F(3) = X(1)-FC*DEXP(A*(PHI1-PHI0))
C
IF(DABS(X(4)-(PI/2.D0)).LE.1.E-8) THEN
PHI3 = PI/2.D0
ELSE
PHI3 = DATAN(A + DTAN(PI-X(4))/B)
ENDIF
IF(PHI3.LE.0.D0) PHI3 = PI + PHI3
PHI4 = PI + DATAN(A)
C = 1.D0-PSI*DSIN(2.D0*(PI-X(4)))
D = 1.D0-PSI*DSIN(2.D0*PI)
FC = DSQRT(C/D)
F(4) = (2.D0*VON)-X(2)*FC*DEXP(A*(PHI4-PHI3))
C
C
RETURN
END
C
C#####
C
C SUBROUTINE TO DEFINE THE HOMOGENEOUS
C NONLINEAR SYSTEM.BOUNDARY B-A.(CCM DCM IN REGION A)
C
C#####
C
SUBROUTINE FBOUNDBA(X,F,N)
C
C VARIABLES DECLARATION
C
COMMON RBETA,PSI,WN,VON,PI
C
INTEGER N
REAL X(N),F(N),PSI,WN,VON,PI
REAL A,B,C,D,FC

```

```

REAL PHI0,PHI1,PHI2,PHI3,PHI4
C
C MAIN PROGRAM
C
C VARIABLES DEFINITION:
C X(1)= R1 ;FIRST RADIUS AFTER BETA13
C X(2)= R2 ;FINAL " " ALFA3
C X(3)= ALPHA3
C X(4)= BETABA
C
C PARAMETERS
C
B = DSQRT(1.D0-PSI*PSI)
A = -PSI/B
C
C MAIN PROGRAM
C
F(1) = 1.D0 + X(1)*X(1)-X(2)*X(2) + 2.D0*X(1)*DCOS(X(3))
F(2) = 1.D0 + X(2)*X(2)-X(1)*X(1) + 2.D0*X(2)*DCOS(X(4))
C
C
PHI0 = DATAN(A)
IF((X(3)-PI/2.D0).LE.1.E-8) THEN
PHI1 = PI/2.D0
ELSE
PHI1 = DATAN(A + DTAN(X(3))/B)
ENDIF
IF(PHI1.LT.0.D0) PHI1 = PI + PHI1
C = 1.D0-PSI*DSIN(2.D0*0.D0)
D = 1.D0-PSI*DSIN(2.D0*X(3))
FC = DSQRT(C/D)
F(3) = X(1)-FC*DEXP(A*(PHI1-PHI0))
C
IF(DABS(X(4)-(PI/2.D0)).LE.1.E-8) THEN
PHI3 = PI/2.D0
ELSE

```

```

PHI3 = DATAN(A + DTAN(PI-X(4))/B)
ENDIF
IF(PHI3.LE.0.D0) PHI3 = PI + PHI3
PHI4 = PI + DATAN(A)
C = 1.D0-PSI*DSIN(2.D0*(PI-X(4)))
D = 1.D0-PSI*DSIN(2.D0*PI)
FC = DSQRT(C/D)
F(4) = (2.D0*VON)-X(2)*FC*DEXP(A*(PHI4-PHI3))
C
C
RETURN
END

```

Appendix C

Spice listings

C.1 Simulation of the model including loss

```
*CLAMPED MODE RES CIRCUIT BELOW RES. FREQ. HIGH LINE
V1 1 0 PULSE(-150,150,0.,35N,35N,1155N,2380N)
V2 0 2 PULSE(-150,150,750N,35N,35N,1155N,2380N)
D1 1 5 DR
D4 3 5 DR
D3 6 1 DR
D2 6 3 DR
;MODEL DR D(CJO = 1P)
LO 3 41 79U IC = -1.5
RO 41 4 16.5
CO 4 2 1.16N IC = 0.
VO 5 6 DC 150.
;TRAN .05U 20U 15.5U UIC
;PLOT TRAN V(2,1) I(V1) V(4,2) V(1,3) V(3,2)
```

```
;OPTIONS LIMPTS = 10000 ITL5 = 50000 LVLTIM = 2
;END
```

```
*CLAMPED MODE RES CIRCUIT BELOW RES. FREQ. LOW LINE
```

```
V1 1 0 PULSE(-150,150,0.,35N,35N,1155N,2380N)
V2 0 2 PULSE(-150,150,375N,35N,35N,1155N,2380N)
D1 1 5 DR
D4 3 5 DR
D3 6 1 DR
D2 6 3 DR
;MODEL DR D(CJO = 1P)
LO 3 41 79U IC = -1.5
RO 41 4 16.5
CO 4 2 1.16N IC = 0.
VO 5 6 DC 150.
;TRAN .05U 20U 15.5U UIC
;PLOT TRAN V(2,1) I(V1) V(4,2) V(1,3) V(3,2)
;OPTIONS LIMPTS = 10000 ITL5 = 50000 LVLTIM = 2
;END
```

```
*CLAMPED MODE RES CIRCUIT ABOVE RES. FREQ. LOW LINE
```

```
V1 1 0 PULSE(-150,150,0.,35N,35N,837N,1764N)
V2 0 2 PULSE(-150,150,165N,35N,35N,837N,1764N)
D1 1 5 DR
D4 3 5 DR
D3 6 1 DR
D2 6 3 DR
;MODEL DR D(CJO = 1P)
LO 3 41 100U IC = -2.
RO 41 4 12.25
CO 4 2 1.09N IC = 0.
VO 5 6 DC 100.
```

```
;TRAN .1U 24U 22.U UIC
;PLOT TRAN V(2,1) I(V1) V(4,2)
;OPTIONS LIMPTS = 10000 ITL5 = 50000 LVLTIM = 2
;END
```

***CLAMPED MODE RES CIRCUIT ABOVE RES. FREQ. HIGH LINE**

```
V1 1 0 PULSE(-150,150,0,.35N,35N,837N,1764N)
V2 0 2 PULSE(-150,150,475N,35N,35N,837N,1764N)
D1 1 5 DR
D4 3 5 DR
D3 6 1 DR
D2 6 3 DR
;MODEL DR D(CJO = 1P)
LO 3 41 100U IC = -2.
RO 41 4 12.25
CO 4 2 1.09N IC = 0.
VO 5 6 DC 100.
;TRAN .1U 24U 22.U UIC
;PLOT TRAN V(2,1) I(V1) V(4,2)
;OPTIONS LIMPTS = 10000 ITL5 = 50000 LVLTIM = 2
;END
```

C.2 Simulation of switching conditions

***CLAMPED MODE SERIES RES. CONV. SWITCHING**

```
VS 1 0 DC 300
XS1 71 12 2 IRF720
XS2 3 22 5 IRF720
XS3 2 32 0 IRF720
```

```

XS4 81 42 4 IRF720
DS1 4 3 DS
DS2 5 0 DS
DP1 0 3 DP
DP2 3 1 DP
DP3 2 71 DP
DP4 4 81 DP
;MODEL DP D(PB=0.6 BV=400 CJO=150P TT=35NS)
;MODEL DS D(PB=0.6 BV=60 CJO=100P)
*****
*MEASURING VOLTAGE SOURCES
V1 1 71 0
V2 1 81 0
*****
*RESONANT TANK
LO 3 6 84.7U IC=1.
RS 6 7 4
CO 2 8 1.09N IC=-100
RP 2 8 1MEG
*****
*TRANSFORMER
ET 7 9 51 50 29
VT 8 9 0
RT 8 52 1MEG
FT 51 50 VT 29
*****
*RECTIFIER
D1 51 53 DR
D2 50 53 DR
D3 52 51 DR
D4 52 50 DR
;MODEL DR D(PB=0.25 CJO=800P)
*****
*LOAD
VO 54 53 0
RCF 53 55 0.02

```

CF 55 52 600U IC = 5.

RL 54 52 0.245

*GATE DRIVERS

VS1 12 2 PULSE(-10 12 0 10N 10N 1.08U 2.4U)

VS2 22 5 PULSE(-10 12 0.6U 10N 10N 1.08U 2.4U)

VS3 32 0 PULSE(-10 12 1.2U 10N 10N 1.08U 2.4U)

VS4 42 4 PULSE(12 -10 0.49U 10N 10N 1.3U 2.4U)

*CIRCUIT TO CALCULATE SWITCHING LOSSES

H1 60 0 V2 1

RI 60 0 1

G1 0 61 POLY(2) 60 0 81 4 0 0 0 0 1 IC=0

RG1 61 0 1G

CG1 61 0 2.4U IC=0.

*SUBCIRCUIT IRF720

;SUBCKT IRF720 1 2 3

MF 1 21 3 3 MOSSFET AD=1.0 W=1.0 L=1.0

RG 21 2 10

D1 3 1 BD

;MODEL MOSFET NMOS(VTO=3.335 KP=3.42 LAMBDA=0 RD=1.381 RS=0.115

+ CGS=510P CGD=20P CBD=500P PB=1 LEVEL=1)

;MODEL BD D(PB=0.6 BV=400)

;ENDS

;TRAN 0.01 U 5.U UIC

;PLOT TRAN V(2,3) I(VT) V(51,50) V(2,8) V(54,52)

;PLOT TRAN V(71,2) V(81,4) I(V1) I(V2) V(61,0) V(63,0)

;PLOT TRAN V(91,0) V(93,0)

;PLOT TRAN I(VO) I(VS)

;END

References:

1. **Vorperian V., and Cuk S.**, "A Complete DC Analysis of the Series Resonant Converter," IEEE PESC, 1982 Record, pp. 85-100.
2. **Vorperian V., and Cuk S.**, "Small Signal Analysis of Resonant converters," IEEE PESC, 1983 Record , pp. 269-282.
3. **Vorperian V.**, "Analysis of Resonant Converters," Ph.D. Thesis, California Institute of Technology, May 1984.
4. **King R., and Stuart T. A.**, "A Normalized Model for the Half Bridge Series Resonant Converter," IEEE Transactions on Aerospace and Electronic Systems, AES-17 March 1981, pp. 190-198.
5. **King R., and Stuart T. A.**, "Modelling the Full Bridge Series Resonant Power Converter," IEEE Transactions on Aerospace and Electronic Systems. AES-18 July 1982, pp. 449-459.
6. **Oruganti R., and Lee F.C.**, "Resonant Power Processors, Part I- State Plane Analysis," IEEE Transactions on Industry Applications, Nov/Dec 1985.
7. **Oruganti R., and Lee F.C.**, "Resonant Power Processors, Part II- Methods of Control," IEEE Transactions on Industry Applications, Nov/Dec 1985.
8. **Oruganti R., and Lee F.C.**, "Effects of Parasitic Losses on the Performance of Series Resonant Converter," IAS annual meeting, 1985.
9. **Oruganti R.**, "State-Plane Analysis of Resonant Converters," Ph.D. Dissertation , Virginia Polytechnical Institute & S.U., May 1987.
10. **Tsai F.S., Materu P.N., and Lee F.C.**, "Constant-Frequency, Clamped Mode Resonant Converters," IEEE PESC, 1987 Record.

11. **Tsai F.S., and Lee F.C.,** "A Complete DC Characterization of a Constant-Frequency, Clamped-Mode Series Resonant Converter," IEEE PESC, 1988 Record.
12. **Tsai F.S.,** "Constant-Frequency Resonant Power Processors," M.S. Thesis. Virginia Polytechnical Institute & S.U., 1985.
13. **Materu, and Lee F.C.,** "Constant-Frequency Resonant Converter" Final Report EG&G Almond Inst., 1986.
14. **Pitel I.J.,** "Phase Modulated, Resonant Power Conversion Techniques for High-Frequency Link Inverters," IAS annual Meeting 1985.
15. **King R.J.,and Laubacher R.L.,** "A Modified Series Resonant DC/DC Converter,". IEEE PESC, 1986 Record.
16. **Schwartz F.C.,** "A Method of Resonant Current Pulse Modulation for Power Converters," IEEE Transactions on Industrial Electronics and Instrumentation. , May 1970 ,Vol IEC1-17 No.3, pp. 209-221.
17. **Nienhaus H.A., and Bowers J.C.,** "A High Power Mosfet Computer Model," IEEE PESC , 1980 Record.
18. **International Rectifier,** HEXFET Data Book, HBB-3, 1985.
19. **Jovanovic M.M., Tabisz W.A., and Lee F.C.,** "Zero Voltage Switching Technique in High Frequency Off-line Converters," APEC 1988.
20. **Jovanovic M.M.,** "Off-Line Zero Voltage Switched Quasi-Resonant Converters," VPEC Seminar 1987.
21. **Hopkins D.C., Jovanovic M.M., Lee F.C., and Stephenson F.W.,** "Two-Megahertz, Off-Line Hybridized Converter," APEC 1987.
22. **Khair D.T. Ngo,** "Analysis of a Series Resonant Pulsewidth Modulated or Current Controlled for Low Switching Loss," IEEE PESC , 1987 Record.
23. **Kwang Hwa Liu,** "High Frequency Quasi-Resonant Conversion Techniques," Ph.D. Dissertation, Virginia Polytechnical Institute & S.U., 1986.
24. **Yuan Chin,** "Constant-Frequency Parallel-Resonant Converter," M.S. Thesis , Virginia Polytechnical Institute & S.U., 1986.

25. **Savary P., Satoshi N., Nakaoka M., Maruhashi T.**, "A 450 KHz Multi-kilowatt Resonant Power Supply with Phase-Shifting Regulation Technique," Proceedings HFPC Conference, April 1987.
26. **Unitrode**, "Application Notes," Semiconductor Data Book 1984-85.
27. **Tsai F.S.**, "Clamped-Mode Resonant Converters," Ph.D. Dissertation , Virginia Polytechnical Institute & S.U., September 1988.

Vita

The author was born on July 21, 1959 in Vilafranca del Penedes, Spain. He graduated in 1982 from Polytechnic University of Catalunya with a degree in Electrical Engineering. After one year of military service in the Spanish Army, he joined the Electronics Department of the Polytechnic University of Catalunya as Research Engineer and Assistant Instructor. He worked part time as design Engineer for Mobba Co.

In September 1986, he enrolled at Virginia Polytechnic Institute and State University and joined the research group of Virginia Power Electronics Center. He is currently doing research work towards a Ph.D. degree.

His main research interest is in the modeling analysis and design of high power density power conversion circuits.